NONLINEARITY OF THE RESIDUAL SHEAR STRENGTH ENVELOPE IN STIFF CLAYS

A THESIS SUBMITTED TO
THE GRADUATE SCHOOL OF NATURAL AND APPLIED SCIENCES
OF
MIDDLE EAST TECHNICAL UNIVERSITY

BY

ARASH MAGHSOUDLOO

IN PARTIAL FULFILLMENT OF THE REQUIREMENTS
FOR
THE DEGREE OF THE MASTER OF SCIENCE
IN
CIVIL ENGINEERING

JANUARY 2013

Approval of the thesis:

NONLINEARITY OF THE RESIDUAL SHEAR STRENGTH ENVELOPE IN STIFF CLAYS

submitted by **ARASH MAGHSOUDLOO** in partial fulfillment of the requirements for the degree of **Master of Science in Civil Engineering Department, Middle East Technical University** by,

Prof. Dr. Canan Özgen
Dean, Graduate School of **Natural and Applied Science** _____

Prof. Dr. Ahmet Cevdet Yalçıner
Head of Department, **Civil Engineering** _____

Asst. Prof. Dr. Nejan Huvaj Sarıhan
Supervisor, **Civil Engineering Dept., METU** _____

Examining Committee Members:

Prof. Dr. Erdal Çokça
Civil Engineering Dept., METU _____

Asst. Prof. Dr. Nejan Huvaj Sarıhan
Civil Engineering Dept., METU _____

Prof. Dr. Sadık Bakır
Civil Engineering Dept., METU _____

Prof. Dr. Tamer Topal
Geological Engineering Dept., METU _____

Inst. Dr. Nabi Kartal Toker
Civil Engineering Dept., METU _____

Date: 31/01/2013

I hereby declare that all information in this document has been obtained and presented in accordance with academic rules and ethical conduct. I also declare that, as required by these rules and conduct, I have fully cited and referenced all material and results that are not original to this work.

Name, Last name : **Arash Maghsoudloo**

Signature :

ABSTRACT

NONLINEARITY OF THE RESIDUAL SHEAR STRENGTH ENVELOPE IN STIFF CLAYS

Maghsoudloo, Arash
M.Sc., Department of Civil Engineering
Supervisor: Asst. Prof. Dr. Nejan Huvaj Sarıhan

January 2013, 103 pages

During shearing of stiff clays, plate-shaped clay particles are parallel-oriented in the direction of shear reaching the minimum resistance of "residual shear strength". The residual shear strength envelopes of stiff clays are curved, but for practical purposes represented by linear envelopes. This study investigates the nonlinearity of the residual shear strength envelope using experimental evidence (i) from laboratory reversal direct shear tests on two stiff clays (Ankara clay and kaolinite) at 25 to 900 kPa effective normal stresses and (ii) from laboratory data collected from literature. To evaluate the importance of nonlinearity of the envelope for geotechnical engineering practice, by limit equilibrium method, (a) case histories of reactivated landslides are analyzed and (b) a parametric study is carried out. Conclusions of this study are: (1) The residual shear strength envelopes of both Ankara clay and kaolinite are nonlinear, and can be represented by a power function (cohesion is zero). (2) At least 3 reversals or cumulative 20 mm shear displacement of direct shear box is recommended to reach residual condition. (3) Empirical relations between plasticity index and residual friction angle can accurately estimate the residual strength of stiff clays. (4) Nonlinearity is especially important for landslides where average effective normal stress on the shear plane is less than 50 kPa, both for translational and rotational failures. For such slopes using a linear strength envelope overestimates the factor of safety (more significantly for the case of high pore pressures). (5) As the plasticity index increases, the power "b" of the nonlinear shear strength envelope decreases, indicating more significant nonlinearity. For less plastic materials, using linear and nonlinear shear strength envelopes does not affect the factor of safety.

Keywords: Residual shear strength, failure envelope, nonlinearity, stiff clay, reversal direct shear test

ÖZ

KATI KİLLERDE DOĞRUSAL OLMAYAN REZİDÜEL KAYMA DAYANIM ZARFI

Maghsoudloo Arash
Yüksek Lisans, İnşaat Mühendisliği Bölümü
Tez Yöneticisi: Asst. Prof. Dr. Nejan Huvaj Sarıhan

Ocak 2013,103 sayfa

Kesme deformasyonları süresince, katı killerde, ince levha-şeklindeki kil mineralleri kayma yönüne paralel şekilde üst üste gelerek kesmeye karşı en az direnci göstererek "rezidüel kayma dayanımı"na erişir. Katı killerin rezidüel kayma dayanım zarfları doğrusal olmayan bir şekle sahiptir, fakat pratikte kolaylık açısından doğrusal yenilme zafı ile ifade edilir. Bu çalışmada, rezidüel kayma dayanım zarfının doğrusal olmayışı: (i) iki katı kilde (Ankara kili ve kaolin) 50 ila 900 kPa efektif normal gerilmeler altında tekrarlı direk kesme deneyleri ile ve (ii) literatürde yayınlanmış rezidüel kayma dayanımı verileri kullanılarak ele alınmaktadır. Rezidüel kayma dayanım zarfının doğrusal olmayışının önemini değerlendirebilmek için, limit denge metodu ile (a) reaktive heyelanlarda vaka analizleri ve (b) parametrik çalışma yapılmıştır. Bu çalışmanın sonuçları (1) Ankara kili ve kaolinin rezidüel kayma dayanım zarfları doğrusal değildir, bir üslü fonksiyonla ifade edilebilir ve kohezyon sıfırdır (2) Rezidüel dayanıma ulaşmak için tekrarlı direk kesme deneylerinde 3 kere tekrarlı kesme veya 20 mm kumulatif kayma deformasyonları uygulanması önerilmektedir (3) Plastisite indisi ve rezidüel kayma dayanımı arasındaki ampirik ilişkiler katı killerde rezidüel dayanımı başarılı bir şekilde tahmin edebilmektedir. (4) Rezidüel yenilme zarfının doğrusal olmayışı özellikle averaj efektif normal gerilmelerin 50 kPa'dan az olduğu, dönel ve ötelenmeli heyelanlar için önemlidir. Bu tür heyelanlarda doğrusal kayma dayanımı zarfı kullanılırsa şev güvenlik sayısı gerçekte olduğundan fazla bulunacaktır (özellikle su seviyesi yüksek olan heyelanlarda). (5) Plastisite indisi arttıkça, üslü fonksiyonun üs "b" değeri azalmakta, ve dolayısıyla yenilme zarfı doğrusal olmaktan daha çok uzaklaşmaktadır. Düşük plastisiteli malzemelerde doğrusal veya doğrusal olmayan yenilme zarfıı kullanmak güvenlik sayısı üzerinde çok büyük etki yapmamaktadır.

Anahtar Kelimeler: reziduel kayma dayanımı, yenilme zarfı, doğrusal olmama, katı kil, tekrarlı direk kesme deneyi .

To My Family

ACKNOWLEDGEMENTS

My first and sincere appreciation goes to Asst. Prof. Dr. Nejan Huvaj Sarıhan, my advisor, for all I have learned from her and for her continuous help and support in all stages of this thesis. In addition to her supports, her friendship has been invaluable on both an academic and a personal level, for which I am extremely grateful.

I would like to express my deep gratitude and respect to Dr. Nabi Kartal Toker whose advices and insights were invaluable to me. For all I learned from him during the courses, researches and laboratory works.

I also would like to thank Prof. Dr. Şebnem Düzgün for providing me the opportunity of working in a real life project of Balikesir mine that was one of the starting points of my thesis.

My greatest appreciation and friendship goes to my closest friend, Reza Ahmadi Naghadeh, who was always a great support in all my struggles in my studies.

I am thankful to all my friends who endured the difficult and happy moments of this adventure. Very special thanks must go to Javad khalaj, Alvand Mehrabzadeh, Okan Köksalan, Mohammad Ahmadi Adli, Fatma Nurten Şişman and Zeynep Çekinmez.

I would also like to thank Mr. Ulaş Nacar, Mr.Kamber Bilgen and Mr.Ali Bal for their helps and supports during the experiments in the soil mechanics laboratory of the Middle East Technical University.

Finally yet importantly, the support, encouragement and patience, my family has been constantly showing are truly appreciated.

TABLE OF CONTENTS

LIST OF TABLES

TABLES

LIST OF FIGURES

FIGURES

CHAPTER 1

INTRODUCTION

Residual shear strength mobilizes along pre-existing shear surfaces in stiff clays and shales in reactivated landslides. It is now well known that residual shear strength condition also exists along horizontal/subhorizontal portions of the failure surfaces in first-time slope failures (Mesri and Shahien 2003). Therefore it is an important concept for the correct understanding and evaluation of slope stability and stabilization alternatives in stiff clays. Stiff clays are typically stratified, and may include bedding planes, laminations, or thin weak continuous seams. During shearing, the plate-shaped clay particles are parallel-oriented to the maximum extent possible in the direction of shearing. This is defined as the "residual condition". The intact, fully softened, and residual shear strength envelopes of stiff clays are curved (i.e. the relationship between effective normal stress and shear strength is nonlinear), and there is no shear strength at zero effective normal stress (i.e. the cohesion is zero) (Bishop et al. 1971, Morgenstern 1977, Stark and Eid 1994, Terzaghi et al. 1996). In this study the importance and significance (or lack thereof) of the nonlinearity of the envelope will be investigated.

1.1 Problem Statement

In slope stability analyses, the most important factor that controls the stability is the shear strength of the material. The residual shear strength is a special condition where platey clay particles align in the direction of shearing and under effective normal stresses, creating the weakest plane. The shear strength envelope is in fact nonlinear, instead of a more commonly employed Mohr-Coulomb (c', ϕ' type) linear envelope. The use of different shear strength envelopes may influence the results of slope stability analyses, e.g. in limit equilibrium solutions. In geotechnical engineering practice the actual nonlinear envelope is typically represented as a linear envelope using (c', ϕ') for the effective vertical stress range considered relevant for the slope. Therefore it is important to understand the effect of shear strength envelope nonlinearity on the F.S. value, since it may lead to unconservative design and may create dangerous consequences.

1.2 Research Objectives

The main objective of this study is to investigate the importance (or lack thereof) of the nonlinearity of the residual shear strength envelope . Other objectives of this study are:

(1) to demonstrate that the residual shear strength envelope is, in fact, nonlinear, (also under high effective normal stresses that may exist in deep landslides, open mine pits etc.).
(2) to find the residual shear strength of stiff overconsolidated Ankara clay
(3) to see whether the residual shear strength envelope is affected by two different laboratory specimen preparation methods and to determine the displacement required to reach to residual conditon in both of these sample preparation methods.

(4) To evaluate the applicability of empirical correlations betwen residual friction angle and index properties existing in the literature in estimating the residual shear strength measured in our tests.
(5) To evaluate whether the nonlinearity has any major significance in geotechnical engineering practice, especially in slope stability problems, and if so under what conditions it becomes important. To determine the factors/conditions for which nonlinear shear strength envelope must be used, otherwise the slope would be dangerous.
(6) To demonstrate that reversal direct shear test can successfully be used to determine residual shear strength of stiff clays.

1.3 Scope

This study investigates the nonlinearity of the residual shear strength envelope using experimental evidence (i) from laboratory reversal direct shear tests on two different stiff clays carried out at Soil Mechanics Laboratory of Middle East Technical University, and (ii) from laboratory data collected from the published literature. To evaluate the possible importance of the nonlinearity of residual shear strength envelope for geotechnical engineering practice, by using limit equilibrium method, (1) a number of case histories of reactivated landslides are analyzed and (2) a parametric study is carried out. The findings in this study can be useful in proper evaluation of stability of existing slopes and to propose effective remedial measures.

CHAPTER 2

LITERATURE REVIEW

2.1 Shear strength of soils

Shear strength of the soil originates from combination of available normal stress, internal friction angle and cohesion of the soil particles. Coulomb in 1776 showed that these parameters are in a linear equation, Eq.2.1, which creates a boundary for illustration of failure in different stress states. Failure occurs when a combination of shear and normal stress exceeds the failure envelope.

$$\tau = c + \sigma . \tan \varphi \tag{2.1}$$

Where τ is shear stress, c is cohesion, σ is normal stress and φ is the angle of friction of the soil.

Culmann (1866) illustrated the stress states in a graphical method, which was developed further by Mohr (1882). In this method, the stress states in different planes of the soil can be calculated from the circles. Figure 2.1 depicts the stress circle, rupture line and the relation between the angles of different planes and internal friction angle of the soil particles.

When the soil is saturated the effective stresses must be considered, effective stress is the stress carried by soil particles. Consequently, for these circumstances the Eq.2.1 would be modified as follows;

$$\tau = c + (\sigma - u) . \tan \varphi = c + \sigma' . \tan \varphi \tag{2.2}$$

Where u is the pore water pressure and σ' is the effective stress

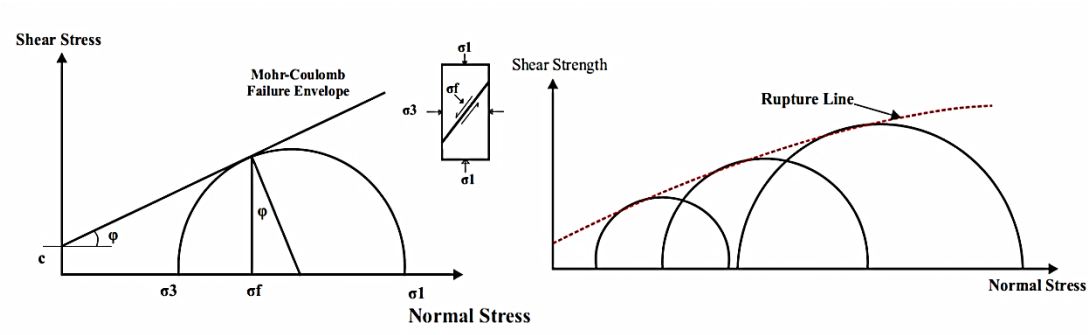

Figure 2.1 Mohr-Coulomb failure envelope (After Terzaghi et al, 1966)

2.2 Shear strength of saturated cohesive soils in drained conditions

In drained conditions, excess pore water pressure is not generated. Consequently, in all conditions total stresses are the effective stresses. Studies have shown that drained shear strength of saturated cohesive soils depends on different factors such as mineralogy, clay size fraction and magnitude of effective normal stress on the failure plane (Mesri and Cepeda-Diaz 1986, Dewoolkar and Huzjak 2005, Mesri and Shahien 2003). Normally consolidated and overconsolidated clays have different shear strength behaviors in drained conditions. A clay is called overconsolidated when it experienced an effective vertical pressure larger than the current overburden pressure (Skempton 1964). Lower void ratio before shearing in overconsolidated clays results in higher peak shear strength in comparison to normally consolidated clays (Terzaghi et al. 1996). In slope failures, mobilized drained shear strength may be the intact, fully softened, or the residual shear strength.

Intact or peak shear strength is the strength mobilized in overconsolidated clay, which remains in the same state as it was during geological alteration of overburden loads, in unloading phase. Available intact shear strength and its envelope are strongly dependent on the preconsolidation pressure and overconsolidation ratio as well as the amount of fissures and softening in the clay. The strength mobilized in highly fissured and jointed conditions without the presence of pre-existing shear surfaces where the plate shaped clay particles are starting to be oriented in horizontal direction is called fully softened shear strength. After passing the peak strength an overconsolidated clay shows a dilation behavior (trend of increasing its volume), during this time clay takes water in through the fissures/cracks, and softens. Fully softened strength corresponds to the time when no further volumetric change is observed. Fully softened shear strength is more or less equal to the shear strength of a normally consolidated clay with the same composition (Terzaghi et al. 1996, Mesri and Shahien 2003).

After passing the peak shear strength, in larger strains, decrement of shear strength which is known as strain-softening is limited to a residual shear strength which has been investigated by pioneer researches such as Tiedemann (1937), Hvorslev (1937), Skempton (1964, 1985), Bishop et al. (1971). Role of residual strength in stability analysis and measurement of residual parameters have been studied in more detail by recent researches such as Mesri and Cepeda-Diaz (1986), Stark and Eid (1992), Stark (1995, 1997), Stark et al. (2005), Stark and Hussein (2010), Mesri and Huvaj (2012) etc. They have developed some empirical correlations between different soil index properties and residual shear strength parameters of the soil in addition to experimental and analytical verification of the shear characteristics of clays that have been provided by previous studies.

Figure 2.2 illustrates shear characteristics of clay under constant normal stress presented by Skempton (1964). This figure also shows the trend of change in water content of the soil sample during the drained shear test. According to Skempton (1964), water content reaches to a constant value in residual state, and there is no further reduction in strength.

2.3 Residual shear strength of clays

In slope failures where the peak and fully softened strength is passed due to large displacements the shear strength reduces. Due to reactivation of pre-existing shear surfaces where clay particles are fully oriented in horizontal direction (as in a slickensided shiny surface), the mobilized shear strength would be in the residual strength level (Skempton 1964, 1985). Figure 2.3 shows some examples of slickensided surfaces observed in the slopes. It is well known that the residual shear strength is the mobilized shear strength in reactivated slope failures where there are pre-existing shear surfaces. As stated by Skempton (1964) and Mesri and Shahien (2003), residual shear strength also exists along the horizontal/sub-horizontal basal portion of the shear surfaces (including bedding planes, laminations, or other stratigraphic and structural discontinuities) of the first-time natural or excavated

slope failures in stiff clays and clay shales. This was a major finding since it says that even in first-time sliding slopes, there could be a portion in the slip surface that is at residual shear strength. Therefore the importance of accurate measurement and correct understanding of residual shear strength is increasing.

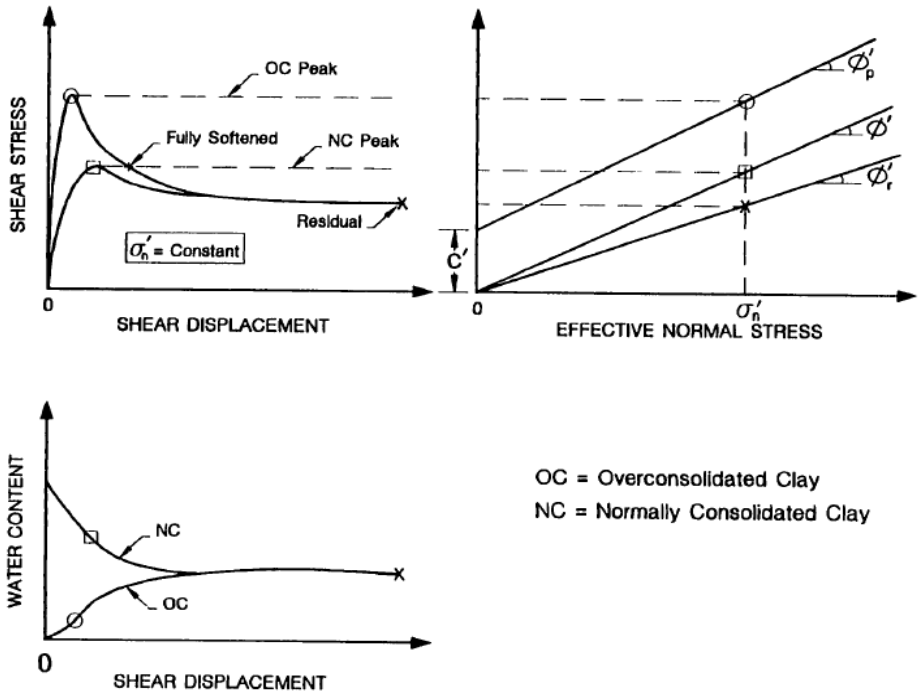

Figure 2.2 Shear characteristics of clays (Skempton 1964, Skempton, 1985, Eid 1996)

It is well established in the literature that there is no shear strength at zero effective normal stress (i.e. cohesion is zero) for the drained residual shear strength (Bishop et al. 1971, Morgenstern 1977, Stark and Eid 1994, Terzaghi et al. 1996). The relationship between shear strength and effective normal stress is curved (Mesri and Shahien 2003, Stark et al. 2005). Relationship between effective normal stress and secant residual friction angle is nonlinear (curved), especially at low effective normal stress range, and one of the earliest studies that illustrates this is the ring shear test results of Bishop et al. (1971) carried out at Imperial College. Therefore, in residual state condition, the cohesion of the soil is equal to zero and the shear strength is defined in terms of the residual friction angle as shown in the equation bellow;

$$\tau_r = \sigma' \tan \varphi_r' \tag{2.3}$$

Where φ_r' is the residual friction angle σ' is the effective stress.

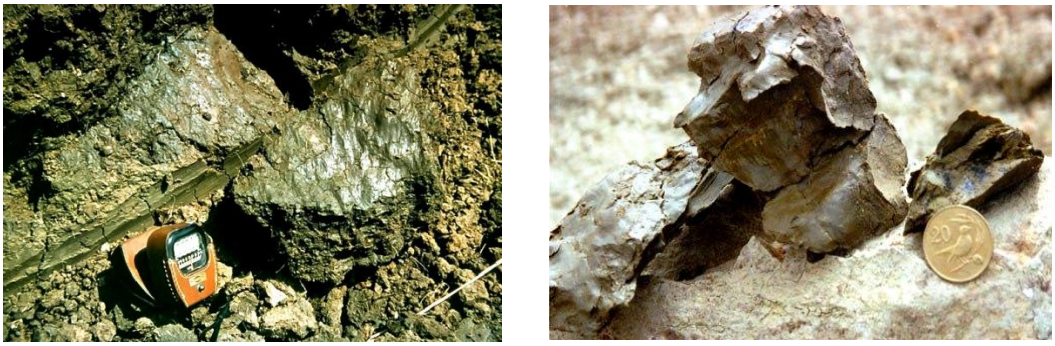

(a) (b)

Figure 2.3 Slickensided surface observed in shear surface (a) University of Idaho College of Agricultural and Life science‘s website (b) British Geological Survey, landslides in Cyprus.

2.3.1 Laboratory measurement of drained residual strength of clays

In the laboratory, residual shear strength is measured by different setups such as direct shear box, triaxial test and ring shear test setups. In each of these setups residual shear strength is investigated under various normal loads, shearing speeds and sample preparation methods for different types of soils. Samples can be “intact specimens” which does not contain a shear surface, or they can be “shear surfaces”. Intact specimens can be either “undisturbed sample” taken from the field, or “reconstituted/remolded sample” prepared in the laboratory. The “shear surface” specimens may be shear surfaces taken from a real landslide shear surface from the field, or they can be reconstitutes/remolded specimen with a pre-cut surface prepared in the laboratory.

2.3.1.1 Intact undisturbed sample (without a shear surface) taken from the field (Direct shear test)

Skempton (1964) conducted tests on intact clay samples and stated that forming the shear surface in the sample without pre sheared surface (remolded sample) needs a shear displacement of 1 to 2 inches to reach residual shear strength after the peak. Consequently, Skempton (1964) proposed the reversal direct shear tests. In reversal direct shear tests after one cycle of shear displacement direction of the box is reversed and the box is brought back to its original position and the sample is re-sheared in the same condition. However, in later years ring shear devices were developed and adopted as well.

Skempton (1964) is one of the earliest fundamental studies defining residual shear strength and its measurement. Figure 2.4 shows the results of reversal direct shear test conducted by Skempton (1964). In this series of tests residual parameters and residual failure envelope are measured under different normal stresses.

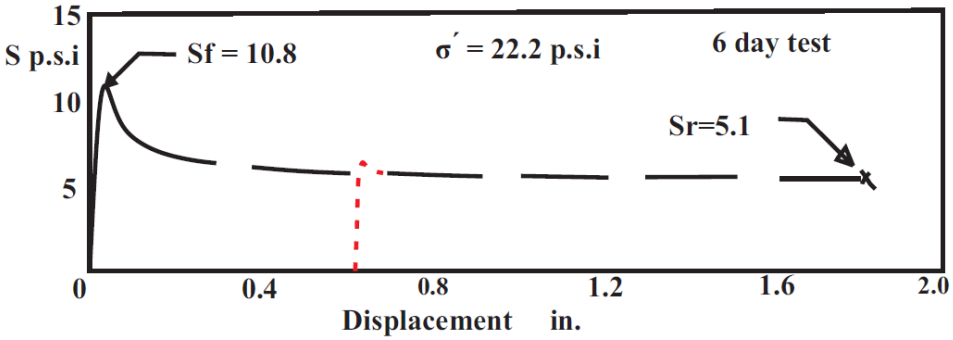

Figure 2.4 Reversal direct shear test results with about 1.8 inch of shear displacement (Skempton 1964)

2.3.1.2 Shear surface sample taken from a natural landslide slip plane (Direct shear test)

Skempton and Petley (1967), tested in direct shear test setup intact stiff clay sample in which there were existing slickensided discontinuities. Comparing the intact residual shear strength test and the test results on the samples with discontinuities Skempton and Petley (1967) concluded that the residual shear strength along slip surface is more or less equal to the residual strength the obtained from the tests without shear surface. In addition they found that the amount of clay-size fraction in slickensided surfaces are greater than the soil portion adjacent to the shear surface. Figure 2.5 shows the test results on intact specimens with and without precut surfaces conducted by Skempton and Petley (1967).

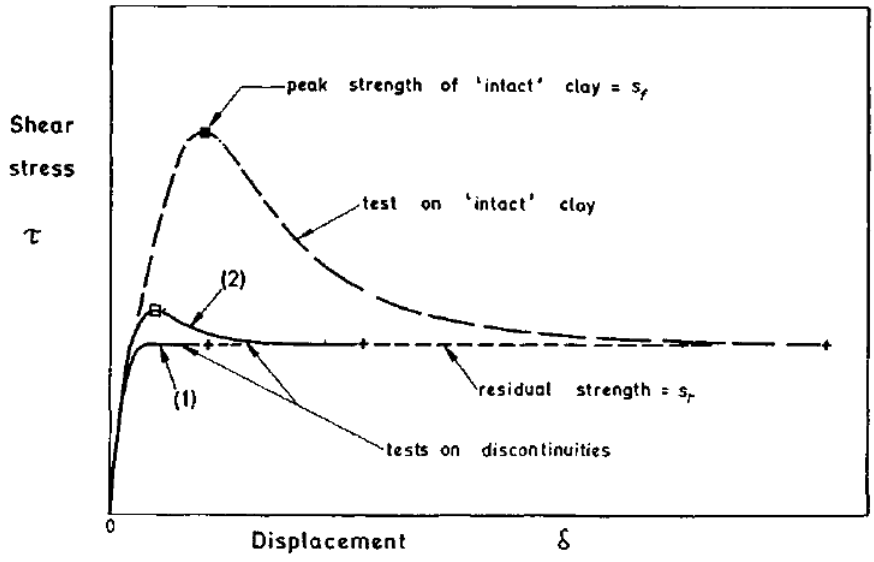

Figure 2.5 Shear stress versus displacement resulted from direct shear test on intact clay and on pre-sheared surface, Skempton and Petley (1967).

2.3.1.3 Shear surface sample prepared in laboratory from reconstituted/remolded specimen by precutting a shear surface (Direct shear test)

Meehan et al. (2010) compares a set of drained ring shear test results with wire-cut reconstituted direct shear test specimens. In these set of experiments Meehan et al. (2010) utilized different soil types and different approaches for creating slickensided shear surfaces to compare the results with ring shear test data with purpose of evaluating the direct shear test results and shear surface forming methods. Meehan et al. (2010) created the slickensided surface in three different methods. They polished the wire-cut surface against the glass plate in wet and dry conditions in addition to polishing against a Teflon plate in dry conditions. The results showed a high sensitivity of the residual shear strength parameters in different soil types and utilized shear surface preparation techniques. Figure 2.6 illustrated three different shear surfaces prepared by Meehan et al. (2010).

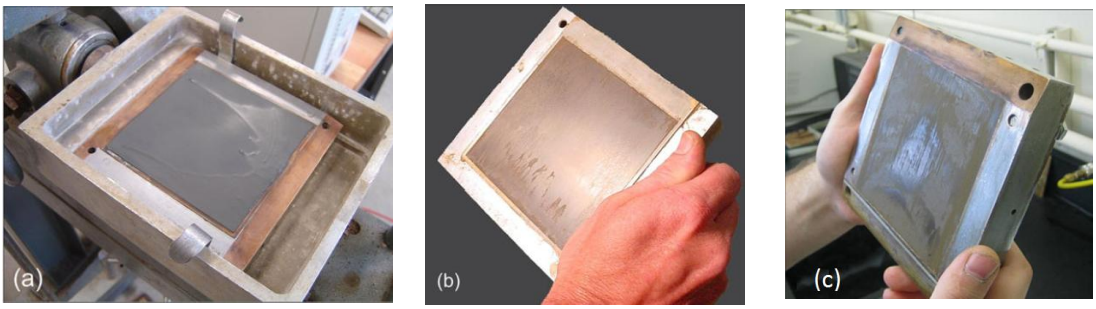

Wet glass Dry teflon Dry glass

Figure 2.6 Shear surface formation (Meehan et al, 2010)

The remolded samples can be pre-cut before the shearing stage to form the failure plane. Mesri and Cepeda-Diaz (1986) proposed a method for creating an overconsolidated remolded precut sample. In their method each part of the conventional direct shear box which is filled with the reconstituted soil paste is consolidated under a load higher than the shearing normal stress. In consolidation stage each face of the failure surface (i.e. the bottom face of the soil placed in the upper half of the shear box, and the upper face of the soil placed in the lower half of the shear box) are placed on a Tetko polyester filter paper that is supported by a smooth Teflon plate. After the samples in two halves of the direct shear box are consolidated to the maximum vertical pressure, the samples are unloaded to the pressure they are to be sheared. Then the two halves of the shear box are assembled together and the shearing normal stress is applied. The shear surface located between the two halves of the shear box was sheared at a slow rate. This sample preparation method has also been used by Huvaj-Sarihan (2009) successfully to obtain the residual shear strength of stiff clays.

2.3.1.4 Intact reconstituted/remolded specimen prepared in laboratory without a shear surface (Direct shear test)

Due to the difficulty of obtaining a naturally sheared surface from the boreholes or other methods of sampling, in the experimental studies shear surface can be formed artificially in the laboratory by continuously shearing a reconstituted specimen (La Gatta 1970). In this method the soil is prepared in the paste form an is placed (remolded) in the direct shear box setup. Enough horizontal displacements must be provided to form a shear surface and reach the residual shear strength. For instance, Kenney

(1967, 1977) conducted multiple reversal direct shear box tests on a 'smear' sample of remolded Cucaracha Shale.

2.3.1.5 Shear surface sample taken from a natural landslide slip plane (Triaxial)

Bishop and Henkel (1962) were the pioneers of using triaxial setup in residual direct shear test measurement. In triaxial testing the intact specimen without preformed shear plane could not be used for residual strength measurement due to the limited shear displacement in triaxial specimens.

In addition to multi reversal direct shear tests on intact specimen, Skempton (1964) conducted a set of triaxial tests on a clay sample collected from Walton's Wood landslides. In the samples there were existing natural shear planes. Skempton (1964) prepared triaxial samples in such a way that the shear surface of the trimmed sample was inclined at 50 degrees to the horizontal direction. As shown in the figure 2.7 the obtained results from the triaxial test correspond very closely to the results attained from intact direct shear test experiments. Skempton and Petley (1967) also conducted a set of triaxial test based on the procedure provided by Skempton (1964) ..

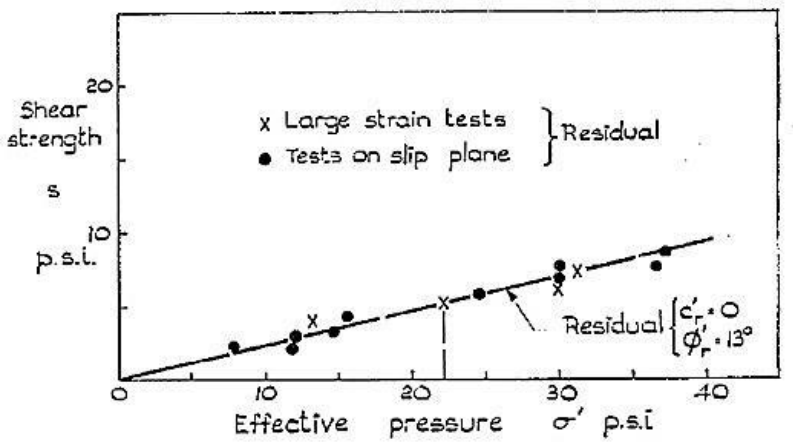

Figure 2.7 Laboratory shear strength tests including shear surface (Skempton 1964)

Meehan (2006) did not recommend triaxial tests for measurement of residual shear strength along pre-formed shear surfaces. Anayi et al. (1988) noted that triaxial test is not suitable for measuring residual strength because of the complex stress distribution across the failure plane that is produced after the test is continued beyond the peak resistance.

2.3.1.6 Shear surface sample prepared in laboratory from reconstituted/remolded specimen by precutting a shear surface (Triaxial)

Following the approach presented by Bishop and Henkel (1962), Chandler (1996) carried out the residual strength measurement test in triaxial setup. Chandler (1996) prepared a remolded and precut specimen in the test. In addition, he developed some corrections for the shearing area of the sample and the effect of membrane. In Chandler (1996)'s experiments, using a mechanism of ball bearings between the top cap and the loading ram provided an even pressure in the shear plane during the shear.

Later on, pre-forming the shear plane in triaxial is utilized by Tiwari (2007) in measurement of the tertiary mudstones residual shear strength parameters. Tiwari (2007) also used ball bearing mechanism in the triaxial setup and remolded precut sample. Meehan et al. (2011) also used the same

triaxial setup and the same sample preparation method and compared the obtained residual strength data with a series of ring shear test tests and reversal direct shear tests with slickensided surfaces to verify the triaxial experiment results. Meehan et al. (2011) concluded that there were noticeable discrepancies between the triaxial, reversal direct shear test and ring shear test results as shown in the figure 2.8 the triaxial test results carried on Rancho Solano Clay by Meehan et al. (2011) were much higher than the ring shear and direct shear results.

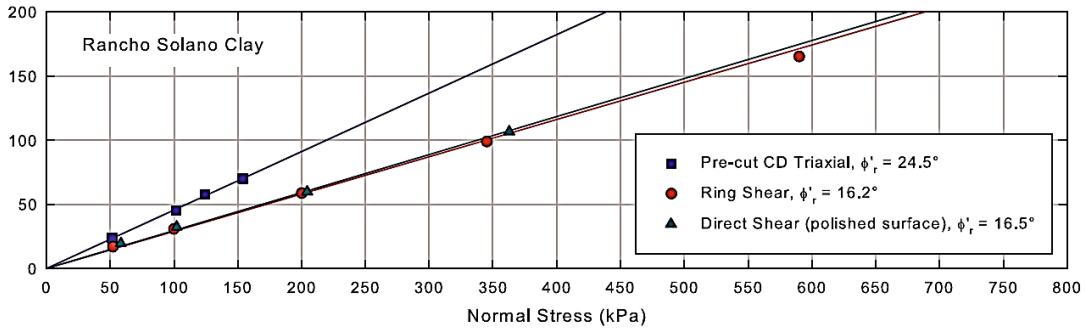

Figure 2.8 Meehan (2011) test results

Figure 2.9 illustrates the setup details and the sample preparation methods utilized by Tiwari (2007) and Meehan et al. (2011).

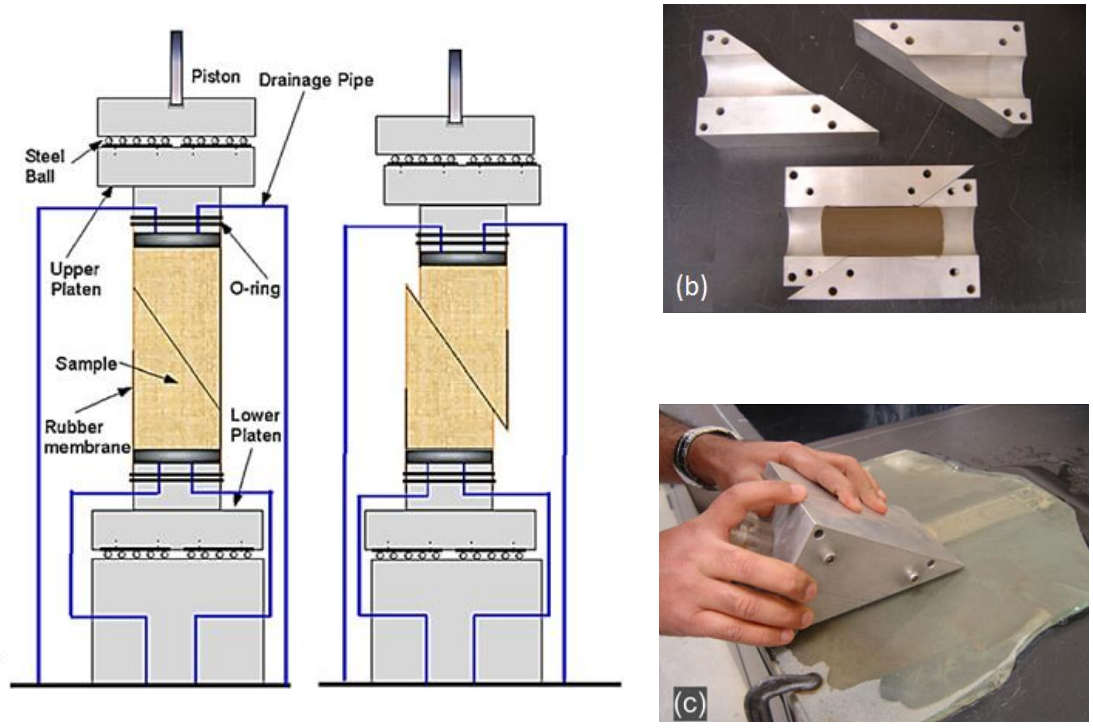

(a)

Figure 2.9 Triaxial test setups, Tiwari (2007), Meehan (2011)

2.3.1.7 Ring Shear Test

Even though torsional ring shear test developed by earlier researches such as Hvorslev (1939), Haefeli (1951), Bishop et al. (1971) and La Gatta (1970) was one of the best methods for measurement of residual parameters, it has a complicated sampling and testing procedures. Bromhead (1979) developed a simplified and robust ring shear device that has become widely used by the researchers as well as in the practical geotechnical enginerring works. Stark and Vettel (1992) investigated the effect of test procedures and proposed some modifications on the Bromhead's ring shear test. Later on, Stark and Eid (1994) modified the specimen container of Bromhead ring shear apparatus which would minimize the settlement of the top platen in addition to minimizing the horizontal displacement required to reach a residual state by allowing remolded, overconsolidated and precut specimen preparation in the setup.

2.3.2 Effect of shear rate on residual shear strength of clays

Increase in residual shear strength by increasing the shearing rate was first investigated by Skempton (1985) for Kalabagh dam project. In this project Skempton (1985) tested Kalabagh dam clay in a ring shear tests at different shearing rates to measure the residual strength in fast shear rates. Initial shearing was done at a slow rate in the order of 0.01 mm/min to form the shear surface in the soil body. In the next steps the test was carried out at higher rates of 10, 100, 400 and 800 mm/min with a slow shearing step in between each fast rate as shown in figure 2.10. Skempton (1985) concluded that probably the shearing mechanism in higher rates would change from "sliding shear" to a "turbulent" stage in which the particles that are oriented parallel to the plane of displacement would be reordered leading to an increase of the shear strength. In addition Skempton (1985) have taken the effect of dissipation of the generated negative pore pressure in the body of the soil sample into account as a reason of shear strength decrement.

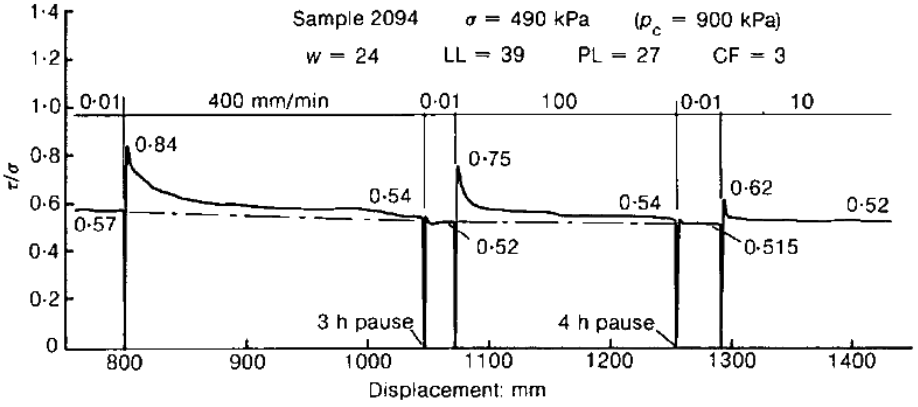

Figure 2.10 Ring shear test on Kalabagh dam, Skempton (1985)

Investigating the shear strength changes at different shearing rates is continued by Lemos et al. (1985) that resulted in four main observations which are illustrated in the figure 2.11. Lemos et al. (1985) concluded that after formation of the shear plane in slow shear by entering the fast shearing stage a peak strength appears which is defined as "fast maximum" strength. The quantity of the fast maximum strength depends on the shearing rate and by increasing the displacement it reduced to a value which is defined as "fast minimum" strength. By transition to slow shearing stage a peak strength known as "slow peak" is observed. Based on the theories of Skempton (1985), slow peak is the result of change in the particle orientation caused by fast shearing.

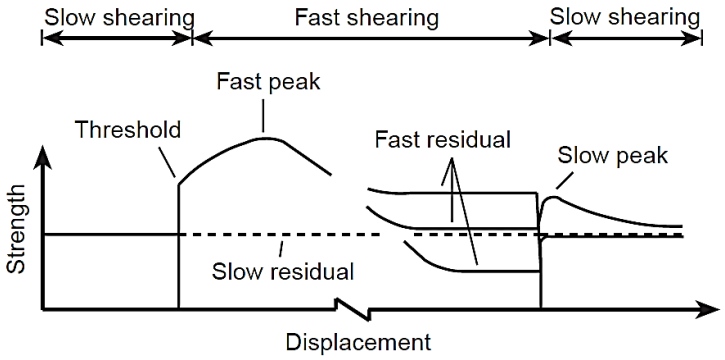

Figure 2.11 Rate dependent changes in shear strength tests, Tika et al. (1996), Tika et al. (1999)

Tika et al. (1996), Tika et al. (1999) also performed a set of ring shear tests in Imperial College (IC) and Norvegian Geotechnical Institute (NGI) ring shear apparatus and observed three different rate effects in the fast shearing phases as shown in Figure 2.12. These three rate effects defined positive, neutral and negative effects, which is a high, equal and lower strength in comparison to slow residual shear strength that is observed in fast shearing stages (Tika et al. 1999). Tika et al. (1996) mentioned that these variations of the shear strength are due to the shear mode of the soils. Lemos (2003) carried out a laboratory investigation on the effect of fast shearing rate on the residual strength of soil. Negative rate effect is described based on the increase in void ratio and water content in the shear zone.

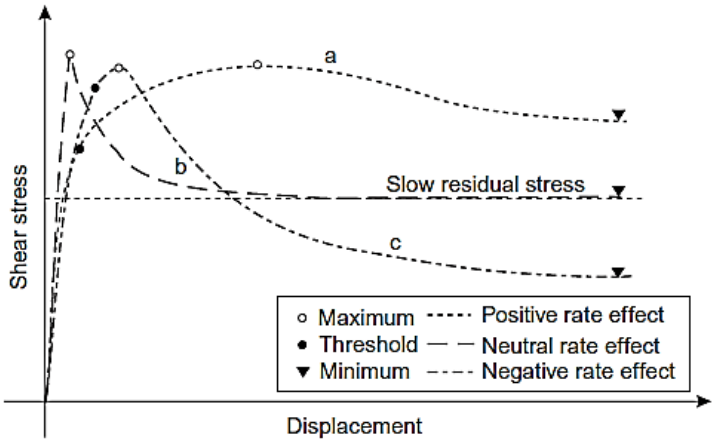

Figure 2.12 Variations of the shear strength in fast shearing (Lemos 2003, Grelle & Guadagno, 2010)

2.3.3 Effect of over consolidation on residual shear strength of clays

Residual shear strength of stiff clays have been shown to be independent of the stress history, overconsolidation ratio and sample preparation because during shear the soil particles adjacent to the slip surface would be reoriented parallel to the direction of shearing (Bishop et al. 1971, Skempton 1964, 1985, Lupini 1981, Stark et al. 2005).

To confirm the negligible effect of overconsolidation ratio experimentally, Vithana et al (2009, 2012) conducted a set of ring shear test on the soil samples obtained from two landslides in Japan. They tested the soils under four over-consolidation ratios (OCR 2, OCR 4 and OCR 6). Vithana et al. (2009,

2012) reported non-significant and minor differences in the residual shear strength parameter due to change in overconsolidation ratios. Residual shear strength is a condition that can only develop in stiff overconsolidated clays, not in normally consolidated (soft) clays. Therefore laboratory tests should be done on overconsolidated samples. The degree of overconsolidation (i.e. the overconsolidation ratio, OCR) does not influence the residual shear strength parameters, i.e. in Morh envelope the cohesion intercept is always zero and residual friction angle does not depend on the OCR value given that the OCR is greater than 1.0. It was also well accepted in the literature that the residual shear strength is independent of stress history (Skempton 1964, Petley 1966, Bishop et al. 1971, Townsend and Gilbert 1976, Morgenstern 1977). Therefore using remolded samples as well as undisturbed samples in laboratory residual shear strength tests is possible. Mesri and Gibala (1972) noted that the residual shear strength of a shale was not influenced by the method of remolding, and that slaked remolded and pre-cut intact specimens gave the same residual friction angle.

2.3.4 Empirical Correlations of residual parameters

Residual shear strength of clays are proved to be controlled by the type and amount of minerals and the properties which is originated from the mineral type, shape and quantities such as index properties and clay-size fraction. Concerning the time and finance needed for soil testing for measurement of residual shear strength of the soils, some researchers have developed correlations between various index properties of the soil and residual shear strength parameters based on the available test data which gave good estimation for the strength parameters (Skempton 1964, 1985, Chandler 1969, Voight 1973, Lupini et al. 1981, Mesri and Cepeda-Diaz 1986, Collota et al. 1989 , Stark and Eid 1994, Mesri and Shahien 2003, Tiwari and Marui 2005, Tiwari and Ajmera 2011, Hatipoglu 2011). Clay particles can hold water since they have high surface area and net negative surface charge. Liquid limit and plasticity index indicates a clay's ability to hold water. As the clay particles become more platey (such as montmorillonite) the particle surface area per unit weight increases and the liquid limit and plasticity index increase. Secant residual friction angle $(\phi'_r)_s$ is also related to particle size and plateyness of particles (Mesri and Cepeda-Diaz 1986). It should be noted that such empirical correlations will not be applicable for clays that have not plate-shaped clay minerals, e.g. attapulgite, and allophane. (Chandler 1984a; Mesri and Cepeda-Diaz 1986; Terzaghi et al. 1996).

Skempton (1964) by collecting some available shear strength and index properties of a number of soils stated that there is a tendency to decrease in residual friction angle of clays with higher clay-size fractions as illustrated in figure 2.13.

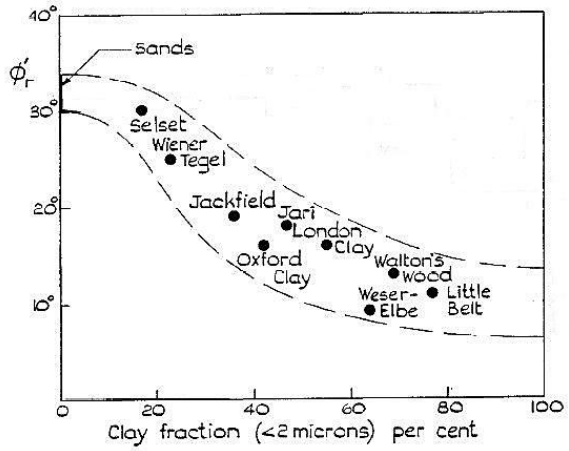

Figure 2.13 Correlation between clay-size fraction and residual friction angle (after Skempton 1964)

Voight (1973) found that the plasticity index is a good material property to estimate the residual shear strength and by collecting the shear strength test data from the literature from different localities and recommending further investigations he illustrated the correlation as shown in Figure 2.14.

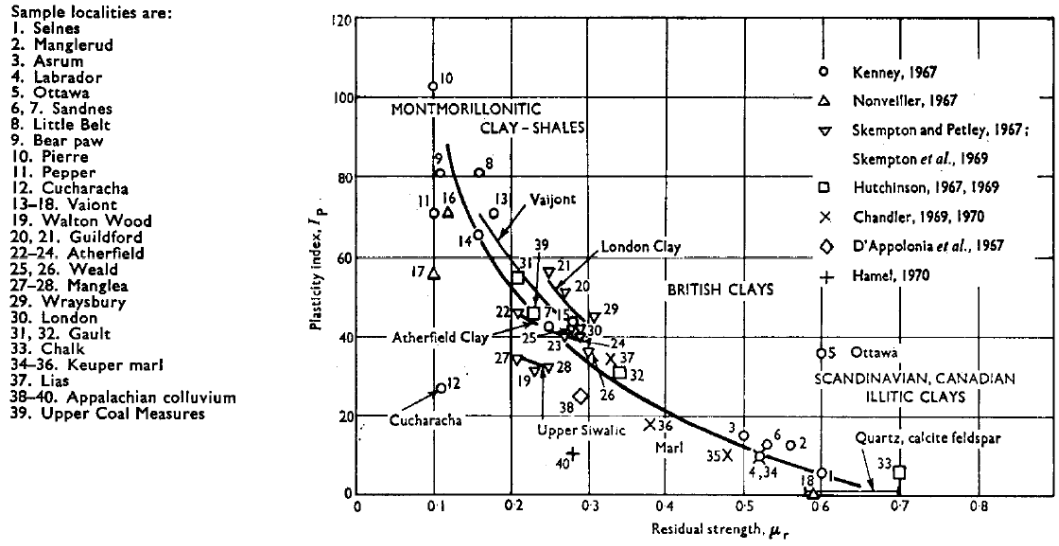

Figure 2.14 Correlation between clay-size fraction and residual friction angle (Voight 1973)

Colloeta et al. (1989) conducted extensive laboratory tests in direct shear and ring shear test setups on more than 150 samples from 20 Italian sites an developed a new correlation for residual friction angle of cohesive soils. Colloeta et al. (1989) proposed the correlation that less steep and less scattered than previous studies and related residual friction angle to liquid limit (LL), clay-size fraction (CF) and plasticity index (PI) of the soil (Eq. 2.4 and 2.5)

$$\emptyset_r' = f(CALIP) \tag{2.4}$$

Where $$CALIP = (\overline{CF})^2 \times LL \times PI \times 10^{-5} \tag{2.5}$$

The correlations proposed before Stark and Eid (1994) were based on one soil index property and the change in the normal stress was not taken into account. Stark and Eid (1994) developed a correlation between residual friction angle which was also dependent on soil index properties as well as effective normal stress which is depicted in Figure 2.15.

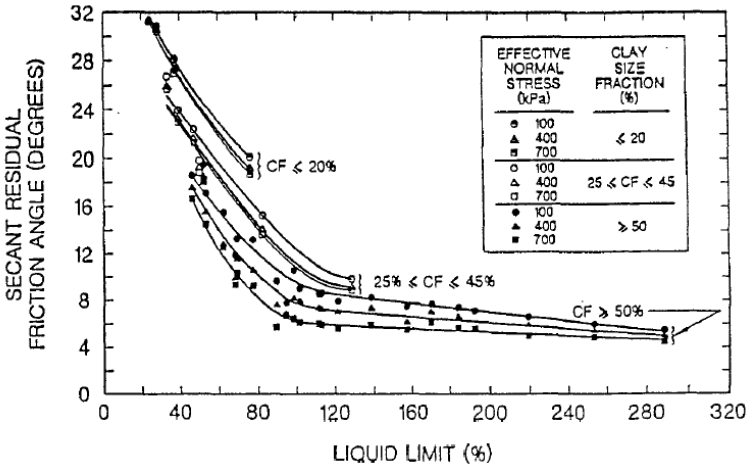

Figure 2.15 Correlation residual friction angle proposed by Stark and Eid (1994)

Mesri and Shahien (2003) also provides a correlation between secant residual friction angle and the plasticity index of stiff clay and developed charts for effective normal stress of 50, 100 and 400 kPa. Mesri and Shahien (2003) proposed nonlinear residual shear strength envelopes as shown in equation 2.6.

$$s(r) = \sigma'_n \tan[\emptyset'_r]_s^{100} \left[\frac{100}{\sigma'_n}\right]^{1-m_r} \tag{2.6}$$

Where $\tan[\emptyset'_r]_s^{100}$ is secant residual friction angle at $\sigma'_n = 100$ kPa.

Tiwari and Maroui (2005) investigated the correlation of the shear strength parameters with mineralogical composition by reconstituting 35 different mixtures from kaolinite, smectite and quartz in addition to collected samples from 80 natural soil sites which contain target minerals. Tiwari and Maroui (2005) stated that proposed correlation based on the amount and type of minerals has less errors in estimating the residual friction angle.

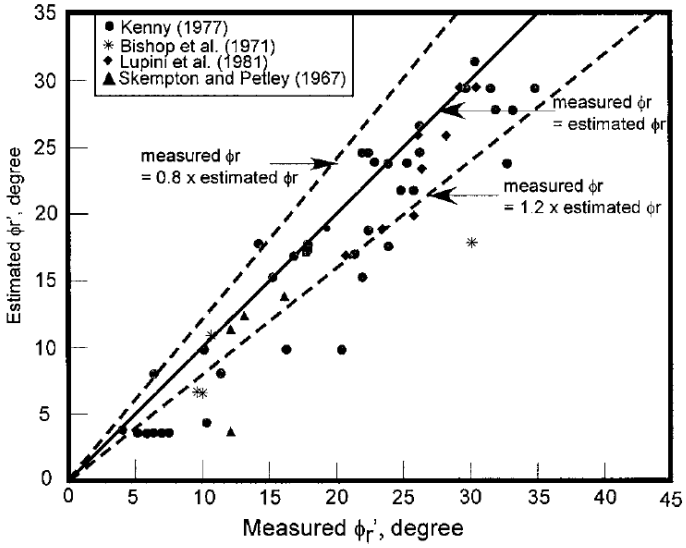

Figure 2.16 Verification of the proposed correlation in cases from the literature (Tiwari 2005)

Tiwari and Maroui (2005) also verified their correlation by comparing the measures and estimated data from available cases in the literature. Figure 2.16 illustrates the verification of the proposed method in case histories.

2.4 Nonlinearity of failure envelope

According to previous experimental studies in the literature, residual shear strength of almost all soil types are non-linear (Figure 2.17 a) but due to its simplicity shear strength envelope of the soil are defined by the Mohr-coulomb failure criterion which is a linear function. The nonlinearity of the shear strength failure envelope and its effect on engineering problems have been investigated by several researches (Bishop et al. 1971, De Mello 1977, Lefebvre 1981,Maksimovic 1989, Perry 1994, Stark and Eid 1994, Mesri and Shahien 2003, Baker 2004, Yang and Yin 2004, Li 2007, Wright 2005, Nusier et al. 2008, Noor and Derahman 2011). The curvature of the nonlinear failure envelope can be addressed by an equivalent linear line, a curve (power) function or secant friction angles. Utilizing a power function and secant friction angles would accurately show the stress dependent values of the internal friction angle (Wright 2005, Stark and Eid 1994). Mesri and Shahien 2003 also states that the relationship between effective normal stress and secant residual friction angle is nonlinear (curved), especially at low effective normal stress range, and one of the earliest studies that illustrate this is the ring shear test results of Bishop et al. (1971) carried out at Imperial College. Available residual shear strength of soils such as Bishop et al. (1971)'s tests on Brown London clay sample from Walthamstow on lower normal stress ranges (Figure 2.17b) shows that the cohesion of the soil is equal to zero in residual condition. All of the aforementioned empirical correlations that estimate the residual secant friction angle can be applied in defining the stress dependent failure envelope.

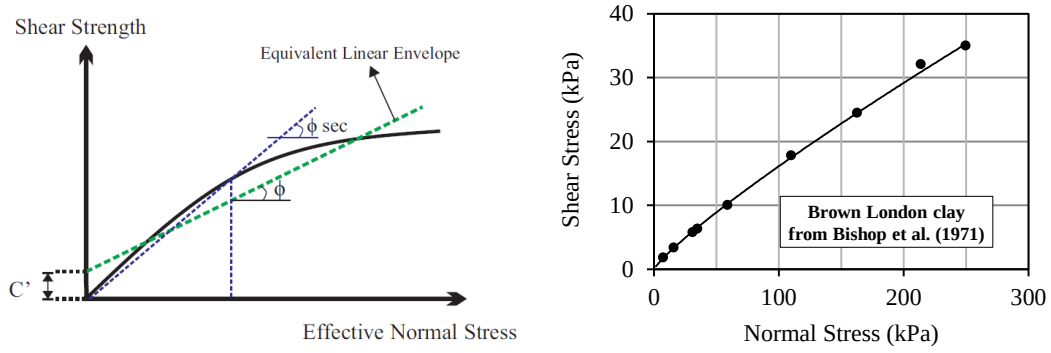

(a) (b)

Figure 2.17 Nonlinearity of failure envelope (a) a typical sketch (b) residual shear strength test results conducted on Brown London clay sample from Walthamstow by Bishop et al. (1971)

The amount of nonlinearity observed in small normal stress ranges is more significant than at larger normal stresses (Baker 2004). In geotechnical problems such as slope stability, nonlinearity of the failure envelope plays a major role in stability analysis due to existence of various normal stresses ranges. Various nonlinear function types have been utilized by the researchers to define the curvature of the failure envelope such as bilinear and tri-linear functions (Baker 2004, De Mello 1977, Lefebvre 1981). Maksimovic (1979, 1988, 1989) states that the hyperbolic functions could describe the nonlinear failure envelopes within a wide stress ranges. Perry (1994) fits power curve on the failure

envelopes to be used in a slope stability method based on the Janbu's rigorous method of slices. The utilized power function has the form of $\tau = A\sigma^b$ in which A and b are the properties of the material (Perry 1994, Nusier et al. 2008). The function's behavior is investigated in the Figure 2.18 by the change of the power b and coefficient A.

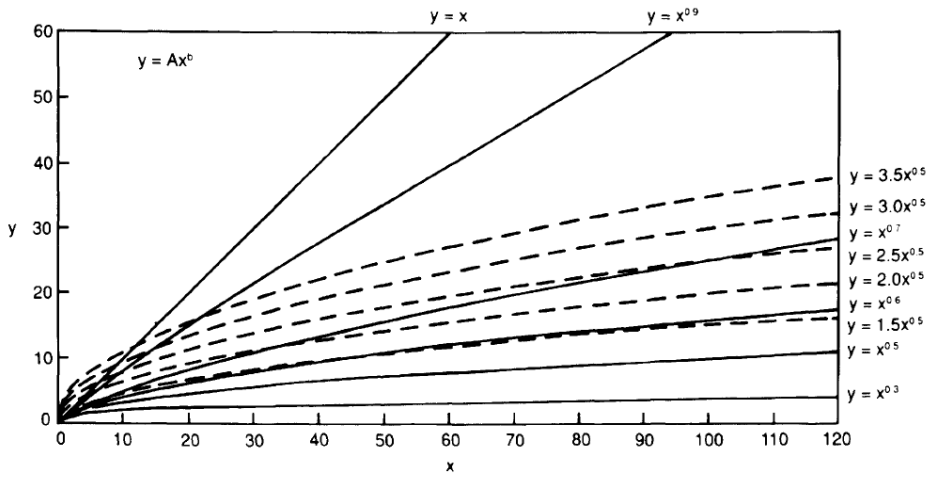

Figure 2.18 Behavior of the function by changing A and b (Perry 1994)

In the nonlinear curve the secant friction angle is a function of stress and material properties as shown in the following equations.

$$\tau = A\sigma^b \tag{2.7}$$

$$s(r) = \tan \emptyset'_{sec} \tag{2.8}$$

$$A(\sigma')^b = \tan \emptyset'_{sec} \tag{2.9}$$

$$A(\sigma')^{b-1} = \tan \emptyset'_{sec} \tag{2.10}$$

Following the above equations and base on the empirical data Mesri and Shahien (2003) developed the correlation in which the amount of curvature in the residual strength envelope is shown by m_r value.

Stark and Eid (1994) in addition to developing a correlation between residual friction angle and soil index properties investigated the amount of nonlinearity in residual failure envelope and its effect in the stability analysis. Stark and Eid (1994) stated that there is a significant nonlinearity in the cohesive soils with a liquid limit between 60% and 220% and the clay size fraction greater than 50%. In addition, Stark and Eid (1998) have investigated the effect of nonlinearity in 2D and 3D slope stability analysis methods in practice and concluded that the linear failure envelope would result in over estimation of the factor of safety.

Yang and Yin (2004), proposed and improved method of estimating the nonlinear failure envelopes of soils by utilizing a "generalized tangential" technique. They have presented the failure envelope by a tangential line, which is always tangential to the curve of a nonlinear failure criterion as shown in the Figure 2.18.

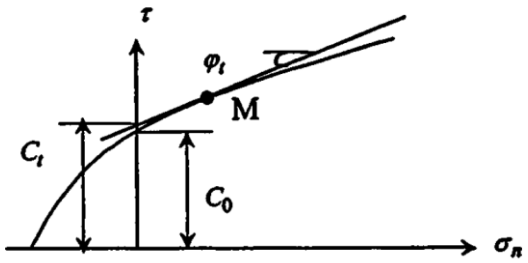

Figure 2.17 Nonlinear envelope presented by tangential line (Yang and Yin, 2004)

The tangential line is defined as

$$\tau = c_t + \sigma_n \tan \varphi_t \tag{2.11}$$

where φ_t is the tangential frictional angle; $c_t$is the intercept of the straight line on the shear stress axis; σ_n is the normal stress; and τ is shear stress. The determination of the intercept and the angle at point M in Figure 2.17 is presented in the equations 2.12 and 2.13.

$$\tan \varphi_t = \frac{1}{m\sigma_t} c_0 \left(1 + \frac{\sigma_M}{\sigma_t}\right)^{(1-m)/m} \tag{2.12}$$

$$c_t = \frac{m-1}{m} c_0 \left(\frac{m\sigma_t \tan \varphi_t}{c_0}\right)^{(1-m)/m} + \sigma_t \tan \varphi_t \tag{2.13}$$

Li (2007) have investigated the effect of nonlinearity in the shear strength failure envelope in finite element modeling of the slopes under earthquake loading and reported a significant influence of the nonlinearity on the stability analysis results.

The curvilinear nature of the shear strength envelope is confirmed by experimental studies such as the set of consolidated drained triaxial tests conducted by Noor and Derahman (2011) on granitic residual soil samples. Emphasizing the importance of nonlinearity at low normal stress ranges in shallow landslides, Noor and Derahman (2011)'s study contains low effective normal stress ranges to show the amount nonlinearity in that range. Noor and Derahman (2011) stated that the shear strength failure envelope is a combination of linear and nonlinear lines as illustrated in the Figure 2.18.

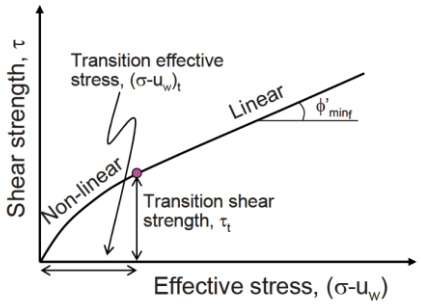

Figure 2.18 Curvi-linear failure envelope of saturated soil (Noor and Derahman, 2011)

CHAPTER 3

DATA FROM LITERATURE

In this chapter a set of available data of clay residual strength tests are collected. These data are reanalyzed and reinterpreted with the purpose of investigating the non-linearity of residual shear strength failure envelope in various clay materials. Here, residual shear strength of a number of different soils are presented in tables and both linear and nonlinear failure envelopes are provided in the following graphs.

3.1 Blue London Clay

Table.1 presents a set of drained multiple reversal direct shear box tests on undisturbed sample of Blue London Clay reported by Agarawal (1967). Later on, Bishop et al. (1971) introduced their modified ring shear apparatus and performed a set of ring shear tests on remolded and undisturbed Blue London Clay samples which has been obtained from Wraysbury, near Staines. The clay was extensively fissured clay with the mineralogy of quartz 30%, chlorite 10%, illite 35%, kaolinite 15%, montmorillonite 10%. Clay-size fraction of these samples was 57%. Bishop et al. (1971)'s test results on new ring shear apparatus are presented in Table 3.2. According to Bishop et al. (1971), even though their test results showed smaller values for residual strength parameters in comparison to reversal direct shear tests of Agarawal (1967), presented in Table 3.1, as the results were less scattered there was less possible error in the test procedure.

Table 3.1 Blue London Clay, Wraysbury (Agarawal, 1967).

LL%	PI%	Effective normal stress (kPa)	shear stress (kPa)	Secant residual friction angle (°)	residual friction angle (°)
82	59	51.7	15.8	17.0	13.5
		103.4	26.2	14.2	
		155.1	36.5	13.2	
		206.8	62.0	16.7	
		310.2	69.0	12.5	
		413.7	105.5	14.3	
		517.1	117.2	12.8	
		620.5	119.3	10.9	

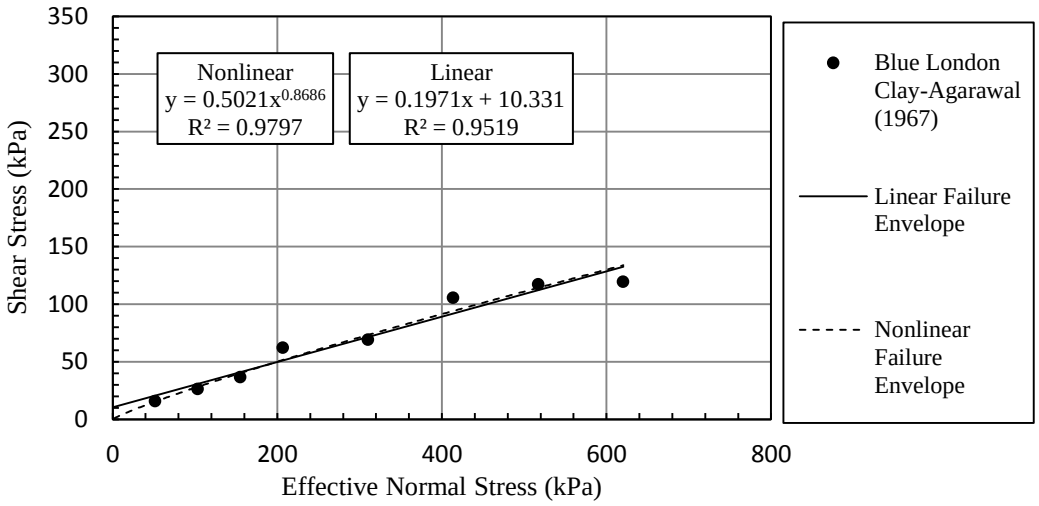

Figure 3.1 Failure envelope of Blue London clay, from reversal direct shear test of Agarawal (1967)

Table 3.2 Blue London Clay, Wraysbury, (Bishop et al, 1971).

LL%	PI%	Effective normal stress (kPa)	shear stress (kPa)	Secant residual friction angle (°)	residual friction angle (°)
		185.5	31.1	9.5	
		144.1	33.0	12.9	
72	43	82.0	13.6	9.4	9.4
		40.7	6.6	9.2	
		280.0	45.6	9.3	

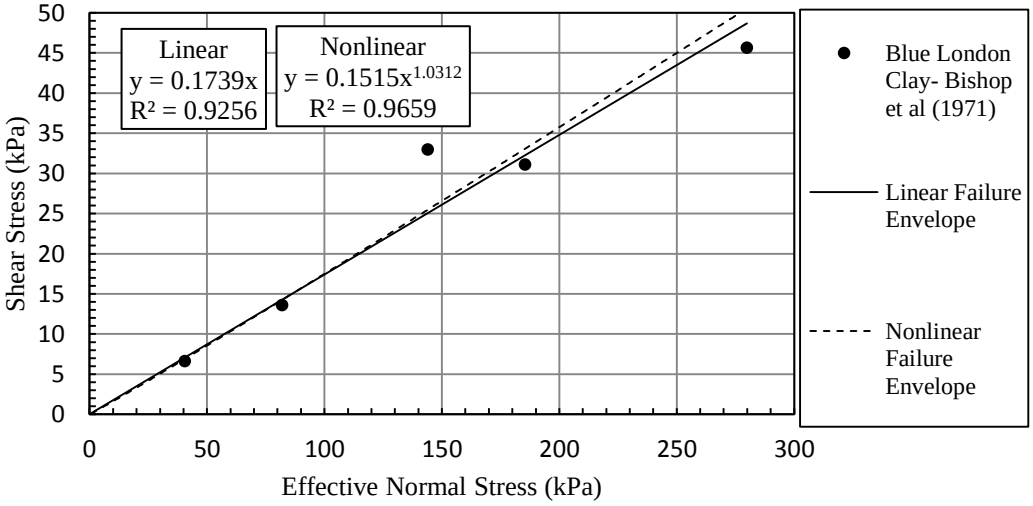

Figure 3.2 Failure envelope of Blue London clay from ring shear test of Bishop et al. (1971).

3.2 Brown London Clay

Another set of data reported by Bishop et al. (1971) contains reversal direct shear tests on undisturbed samples of brown London Clay from Hendon performed by Petley (1966) at Imperial College's laboratory. The soil's clay-size fraction is 60% and its liquid limit and plastic limit is 82 and 33 percent respectively. Table 3.3 summarizes the test data of Brown London clay and linear and nonlinear failure envelopes of residual shear strength are drawn in Figure 3.3.

Table 3.3 Brown London clay

Effective normal stress (kPa)	**shear stress (kPa)**	**Secant residual friction angle (°)**	**residual strength**
27.6	10.3	20.6	
34.5	13.8	21.8	
55.2	17.9	18	
82.7	29	19.3	
91	26.2	16.1	
122	27.6	12.7	
122	30.3	14	c =0.5 kPa
184.1	45.5	13.9	
184.1	48.3	14.7	φ =14.6°
184.1	55.2	16.7	
215.1	55.2	14.4	
215.1	62.1	16.1	
277.2	58.6	11.9	
277.2	62.1	12.6	
308.2	68.9	12.6	
308.2	82.7	15	

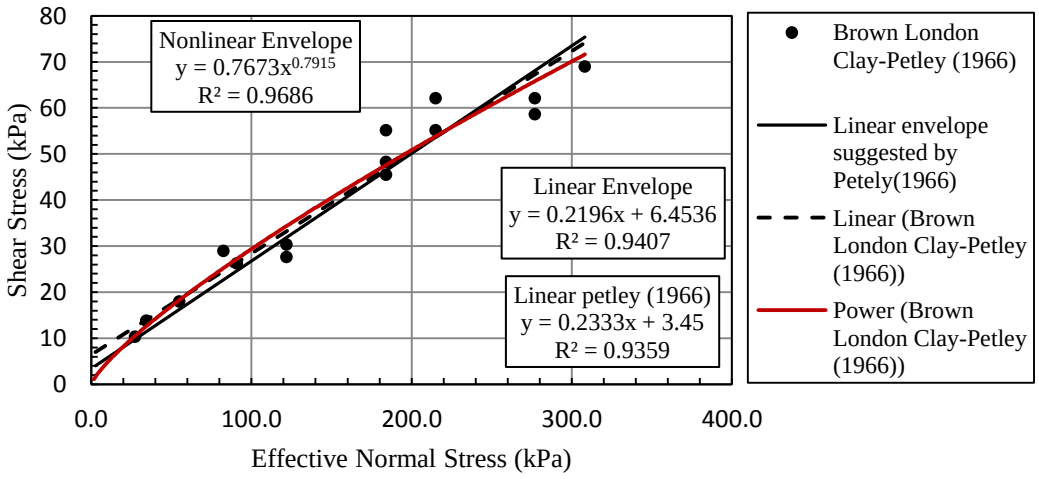

Figure 3.3 . Failure envelope of Brown London clay, (Petley, 1966).

3.3 Clay samples from Colorado

Dewoolkar and Huzjak (2005) have investigated residual shear strength of claystones from Colorado. They prepared the samples from seven different sites. The residual parameters of the clays have been measure by reversal direct shear test and torsional ring shear test setups. In this section the amount of nonlinearity in the residual shear strength failure envelopes are investigated in two of the seven sites.

3.3.1 Clay samples from Site 1

Site 1 samples are obtained from Rueter Hess dam and reservoir. The residual shear strength parameters of the samples from site 1 are measured by torsional ring shear test in the remolded samples which are prepared with the water content near the liquid limit of the soil and the shearing rate was in the range of 0.018 - 0.036 mm/min. In six samples the LL and PI are 81-82% and 55-56%, respectively and in the other six samples the LL and PI are 65-66% and 40-41%. Several researchers mentioned that the amount of nonlinearity of the residual shear strength envelope is related to the mineral type, and index properties of the clayey soils (Wright, 2005; Stark and Eid, 1994). The linear and nonlinear envelope of the residual shear strength of Claystones of site 1 is delineated in Figure 3.4 and 3.5 and the test data of the soil is summarized in Table 3.4 and 3.5.

Table 3.4 Residual shear strength tets data of Site 1 claystones (PI=55-56%) (Dewoolkar and Huzjak, 2005)

LL (%)	PI(%)	Effective Normal Stress (kPa)	Residual Shear Stress (kPa)	Residual friction angle (°)
81	56	70.4	23.9	18.7
81	56	287.7	56.5	11.1
81	56	559.3	96.2	9.8
82	55	70.4	25.9	20.2
82	55	286.3	58.4	11.5
82	55	556.4	97.7	9.9

Table 3.5 Residual shear strength test data of Site 1 claystones (PI=40-41%) (Dewoolkar and Huzjak 2005)

LL (%)	PI(%)	Effective Normal Stress (kPa)	Residual Shear Stress (kPa)	Residual friction angle (°)
66	40	69.9	22	17.5
66	40	283.9	63.2	12.5
66	40	552.1	102.5	10.5
65	41	70.4	22.5	17.7
65	41	286.3	59.9	11.8
65	41	557.3	104.9	10.7

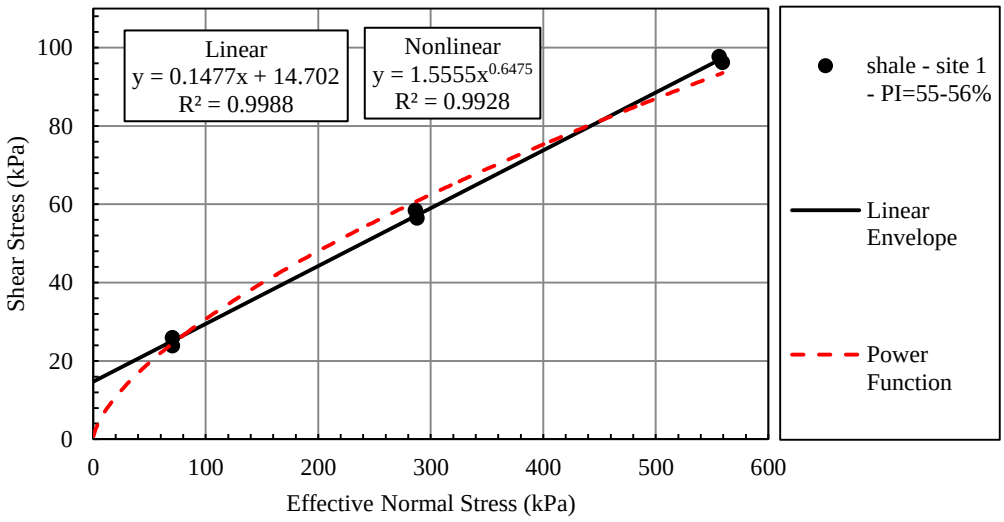

Figure 3.4 Residual Strength failure envelope of Site 1 clay (PI=55-56%)

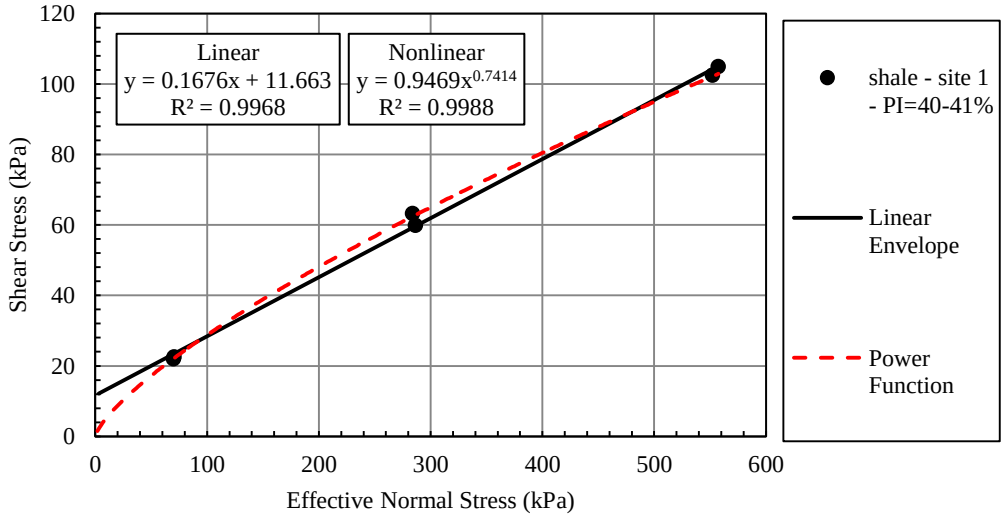

Figure 3.5 Residual Strength failure envelope of Site 1 clay (PI=40-41%)

3.3.2 Clay samples from Site 6

Site 6 is a confidential undisclosed site located in Denver. Sample preparation and testing method of the site 6 samples are the same as site 1 described in section 3.3.1. Liquid limit of the samples are from 45 to 53% and the plasticity indices are in the range of 17 to 22%. The residual shear strength test data of the samples obtained from site 6 is also presented in the Table 3.6.

Table 3.6 Residual shear strength test data of Site 6 clay (Dewoolkar and Huzjak, 2005).

LL (%)	PI(%)	Effective Normal Stress (kPa)	Residual Shear Stress (kPa)	Residual friction angle (°)
53	22	35	7.2	11.6
53	22	104.4	19.6	10.6
53	22	380.2	59.4	8.9
51	21	17.7	7.2	22.1
51	21	82.4	19.2	13.1
51	21	381.1	61.3	9.1
49	22	35	10.5	16.7
49	22	102.5	26.8	14.6
45	17	16.8	6.7	21.7
45	17	80.9	14.8	10.4
45	17	369.2	53.1	8.2

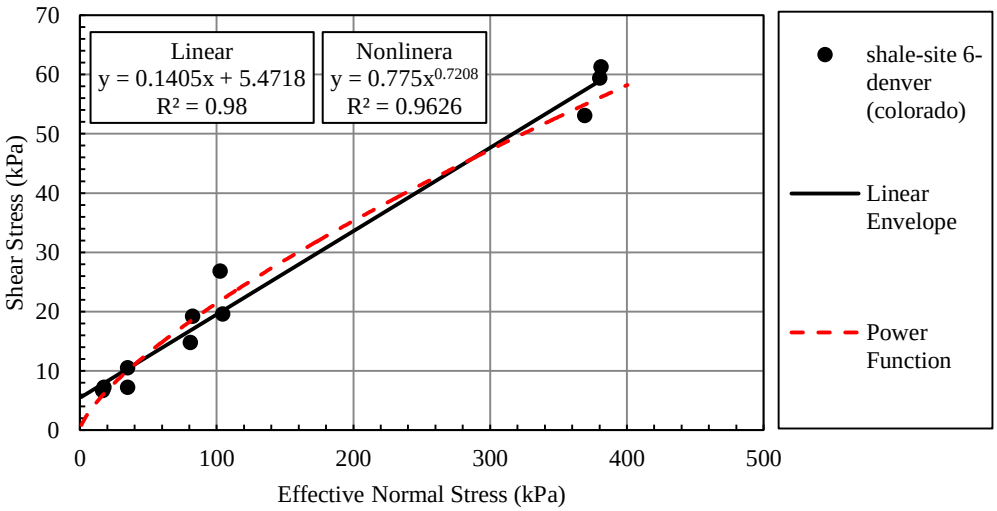

Figure 3.6 Residual Strength failure envelope of Site 6 clay

3.4 Walton's Wood clay

Skempton (1964) investigated the residual shear strength of clay samples obtained from a sliding mass in Walton's Wood, Staffordshire. The thickness of the clay zone was reported to be up to 10 meters. In the collected samples some real failure surfaces have been observed. The residual shear strength test of the clay samples were measured with reversal direct shear test and triaxial setups. In triaxial tests, Skempton (1964) prepared the specimens including actual shear planes and place them into the setup so that the shear plane was inclined at 50 degrees to the horizontal. Obtained residual shear strength from triaxial setup were in a good correspondence with the reversal direct shear tests. All of

the attained residual strength tests data are summarized in the Table 3.7.and the failure envelopes are delineated in Figure 3.7.

Table 3.7 Residual shear strength test data of Walton wood's clay (Skempton, 1964))

LL (%)	PI(%)	Effective Normal Stress (kPa)	Residual Shear Stress (kPa)	Residual friction angle (°)
53	25	90.6	28.3	17.4
53	25	152.1	36.9	13.6
53	25	205.6	43.2	11.9
53	25	214.98	51.8	13.5
53	25	53.5	16.5	17.1
53	25	80.99	15.5	10.8
53	25	82.5	21.4	14.5
53	25	100.5	23.6	13.2
53	25	107.1	30.7	16.0
53	25	168.7	41.1	13.7
53	25	206.3	48.5	13.2
53	25	206.7	54.3	14.7
53	25	251.9	54.2	12.1
53	25	256.2	60.96	13.4

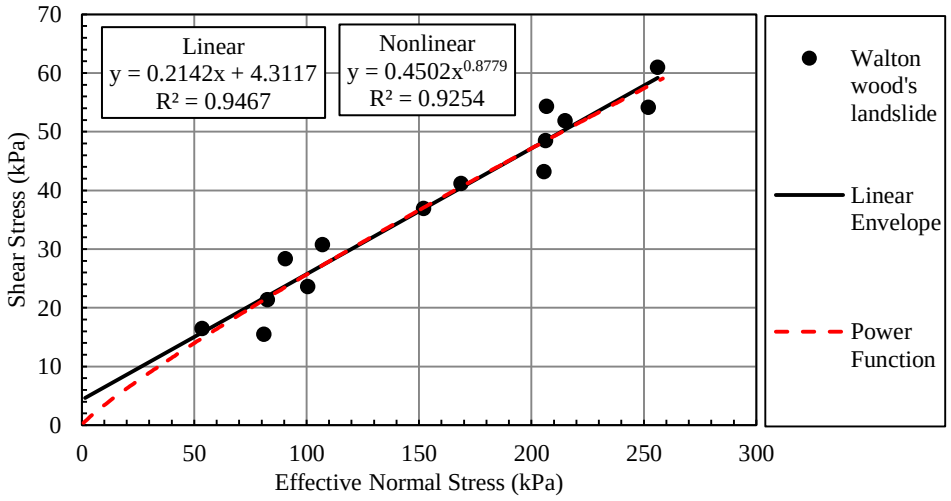

Figure 3.7 Residual Strength failure envelope of Walton wood's clay

3.5 Niigata Prefecture's landslides in Japan

Tiwari et al. (2005) investigated six landslides within a radius of about 6 km at Niigata Prefecture: Okimi,Yosio, Mukohidehara, Engyoji, Iwagami, and Tsuboyama landslides. Tiwari et al (2005) also stated that all the landslides have similar geologic and climatic conditions. Both undisturbed and remolded samples were utilized for residual shear strength tests. Remolded samples were categorized as "shallow" and "deep"samples. Shallow samples were collected from the scarp of the sliding mass and deep samples are obtained from deeper portion of the landslide. Table 3.8 summarizes the index properties of the landslide soil specimens. In this study, the nonlinearity of residual shear strength envelope in the remolded deep samples were investigated by generating the residual shear strength failure envelopes for all six landslides. The nonlinear residual shear strength of the landslides are presented in the Figures 3.8 to 3.13.

Table 3.8 Index properties of the soil samples from landslides in Japan (After Tiwari et al 2005).

Location	Sand (%)	Silt (%)	Clay (%)	Fines (%)	LL (%)	PI (%)	USCS	W (%)	γ (kN/m3)
Okimi	15.7	48.2	36.1	84.3	84	52.9	CH	35.3	14.3
Yosio	16.9	43.1	40	83.1	89	41.9	MH	50.5	14.1
Mukohidehara	35.6	46.3	18.1	64.4	55.8	32.6	CH	35.3	15
Engyoji	73	19.8	7.2	27	94.6	62.4	SC	44.1	15
Iwagami	71.5	22.1	6.4	28.5	94.7	59.2	SC	37.5	15.7
Tsuboyama	6.1	29.9	64	93.9	100	68.3	CH	38.7	14.8

***Note** : All the samples are obtained from deep portion of the sliding masses.*

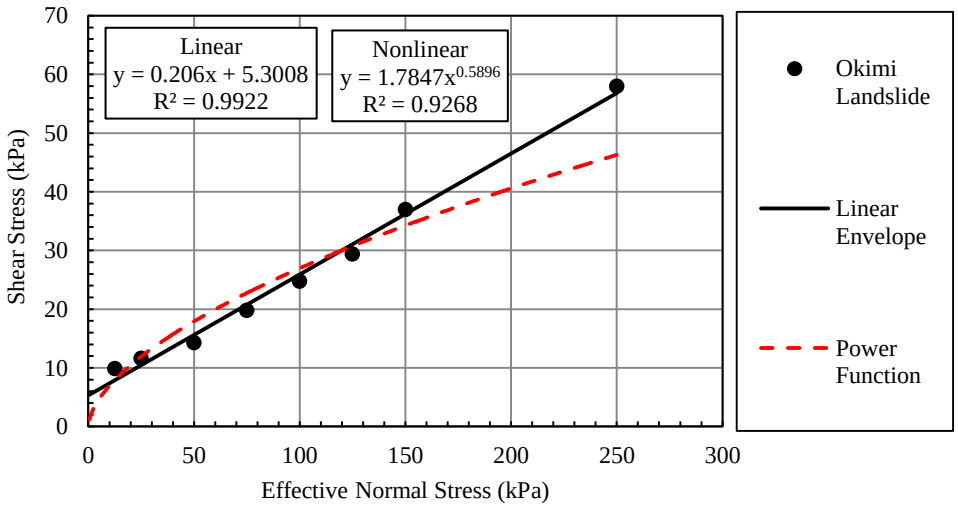

Figure 3.8 Residual strength failure envelope of Okimi landslide.

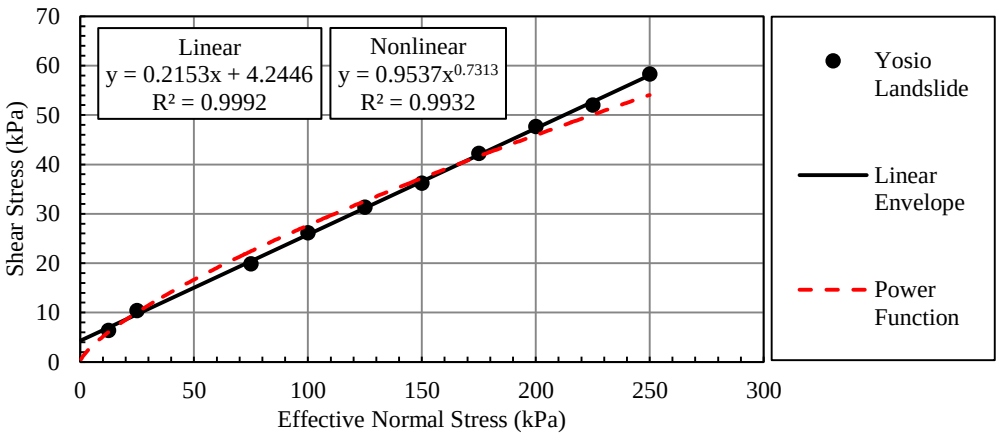

Figure 3.9 Residual strength failure envelope of Yosio landslide.

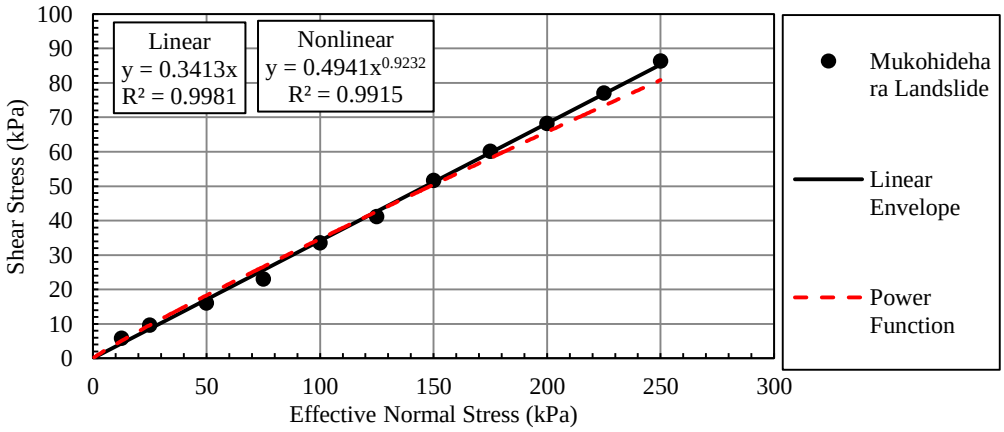

Figure 3.10 Residual strength failure envelope of Mukohidehara landslide.

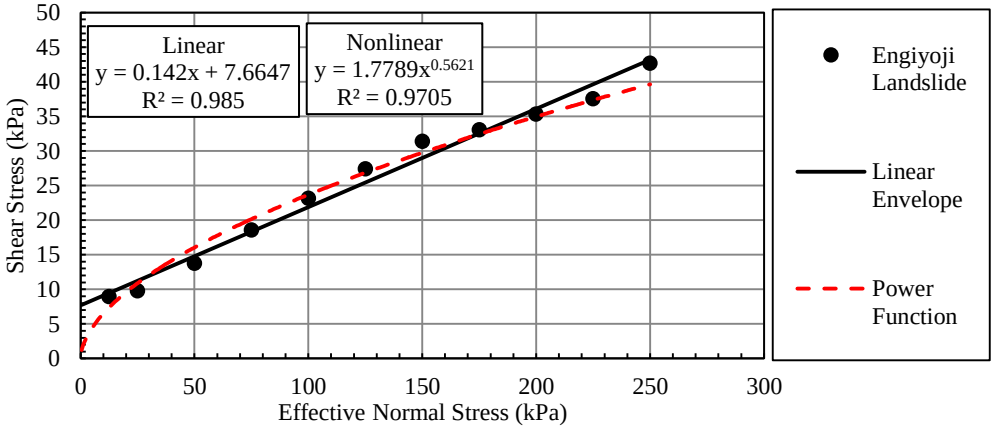

Figure 3.11 Residual strength failure envelope of Engiyoji landslide.

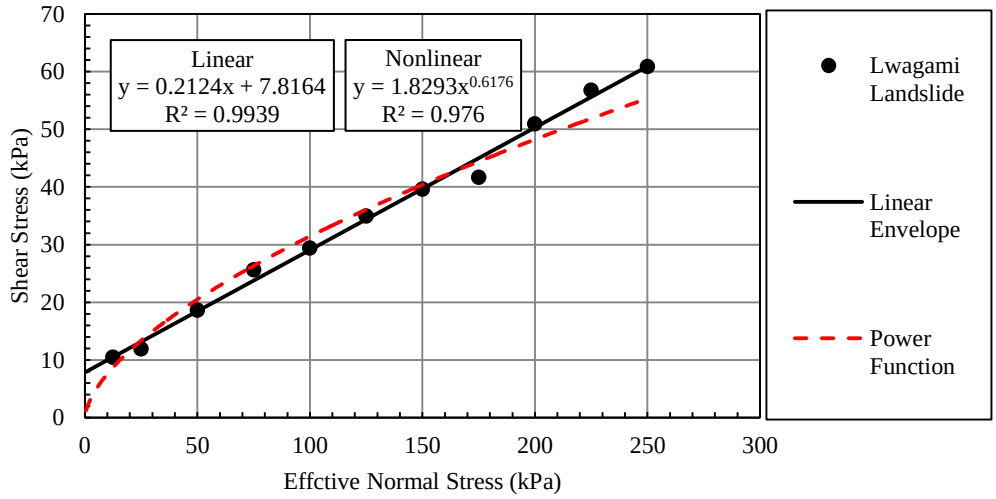

Figure 3.12 Residual strength failure envelope of Lwagami landslide.

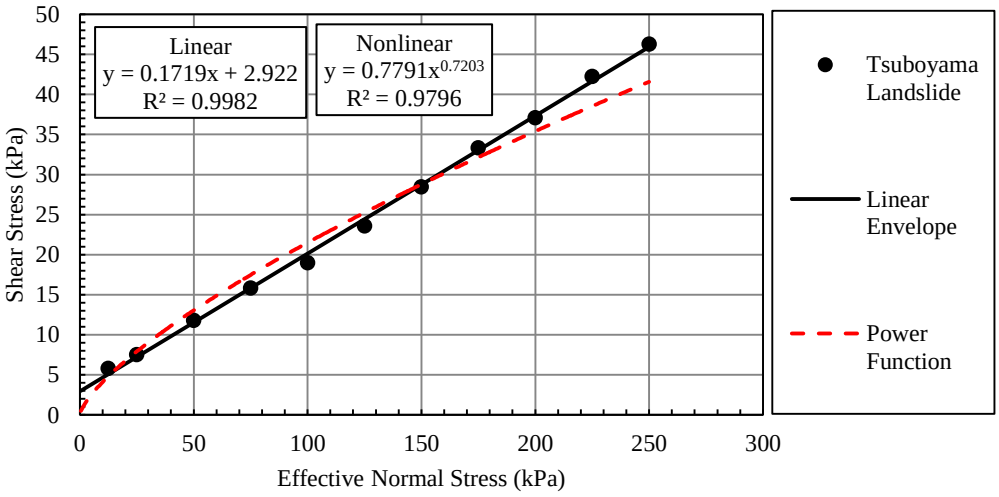

Figure 3.13 Residual strength failure envelope of Tsuboyama landslide.

3.6 Additional collected data from literature

In addition to the presented data, a number of residual shear strength test data are collected. After fitting a power function in the form of $Y=AX^b$ ($\tau = A\sigma'^b$) for the residual shear strength failure envelope on the collected data the *b* values are plotted in the figure 3.13. Mentioned data are collected from Dewoolkar and Huzjak (2005), Huvaj-Sarihan (2009), Experimental studies of this study and the investigated case histories that are described in chapter 5. These added test data are also presented in the Table 3.8.

Table 3.8 Summary of the investigated residual shear strength failure envelopes and its nonlinear functions

Soil	PI (%)	Nonlinear Function ($\tau = A\sigma'^{b}$)	Reference
Blue London Clay	59	$y = 0.5021x^{0.8686}$	Bishop et al. (1971)
Blue London Clay	43	$y = 0.1515x^{1.0312}$	Bishop et al. (1971)
Brown London Clay	33	$y = 0.7673x^{0.7915}$	Bishop et al. (1971)
Rueter Hess dam	56	$y = 1.5555x^{0.6475}$	Dewoolkar&Huzjak (2005)
Rueter Hess dam	40	$y = 0.9469x^{0.7414}$	Dewoolkar&Huzjak (2005)
Colorado site 6	20	$y = 0.775x^{0.7208}$	Dewoolkar&Huzjak (2005)
Rueter Hess dam	56	$y = 1.4023x^{0.6625}$	Dewoolkar&Huzjak (2005)
Rueter Hess dam	50	$y = 1.4023x^{0.6625}$	Dewoolkar&Huzjak (2005)
Rueter Hess dam	55	$y = 1.8436x^{0.6391}$	Dewoolkar&Huzjak (2005)
SENAC dam	59	$y = 1.7252x^{0.6325}$	Dewoolkar&Huzjak (2005)
SENAC dam	29	$y = 0.3449x^{0.9078}$	Dewoolkar&Huzjak (2005)
Standely lake dam	33	$y = 2.5746x^{0.5781}$	Dewoolkar&Huzjak (2005)
South tani reserviour dikes	28	$y = 0.6036x^{0.7985}$	Dewoolkar&Huzjak (2005)
Walton's Wood clay	25	$y = 0.4502x^{0.8779}$	Skempton (1964)
Okimi landslide	52.9	$y = 1.7847x^{0.5896}$	Tiwari et al. (2005)
Yosio landslide	41.9	$y = 0.9537x^{0.7313}$	Tiwari et al.(2005)
Mukohidehara	32.6	$y = 0.4941x^{0.9232}$	Tiwari et al. (2005)
Engyoji landslide	62.4	$y = 1.7789x^{0.5621}$	Tiwari et al. (2005)
Iwagami landslie	59.2	$y = 1.8293x^{0.6176}$	Tiwari et al. (2005)
Tsuboyama	68.3	$y = 0.7791x^{0.7203}$	Tiwari et al. (2005)
Ankara clay	46	$y = 0.9897x^{0.7063}$	Chapter 4 of this thesis
Kaolinite	19	$y = 0.9555x^{0.7691}$	Chapter 4 of this thesis
Texas clay1 (Ring shear)	54	$y = 0.383x^{0.8283}$	Huvaj-Sarihan (2009)
Texas clay2 (Ring shear)	76	$y = 0.242x^{0.8894}$	Huvaj-Sarihan (2009)
Balikesir mine	37	$y = 1.8622x^{0.6924}$	Chapter 5 of this thesis
Jackfield Landslide	25	$y = 0.5686x^{0.9019}$	Chapter 5 of this thesis
Cortes des Pallas	14	$y = 0.5932x^{0.9306}$	Chapter 5 of this thesis
Kuchi-Otani Landslide	63	$y = 0.1578x^{0.9318}$	Chapter 5 of this thesis
Ogoto Landslide (Block A)	57	$y = 0.336x^{0.8868}$	Chapter 5 of this thesis
Ogoto Landslide (Block B)	50	$y = 0.4372x^{0.924}$	Chapter 5 of this thesis
USA mine, S2	75	$y = 0.7628x^{0.7474}$	Unpublished
USA mine, S3	55	$y = 0.4179x^{0.8361}$	Unpublished
USA mine, S4	83	$y = 0.1535x^{0.9483}$	Unpublished

Table 3.8 summarized all the analyzed soils in chapter three with both linear and nonlinear residual shear strength parameters and functions. In order to see if there are any correlations between the nonlinearity of the residual shear strength failure envelope and soil properties such as soil plasticity Figure 3.13 which shows the *b* values taken from the powers in the nonlinear function in the form of $Y=AX^b$, and the soil plasticity. In Figure 3.13 the dashed line is the trend obtained from the average empirical correlation proposed by Mesri and Shahien (2003), which shows the change of nonlinear function's power by the change in the plasticity index of the soils. From the collected data from the literature, a clear correlation cannot be defined, however it may be argued that as the plasticity index of the soil is increasing, the power "b" value is decreasing (indicating a higher degree of nonlinearity in residual shear strength envelope) for the data with plasticity index range of 10-80%. Therefore, it can be concluded that more data in higher plasticity levels must be collected to be able to define a clear correlation between the *b* value and the plasticity index of the soil.

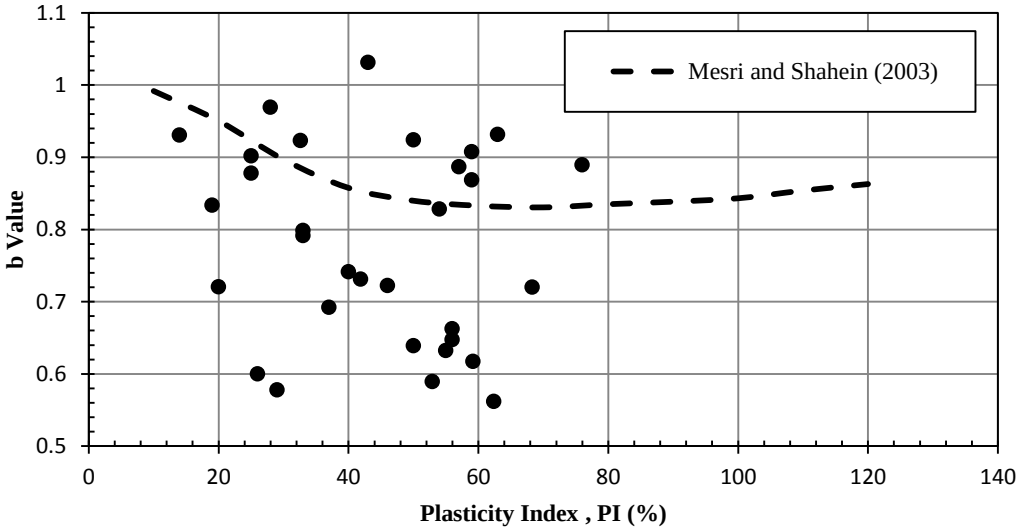

Figure 3.13 Correlation between *b* value in the nonlinear power function ($\tau = A\sigma'^{b}$) and plasticity index (PI)

CHAPTER 4

EXPERIMENTAL STUDY

4.1 Studied Materials

The experimental section of this study investigates the residual shear strength failure envelope of two clayey soils. An overconsolidated natural clay known as Ankara Clay and a commercial kaolinite type of clay are used in the shear strength experiments. These soils have different plasticity; Ankara clay is highly plastic and kaolinite has a lower plasticity. Kaolinite is preferred also because it is a processed, uniform material which will not cause much deviation in shear strength test results.

4.1.1 Ankara Clay

Ankara Clay is a reddish-brown, stiff, fissured, overconsolidated soil. Ankara clay was preconsolidated by overburden subjected to subsequent erosion, by a depression in the groundwater level and by dessication (Ordemir et al. 1977). This clay is available in various thicknesses in different locations of the Ankara Basin (Erol 1973). It is composed of clayey, sandy and gravely particles, which is reported in the grain size distribution test section. Based on a study by Sezer et al. (2003), Ankara clay is a Pliocene age material and it was deposited in a fluvial environment. It mainly consists of illite, smectite, chlorite and kaolinite minerals. The non-clay minerals are quartz, feldspars, calcite and Fe–Ti oxides (Sezer et al. 2003). According to a semi-quantitative whole soil mineralogy and clay mineralogy study on Ankara Clay by Erguler and Ulusay (2003), on average, the clay minerals are about 66% of the whole soil, and clay-size fraction is composed of 34% smectite and 16% illite and 16% kaolinite. Teoman et al. (2004) described three small landslides in Ankara clay and described the material as a clay and silt size material with locally sandy and gravely zones. Fines content was reported as 60-82%. Mineralogy of the material included quartz, plagioclase, calcite and clay minerals. Clay minerals were smectite (%67-79), illite (9-22%) and kaolinite (10-12%) based on the method of semi-quantitaitve clay percentage method of Biscaye (1965).

Ankara clay samples are obtained from a deep excavation site, related to EGE Group construction in the central part of the city of Ankara, Turkey. The location of this construction site and a view of the soil excavation are depicted in Figures 4.1 (a) and (b).

4.1.2 Kaolinite Clay

This type of manufactured clay is preferred due to its uniform composition and grain size distribution to reduce the effect of aggregates in remolded sample preparation and to reduce the effect of inherent variability in natural soils on test results. In addition, difference in the plasticity of the investigated materials was considered in selecting the kaolinite and Ankara clay.

The manufacturer of kaolinite, Kale Maden Company, presented a data sheet, containing the mineralogical and chemical composition of the clay, which is summarized in Table 4.1 and 4.2 respectively.

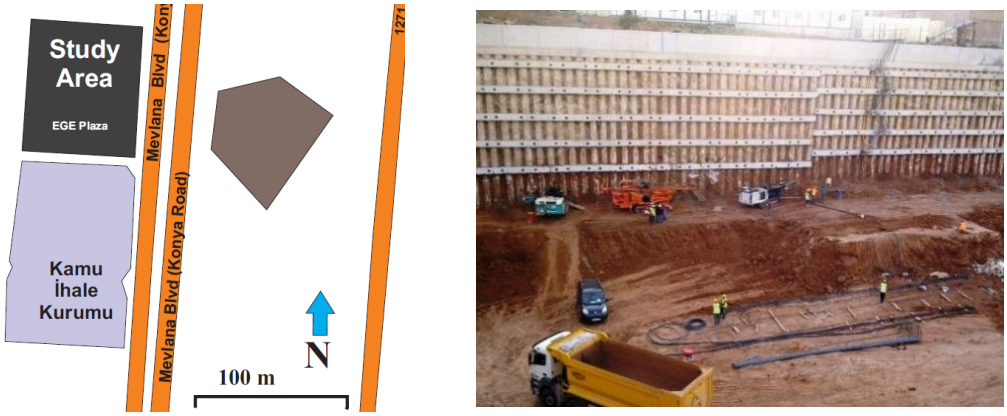

(a) (b)

Figure 4.1 (a) Location of the construction site (b) a view of the excavation site

Table 4.1 Mineralogical composition of Kaolinite (Kale Maden Company, 2012)

Type of mineral	Volumetric content (%)
Clay Mineral	90.97
Sodium Feldspar	0.08
Potassium Feldspar	2.31
Free Quartz	4.45

Table 4.2 Chemical composition of Kaolinite (Kale Maden Company,2012)

Chemical Analysis	(%)
Loss on ignition	12.77
SiO3	48.56
Al2O3	36.62
TiO2	0.64
Fe2O3	0.35
CaO	0.38
MgO	0.1
Na2O	0.01
K2O	0.39

4.2 Index Properties

A series of index properties tests are conducted on the two soils. In these set of tests, Specific Gravity, Atterberg limits and grain size distribution are obtained. The test results are summarized in Table 4.3 and Figure 4.2.

4.2.1 Specific Gravity (Gs)

This test is performed based on standard test method of ASTM D854. Because kaolinite and Ankara clay are both nonreactive to water and heavier than water, submersion technique in water is utilized. For low specific gravity values, or the materials in which the particles react with water, the water must be replaced by another liquid such as kerosene.

4.2.2 Atterberg Limits

Liquid limit and plastic limit values of the two samples are measured. The soil samples are pulverized to pass from sieve No.40 (i.e. <0.425 mm) and are mixed thoroughly with plenty of water for homogeneity of the soil moisture and to provide enough water for the clay minerals to interact. The samples are wrapped and stored overnight (>16 hours) to allow enough time for the hydration of clay minerals. According to standard test method of ASTM D4318, the liquid limit should be determined by obtaining the first drop count at a high water content, i.e. starting from the wet condition. Then, as the sample is air dried in room temperature by continuous mixing throughout the test, the water content is lowered and higher drop counts at lower water contents are obtained. This procedure (starting from wet condition) gives more accurate LL determination as compared to the method, which starts from drier condition and adds water to the sample to obtain smaller drop count values. Figure 4.2 presents some of the Atterberg limit test procedure of the Ankara clay and the kaolinite.

(a) (b) (c) (d) (e)

Figure 4.2. Atterberg limit tests (a-c) the Ankara Clay (d-e) the kaolinite

4.2.3 Grain Size Distribution

This experiment results in the quantitative determination of the grain size distribution of the soil. In this study 100% of the kaolinite's grains were smaller than 75 μm (sieve No.200). Consequently, size distribution was obtained by sedimentation (hydrometer) test. However, in Ankara clay, both sieve analysis and sedimentation tests were conducted. Due to high cohesion of Ankara clay particles, sieve analysis has been done in wet condition based on ASTM D1140.

Figure 4.3 presents the grain size distribution results. An additional grain size distribution for the Ankara clay particles passed from sieve No.40 is provided, because the particle size of the remolded samples used in the shear strength tests are below sieve No.40.

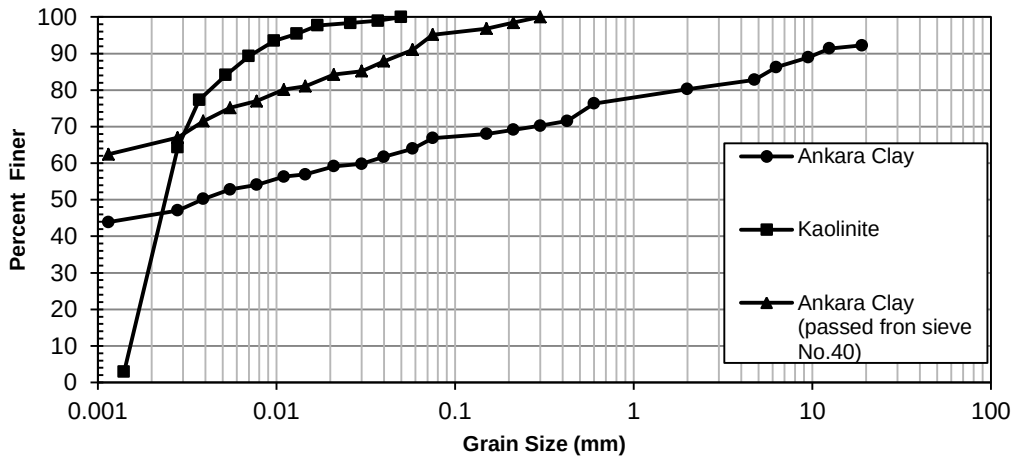

Figure 4.3 Grain Size Distribution

Table 4.3 Summary of the index properties test results

Properties	Ankara Clay	Kaolinite
Fines Content (%) (<0.074 mm)	68 (in whole sample)	100
Gs	2.66	2.62
LL (%)	72	47
PI (%)	46	19
Clay-size Fraction (%) (<0.002 mm)	65	30
USCS Classification	CH	CL

4.2.4 Soil Classification

Based on the Unified Soil Classification System (USCS), the Ankara clay and kaolinite are classified in CH and CL categories, respectively. Figure 4.4 presents the related data on the Casagrande's plasticity chart.

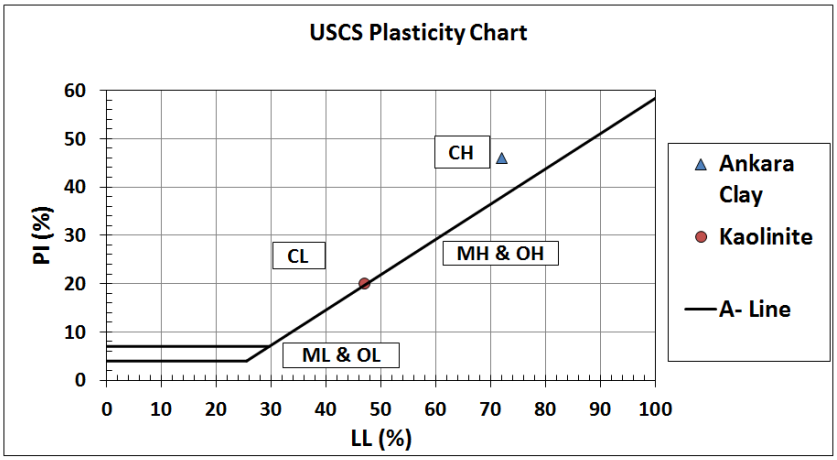

Figure 4.4 USCS Plasticity Chart

4.3 Residual Shear Strength Tests

Ring shear tests and reversal direct shear tests are widely used in geotechnical engineering to determine the residual shear strength envelope of stiff clays. A set of shear strength tests are performed on soils by reversal direct shear test technique in which there will be continuous forward shearing process until the measured shear strength reaches a constant value at relatively large shear displacements that shows the residual state.

4.3.1 Shear Rate Determination

Shear rate is one of the most important factors in drained direct shear testing. The rate of shear should be selected such that it provides fully drained condition of the sample during shearing. This rate must be initially determined based on the consolidation properties of the soil and it should be kept constant throughout the tests. According to the standard test method of ASTM D3080, the shear rate to be used drained direct shear tests is defined based on the coefficient of consolidation (or t_{90}) of the soil sample in order to provide enough time for drainage throughout the test. In this study, during the consolidation stage of each clay, the shear rates are calculated and used for all clay samples as **0.024 mm/min.** This value is in agreement with the typical shear rates used in the literature for drained direct shear testing (e.g. Stark and Eid (1994) used 0.018 mm/min shear rate in ring shear tests). After finishing each forward shearing, the shear direction is reversed and the sample was brought back to its initial position by the motor of the direct shear machine, then the screws that connect the two halves of the shear box together are tightened. The sample was rested overnight to allow enough time for dissipation of excess pore water pressures that might be originated during the reversing step. For the sake of having uniformity in the reversing conditions, all of the tests are reversed in a constant rate of 0.122 mm/min.

4.3.2 Normal Stress Range

To obtain residual shear strength envelope and to check for the nonlinearity of the envelope a wide range of normal stresses are selected. Both small and large normal stresses should are considered, therefore an effective normal stress range used in laboratory reversal direct shear tests is from 25 to 900 kPa.

4.3.3 Sample Preparation

It is important to emphasize that residual shear strength condition develops in stiff overconsolidated clays and shales in the field, and not an observed phenomenon in normally consolidated (soft) clays. Therefore if remolded specimens are prepared in the lab, they should be overconsolidated.

As illustrated in the Figure 4.5, Huvaj-Sarihan (2009) noted that in reversal direct shear or in ring shear tests, the samples can be (1) intact specimens (undisturbed or reconstituted) or (2) shear surfaces: such as an undisturbed sample containing a natural pre-sheared surface taken from the field, or a remolded specimen with a pre-cut surface prepared in the laboratory. When determining the residual shear strength of stiff clays it is in fact best to take an undisturbed sample from the natural existing shear surface in the field from existing landslides and carefully align the natural shear surface in the level of the plane between the two halves of shear box and shear in the natural direction of movement. Specimens containing a natural pre-sheared surface can be obtained from the exposed shear plane of an existing landslide, from trenches, shafts, open faces, and boreholes (preferably obtained by block-sampling in trenches or shafts) (Skempton 1964; Eid 1996). In this way, the shear strength of the existing shear surface can be measured very realistically in the laboratory in a relatively short period of time. This kind of specimen, tested in direct shear test, is known to provide a good estimate of the field residual strength (Skempton 1964, 1985).

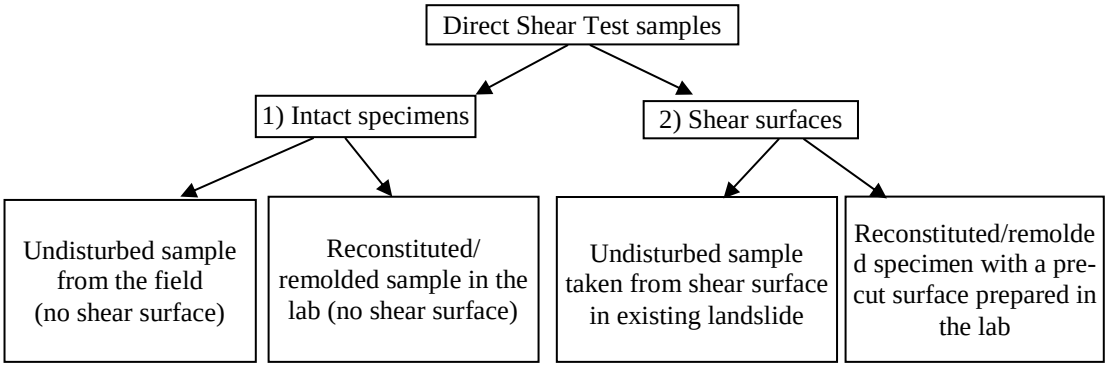

Figure 4.5 Sample preparation in residual direct shear test

However most of the time, taking an undisturbed sample from the shear plane is not possible; or it might be difficult to locate the slip surface in the case of borehole samples; or sampling, trimming and properly aligning the specimen in the shearing apparatus may be difficult. The other option is to use remolded specimens (with or without artificially prepared shear surfaces formed in the laboratory). In this study (1) intact reconstituted/remolded specimens, and (2) reconstituted/remolded specimens with a pre-cut surface prepared in the laboratory are used.

4.3.3.1 Clay samples without pre-sheared surface

This is the method where we prepare remolded clay sample without a shear plane. In this method the clay sample (pulverized to pass No. 40 sieve) has been hydrated for three days at about its liquid limit to satisfy the initial saturation of the sample and for easier placement of the clayey paste into the direct shear boxes so that there would not be any trapped air bubbles. Sample is gradually filled in the lower half of the direct shear box with a spatula as shown in Figure 4.7 (b). In the square shear box, the corners of the shear box, then along the sides of the square clay is filled by pressing with a spatula, moving toward the inner central part of the box. After filling the lower box, the upper box is fixed on the filled lower box with screws and with the same procedure, the whole box is filled with remolded clay to a certain height and the top of the clay is leveled. The lower box is filled separately first, because if the two halves of the box are initially fixed together, that would mean sample placement is done in a deeper box where uniform placement and leaving no air bubble may be difficult. It should be noted that, during the filling, it is made sure that there was no weak plane, or no interface boundary, in the clay. The initial density of the samples after placement (before consolidation) is in the range of 1.6 to 1.7 kg/cm^3. The consolidation loading is started from a small load and carried out with a load increment ratio of one (LIR=1.0) to prevent the clay from squeezing out and to have all the vertical deformation due to 1D vertical deformation of the clay (consolidation behavior).

Since the goal is to produce artificially an “overconsolidated clay” sample, after the final consolidation pressure is reached, the vertical pressure on the sample is reduced and the it is allowed to rebound. In this way, an overconsolidated stiff clay, having a pre-determined overconsolidation ratio, is obtained. It should be noted that during all consolidation pressure increments, void ratio versus log effective stress plots are obtained and especially in the final pressure and in unloading/rebound the e-log σ'_v plots are checked for complete consolidation. Then the spacer screws are used to create a gap between the two halves of the shear box and sample is sheared as illustrated in the Figure 4.6. Shearing rate is set to 0.024 mm/min to have a perfect drainage condition based on

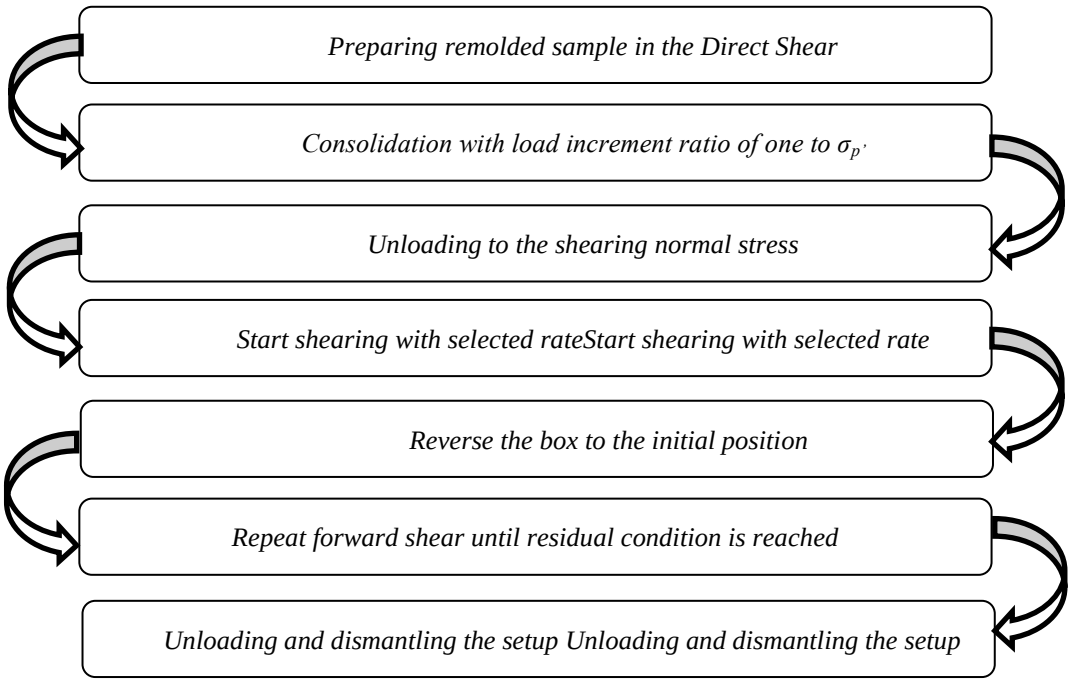

Figure 4.6 Multi-Reversal Direct Shear Test Flowcharts

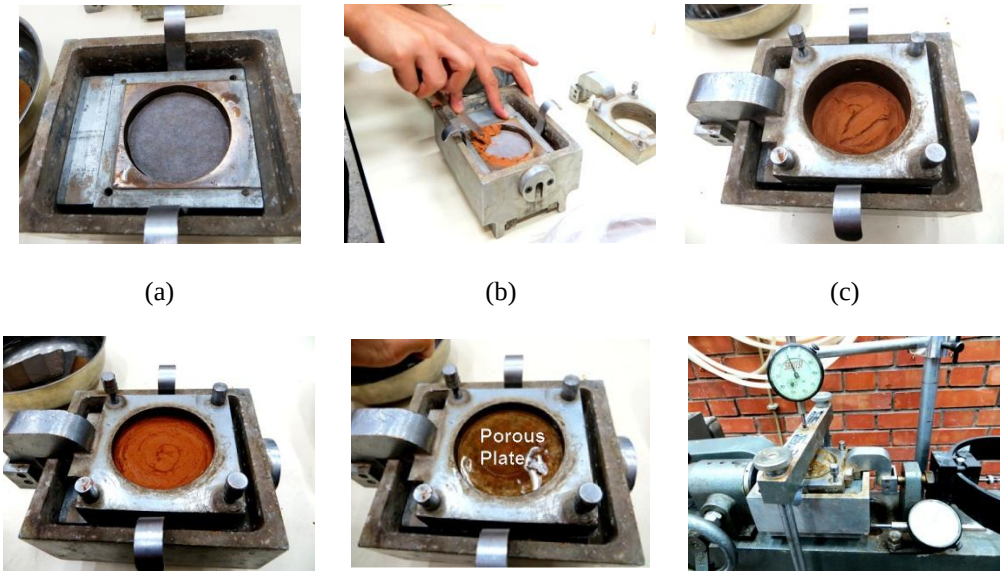

(a) (b) (c)

(d) (e) (f)

Figure 4.7 Remolded sample preparation

the consolidation results of the sample according to ASTM D3080 standard and the reversing rates is set at a relatively higher rate about 0.122 mm/min, but low enough to prevent generation of excess pore water pressure in both Ankara Clay and Kaolinite. Consolidation time of Kaolinite clay was

much faster than Ankara Clay, i.e. it had higher t_{90} and the calculated direct shear test shearing rate was higher. Therefore, kaolinite samples could have been sheared at a faster rate compared to Ankara clay, however, as the experiments were planned in a unified lowest possible shearing rate, both clays have been sheared in the same forward and revers rates.

4.3.3.2 Clay samples with pre-sheared surface

This is the method where we prepare remolded clay sample with a shear plane. After normal sample preparation (pulverization and hydration) procedure as described in section 4.3.3.1, a different method is utilized for consolidation. Separate consolidation of the clay in each half of the direct shear box and therefore generation of a distinct shear plane between the two halves of the direct shear box was the main idea of second approach (that simulates a pre-existing shear surface in the reactivated slopes). This procedure was originally used by Mesri and Cepeda-Diaz (1986). In this method a consolidation cylinder and a smooth steel plate is used in consolidation stage. As shown in Figure 4.8, each half of the box is screwed to the consolidation cylinder. Remolded sample is prepared similar to previous method in a water content near the liquid limit of the material and each half of the direct shear box is filled separately and consolidated to the target load for predetermined overconsolidation ratio of 4 with load increment ratio of one. Under each half of the box, a smooth steel surface is mounted to form the smooth surface as shown in Figure 4.8. After the sample is consolidated to the highest pressure, unloaded to the desired normal stress, the two halves of the shear box are then assembled together, quickly taken to the direct shear device (without allowing much time for swelling under zero normal stress), loaded to the same normal stress, and axial deformation, if any, is observed. After equilibrium, a gap is created between the two halves of the shear box with the help of spacer screws, and shearing is started. Loading/consolidation to the highest pressure and unloading/ rebound/ reloading stages can be finished in about 7-10 days depending on the pressure ranges required. In all tests, the thickness of the specimen in each half of the shear box was about 6 to 8 mm at the end of consolidation/rebound.

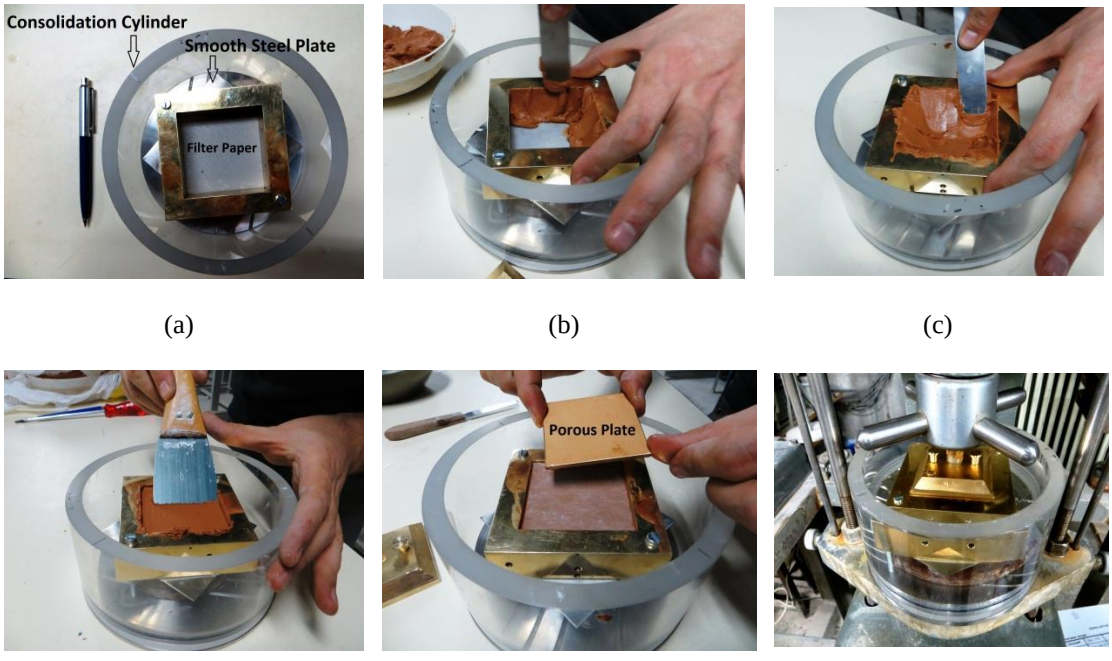

Figure 4.8. Remolded sample with pre-sheared surface.

4.3.3.3 Additional Designed Apparatuses

High overconsolidation ratio used in the laboratory tests, specifically in Ankara Clay samples OCR=4, demands very high pressures to be applied. For example, to shear the Ankara clay sample at 900 kPa normal stress, the sample has to be consolidated under 3600 kPa for OCR=4. The safe loading capacity of direct shear device was for about 900 kPa normal stress. Therefore the samples had to be consolidated elsewhere. Another benefit of consolidating the samples elsewhere is that, direct shear device would be free and could be used for shearing an already-consolidated, ready-specimen while another is being consolidated elsewhere. Furthermore, creation of a pre-sheared surface by separately consolidating the two halves of the direct shear box was not possible in the direct shear set up. Consequently, some additional parts were designed to make the consolidation stage possible with an oedometer setup. This additional part is a Plexiglass cylinder container in which the direct shear boxes could be fixed (both two boxes together and separately) and the cylinder could be mounted in an oedometer setup. Furthermore, an additional direct shear box is designed and manufactured to be used in precut sample preparation. Figure 4.9 shows a sketch of the designed set up with mounted direct shear box in it.

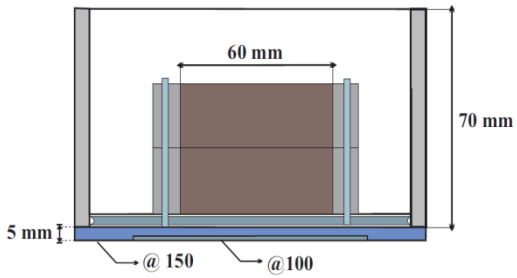

(a)

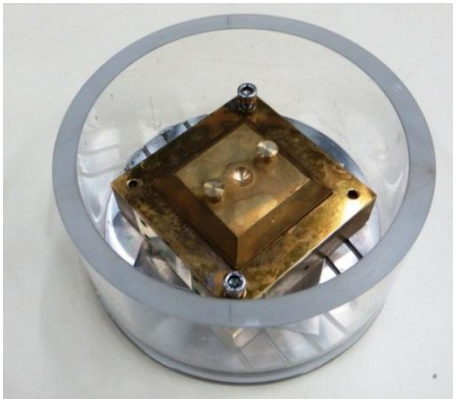

(b)

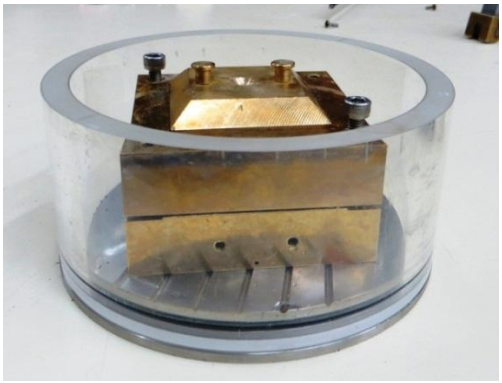

(c)

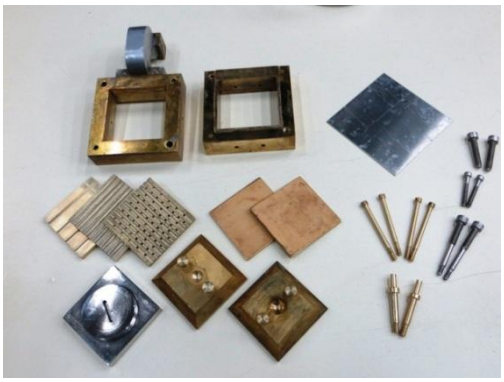

(d)

Figure 4.9 Designed parts of the setup (a) Consolidation container and shear box's section cut (b) Mounted direct shear box and smooth steel plate to form precut shear (c) together consolidation of the direct shear box (d) other manufactured parts of the setup

4.4 Determination of the Residual Shear Strength Parameters

Table 4.4 and 4.5 present the summarized results of the residual shear strength tests for both sample preparation methods and both soil types. Furthermore, determination of residual shear strength parameters are described on the following graphs in more detail.

Table 4.4 Test results without shear plane *

Soil Type	Box Shape	Shearing σ'_n (kPa)	Consolidation σ'_p (kPa)	OCR	w % Sample Preparation	w % After Shearing	τ_r (kPa)	Disp. to reach residual (mm)	φ'_r sec (°)
Ankara Clay	Square	25	100	4	69	47	10.1	21	22
	Circle	50	200	4	67.5	46.8	16.0	23	17.7
	Square	100	400	4	68.4	41.4	24.7	23	13.9
	Square	200	800	4	60.1	42.4	40.0	22	11.3
	Square	400	1600	4	51.2	39.1	60.5	17	8.6
	Square	900	3600	4	80.5	36.1	135	22	8.6
Kaolinite	Circle	25	50	2	44	33	13.6	25	28.6
	Circle	50	100	2	48.5	34.3	20	37	21.8
	Square	100	200	2	47.5	-	28-30	31-23	15.6-16.7
	Circle	200	400	2	52	39.5	51-55.5	21-16	14.3-15.5
	Square	400	800	2	42.2	34.9	95.5	24	13.4
	Circle	900	1800	2	43.6	32.4	210	24	13.1

Notes:
** Rates are the same in all tests: Forward rate = 0.024 mm/min, Reverse rate = 0.122 mm/min*
** The density of both Ankara clay and kaolinite is in the range of 1.6-1.7 gr/cm^3.*
**All the samples were controlled to have enough height in the upper and lower box before shearing. (6-8 mm in each box)*

Table 4.5 Test with precut shear plane

Soil type	Box shape	Shearing σ_n (kPa)	Consolidation σ_p (kPa)	OCR	W% Sample Preparation	W% After shearing	τr (kPa)	Disp. required to reach residual (mm)	φ'_r sec (°)
Ankara Clay	Square	400	1600	4	68.5	36	53.5	20	7.6

When the shear strength of the sample reaches to a constant state after the post peak strain softening phase in over-consolidated clays, corresponding strength presents the residual shear strength parameters. During the test procedure, sample preparation and shearing stages there might be some conditions which may result in some fluctuations in the shear strength of the sample in large strains in direct shear test. Consequently, the linearized parts of the strength graphs are selected as residual parameters based on the engineering and visual judgments of the test interpreters. Following graphs are presenting the shear stresses and shear displacements of each test stage for both Ankara Clay and Kaolinite and the comments that describe the selected residual parameter values or ranges.

4.4.1 Ankara Clay (Intact Samples)

Ankara clay has been tested under five different effective normal stresses in direct shear test setup. In each normal stress the graphs of shear stress versus normal stress in both cumulative and non-cumulative displacement versions are presented for better delineation of the stress and displacement change during the test stages.

4.4.1.1 Ankara Clay (25 kPa)

The test data of Ankara Clay under 25 kPa effective normal stress is presented in the Figures 4.10 to 4.12.

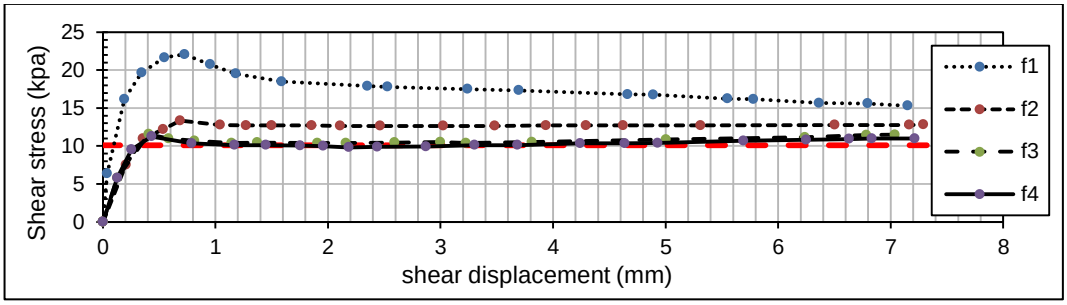

Figure 4.10 Shear Stress – Shear Displacement, Ankara Clay (25 kPa)

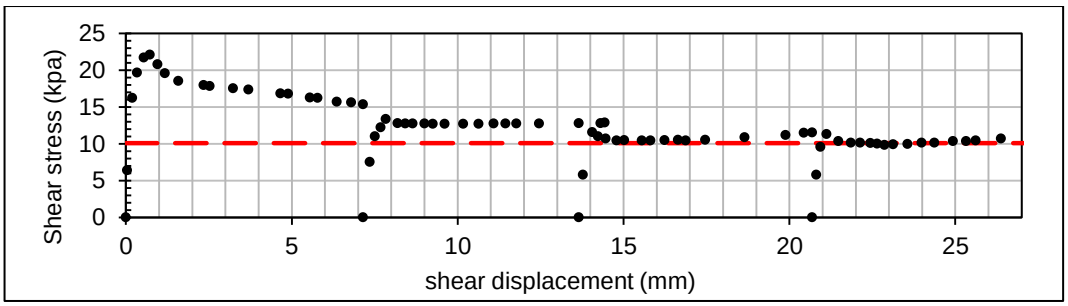

Figure 4.11 Shear Stress – Cumulative Shear Displacement, Ankara Clay (25 kPa)

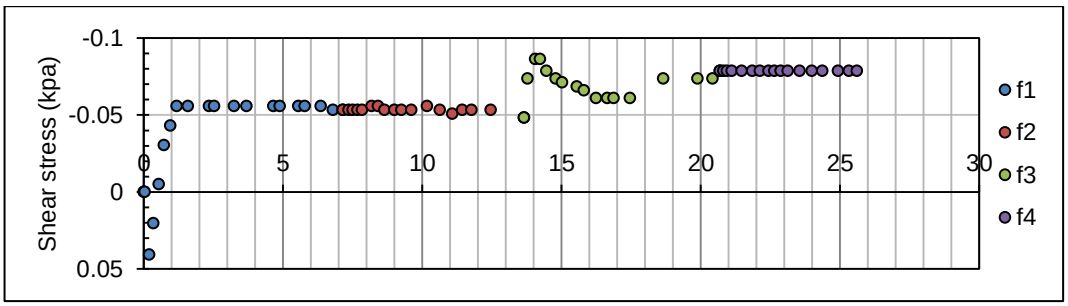

Figure 4.12 Vertical Displacement – Cumulative Shear Displacement, Ankara Clay (50 kPa)

In the presented results, selected residual shear strength is 10.1 kPa. Consequently, secant residual friction angle would be 22 degrees.

4.4.1.2 Ankara Clay (50 kPa)

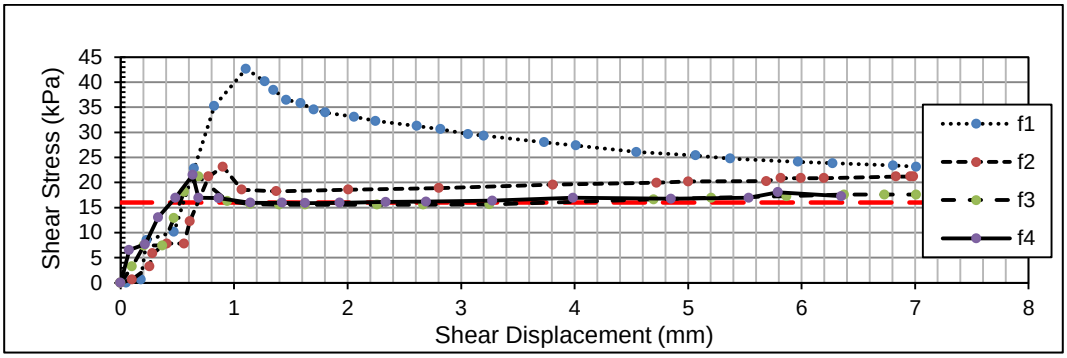

Figure 4.13 Shear Stress – Shear Displacement, Ankara Clay (50 kPa)

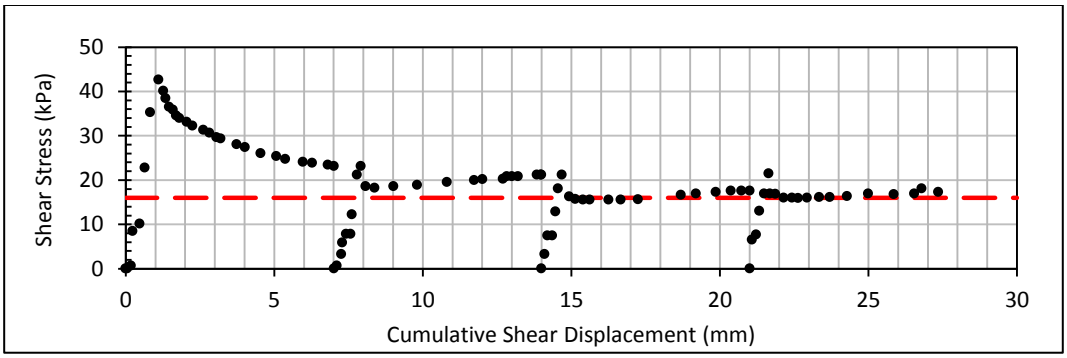

Figure 4.14 Shear Stress – Cumulative Shear Displacement, Ankara Clay (50 kPa)

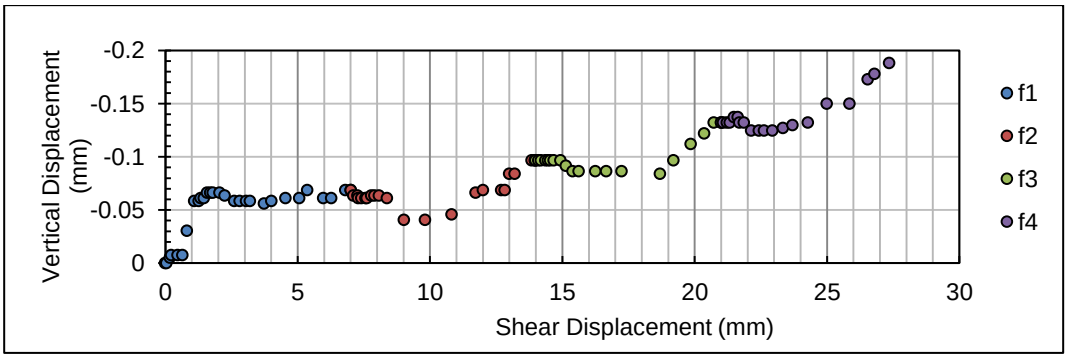

Figure 4.15 Vertical Displacement – Cumulative Shear Displacement, Ankara Clay (50 kPa)

In this test, the linearized portion of the shear strength trend in the fourth shearing forward step at about 23 mm of total horizontal displacement. Selected residual shear strength is 16 kPa. Consequently, secant residual friction angle would be 17.7 degrees. Which is illustrated in the Figures 4.13 to 4.15.

4.4.1.3 Ankara Clay (100 kPa)

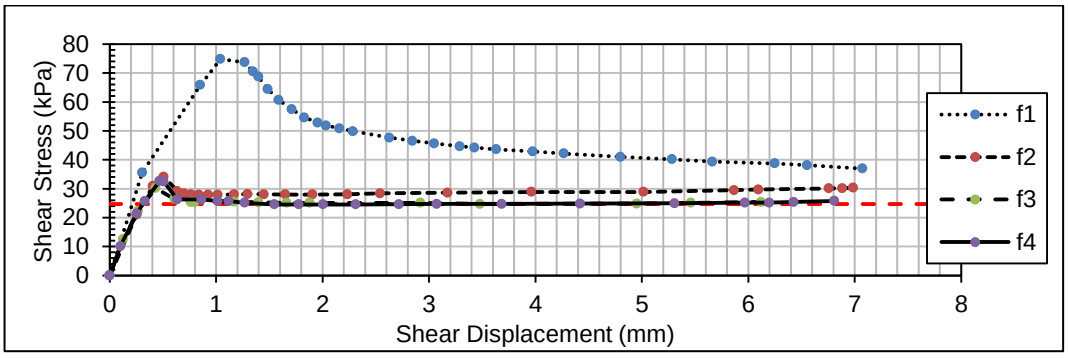

Figure 4.16 Shear Stress – Shear Displacement, Ankara Clay (100 kPa)

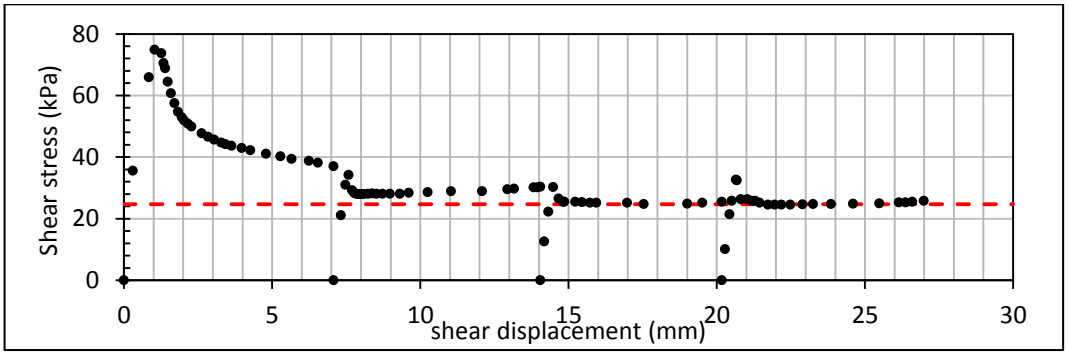

Figure 4.17 Shear Stress – Cumulative Shear Displacement, Ankara Clay (100 kPa)

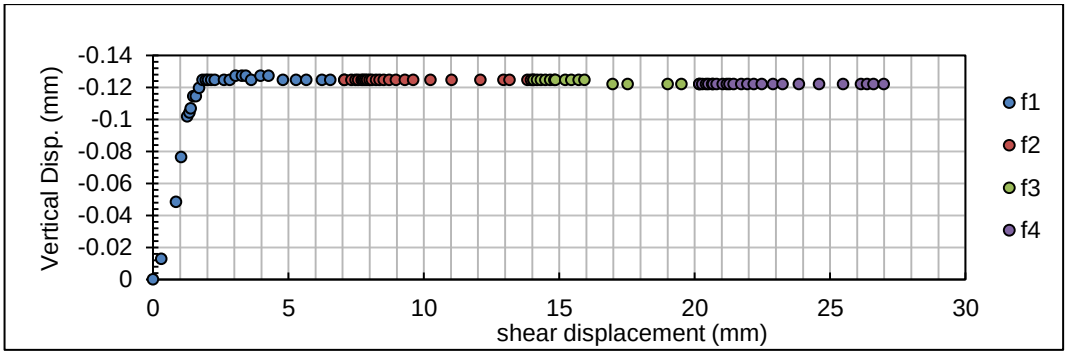

Figure 4.18 Vertical Displacement – Cumulative Shear Displacement, Ankara Clay (100 kPa)

Ankara Clay in shearing under 100 kPa effective normal stress has reached to residual state condition at about 23 mm of shear displacement. As shown in the graphs 4.16 and 4.17, the recorded residual shear strength is 24.7 kPa and calculated secant residual friction angle is 13.9 degrees.

4.4.1.4 Ankara Clay (200 kPa)

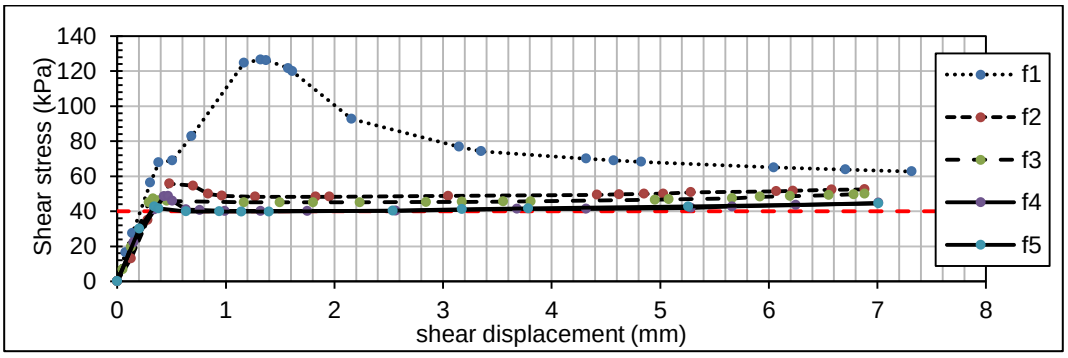

Figure 4.19 Shear Stress – Shear Displacement, Ankara Clay (200 kPa)

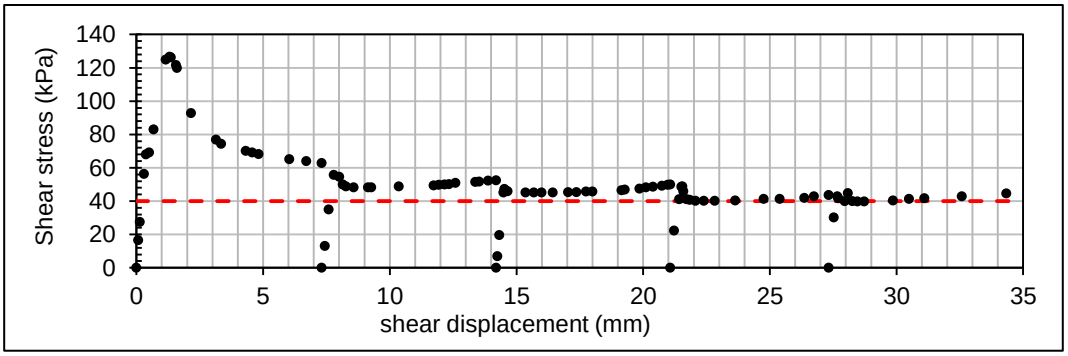

Figure 4.20 Shear Stress – Cumulative Shear Displacement, Ankara Clay (200 kPa)

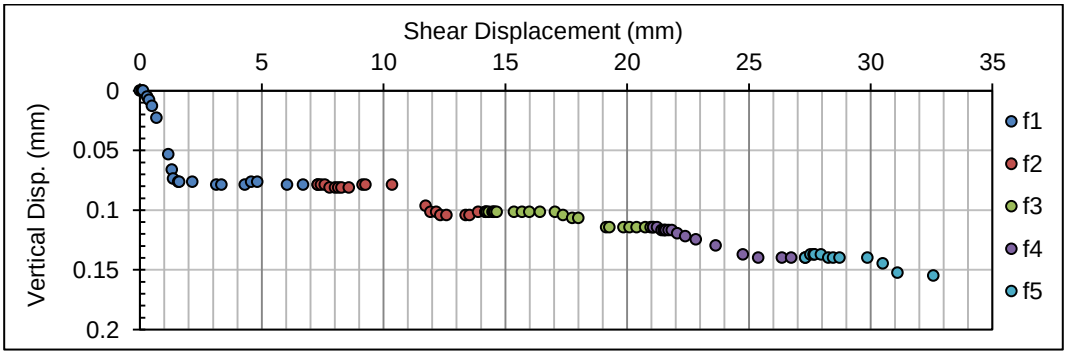

Figure 4.21 Vertical Displacement – Cumulative Shear Displacement, Ankara Clay (200 kPa)

At shear displacement of 22 mm Ankara clay shows residual state behavior. Residual shear strength is 40 kPa under 200 kPa normal effective stress and the residual friction angle is 11.3 degrees. A dashed red line in the graphs illustrates the level of the residual shear strength.

4.4.1.5 Ankara Clay (400 kPa)

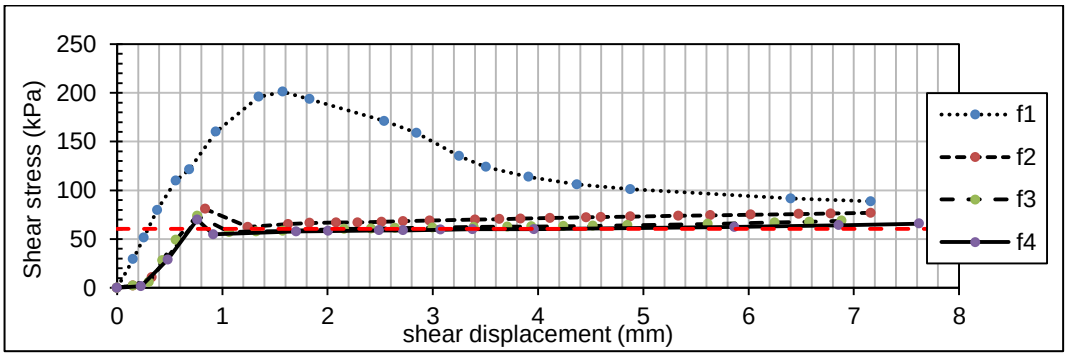

Figure 4.22 Shear Stress – Shear Displacement, Ankara Clay (400 kPa)

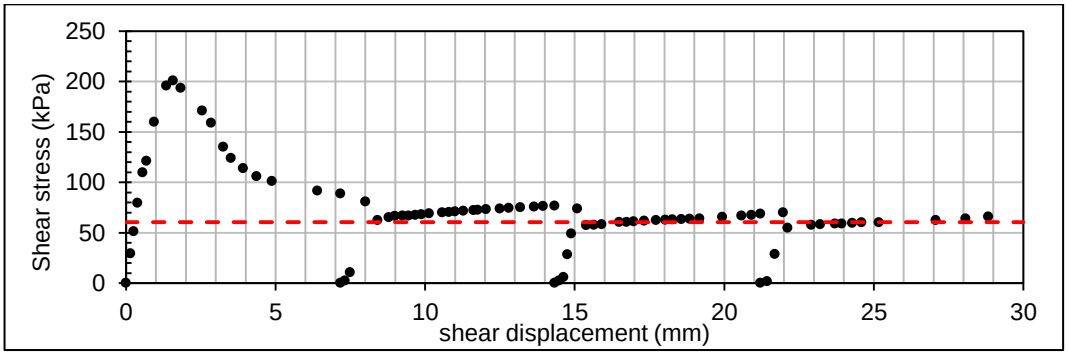

Figure 4.23 Shear Stress – Cumulative Shear Displacement, Ankara Clay (400 kPa)

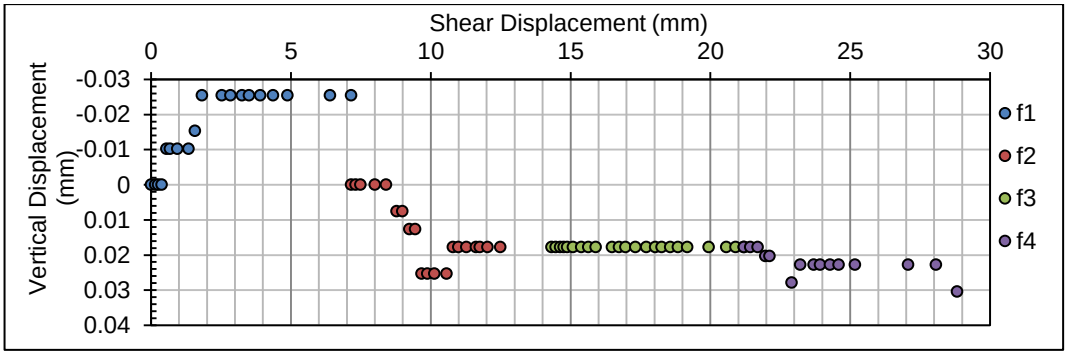

Figure 4.24 Vertical Displacement – Cumulative Shear Displacement, Ankara Clay (400 kPa)

The dashed red line shows the residual shear strength of 60.5 kPa is obtained in the shearing under 400 kPa normal effective shear stress. Residual state is achieved after about 17 mm horizontal displacement. Residual internal friction angle is 8.6 degrees.

4.4.1.6 Ankara Clay (900 kPa)

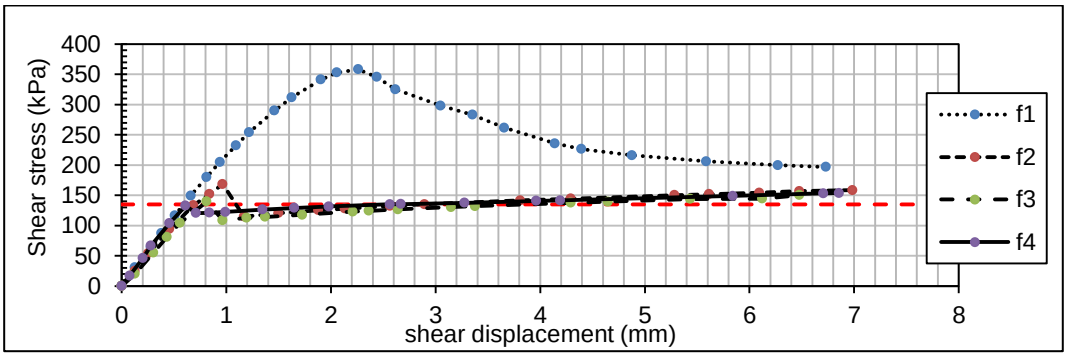

Figure 4.25 Shear Stress – Shear Displacement, Ankara Clay (900 kPa)

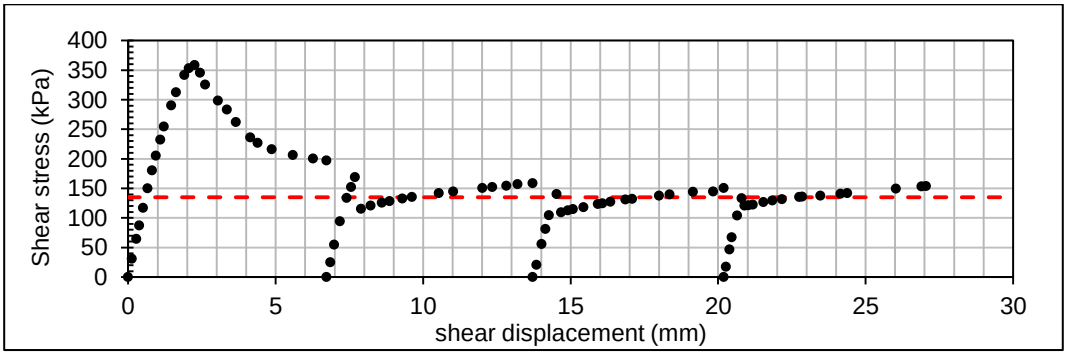

Figure 4.26 Shear Stress – Cumulative Shear Displacement, Ankara Clay (900 kPa)

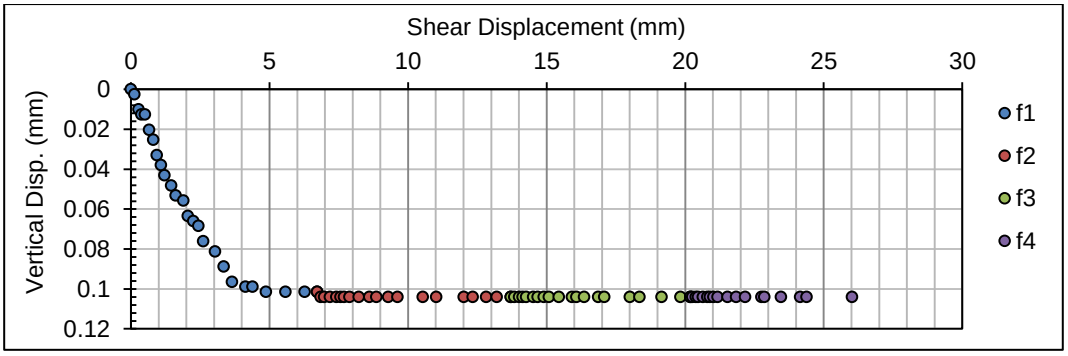

Figure 4.27 Vertical Displacement – Cumulative Shear Displacement, Ankara Clay (900 kPa)

In the highest normal stress load of the test, residual state is approached at 22 mm horizontal displacement. Recorded residual shear strength was 135 kPa. In this case, probably due to high normal load, generated shear surface has begun to deform after the first shear stage and in the next stages and unexpected raise in the shear strength is observed, so the most linearized part of the shearing stage is considered as the residual shear strength. And the selected residual shear strength is 8.6 degrees.

4.4.2 Ankara Clay (Precut Sample)

Ankara Clay sample is also prepared in a different method in which a pre-existing shear surface is artificially formed before shearing, and sheared under the effective normal stress of 400 kPa to be compared with the other sample preparation approach. In this case, final shear surface has much more uniform (and planar) shape and there were les fluctuation in the shearing stage. And the results are reasonably in the same range with the other test method. Figures 4.28 to 4.30 presents the test results.

4.4.2.1 Ankara Clay (400 kPa)

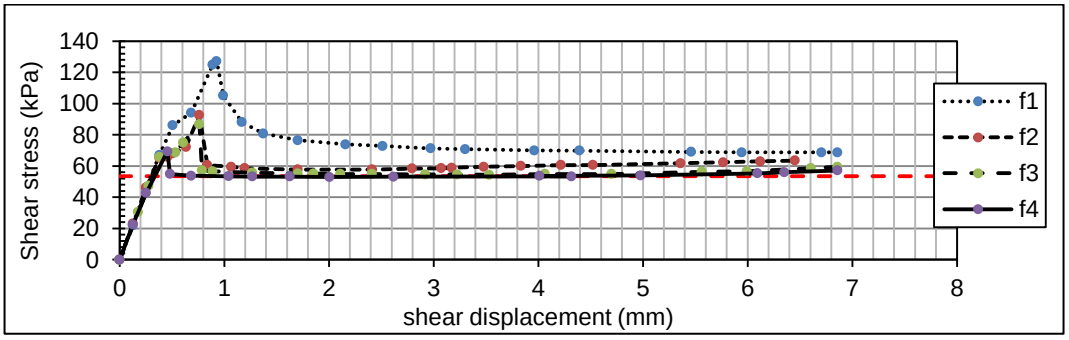

Figure 4.28 Shear Stress – Shear Displacement, Ankara Clay (400 kPa)

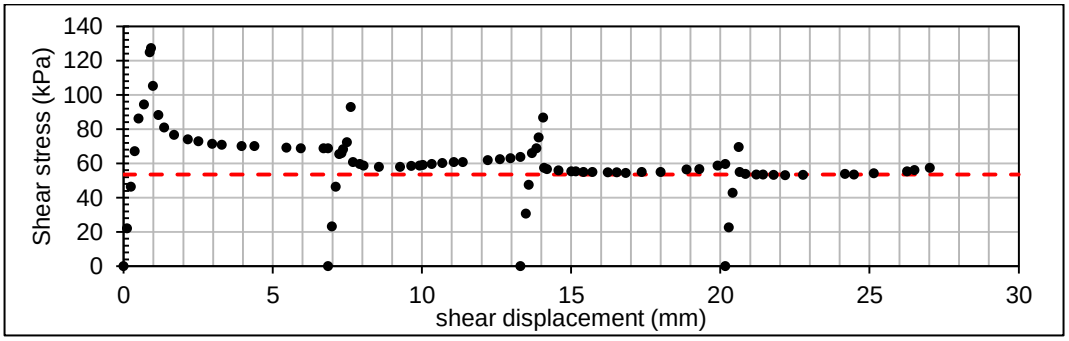

Figure 4.29 Shear Stress – Cumulative Shear Displacement, Ankara Clay (400 kPa)

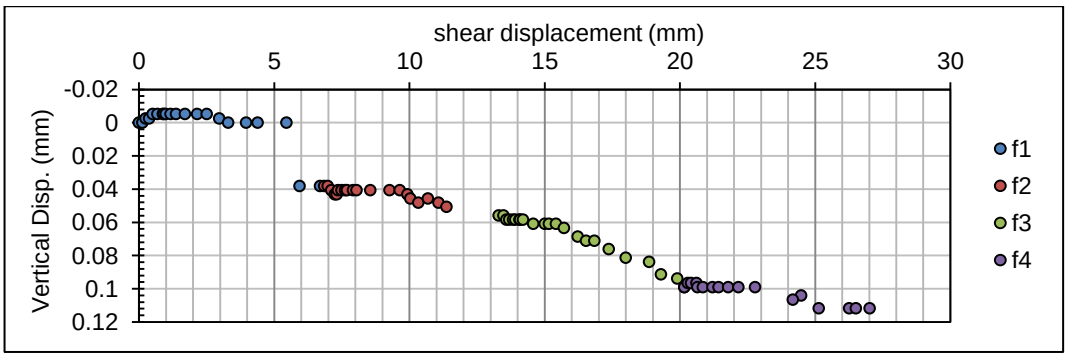

Figure 4.30 Vertical Displacement – Cumulative Shear Displacement, Ankara Clay (400 kPa)

4.4.3 Kaolinite

4.4.3.1 Kaolinite (25 kPa)

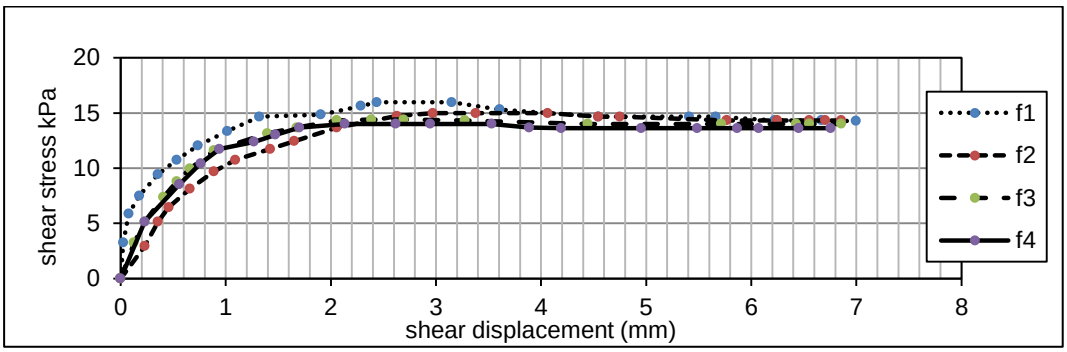

Figure 4.31 Shear Stress – Shear Displacement, Kaolinite (25 kPa)

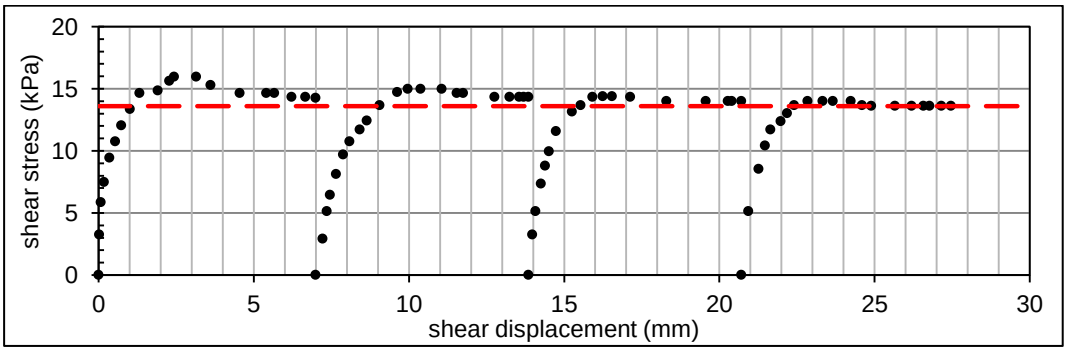

Figure 4.32 Shear Stress – Cumulative Shear Displacement, Kaolinite (25 kPa)

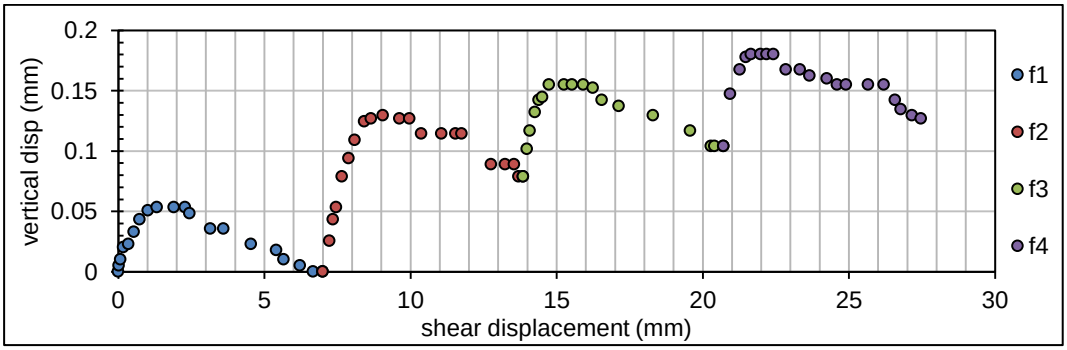

Figure 4.33 Vertical Displacement – Cumulative Shear Displacement, Kaolinite (25 kPa)

The test results illustrated in the Figures 4.31 to 4.33 the residual shear strength of kaolinite under 25kPa effective normal stress is 13.6 kPa which results in a residual friction angle of 28.6 degrees.

4.4.3.2 Kaolinite (50 kPa)

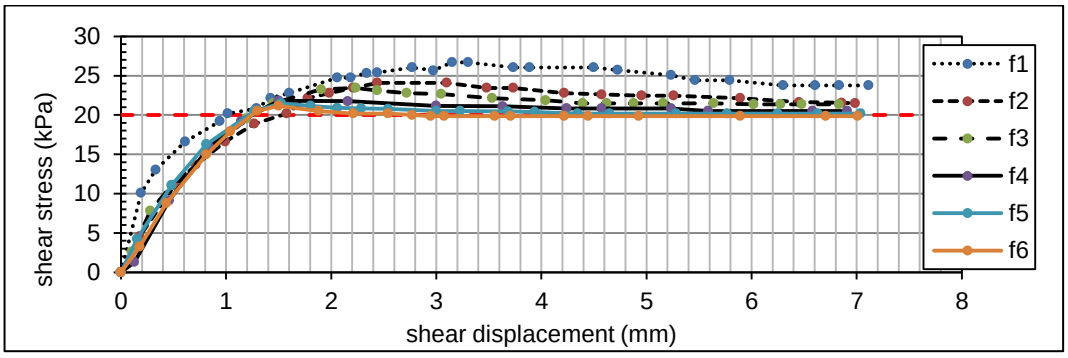

Figure 4.34 Shear Stress – Shear Displacement, Kaolinite (50 kPa)

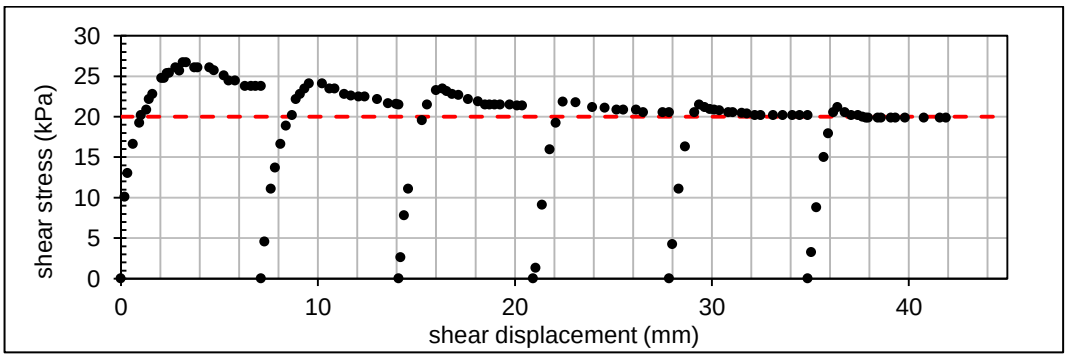

Figure 4.35 Shear Stress – Cumulative Shear Displacement, Kaolinite (50 kPa)

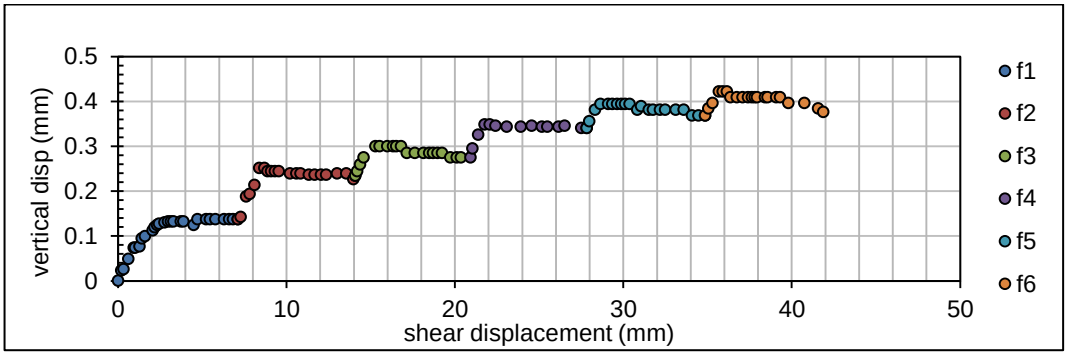

Figure 4.36 Vertical Displacement – Cumulative Shear Displacement, Kaolinite (50 kPa)

With effective normal stress of 50 kPa, Kaolinite's residual shear strength is 20 kPa which is obtained after 37 mm shear displacement. Corresponding residual friction angle is 21.8 degrees.

4.4.3.3 Kaolinite (100 kPa)

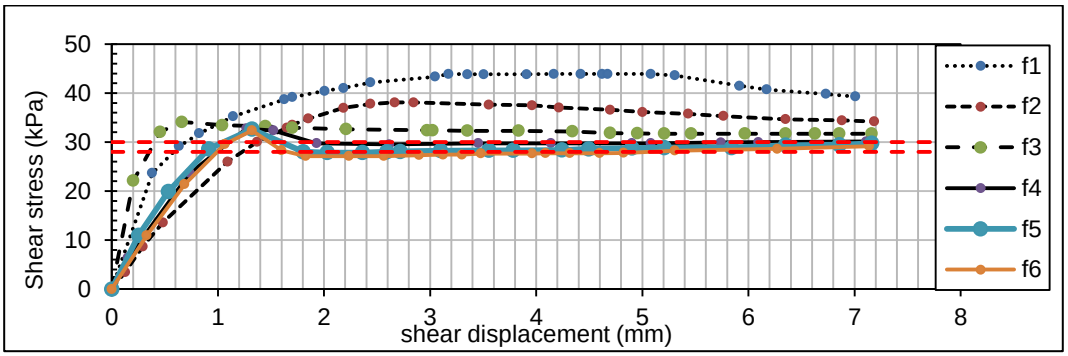

Figure 4.37 Shear Stress – Shear Displacement, Kaolinite (100 kPa)

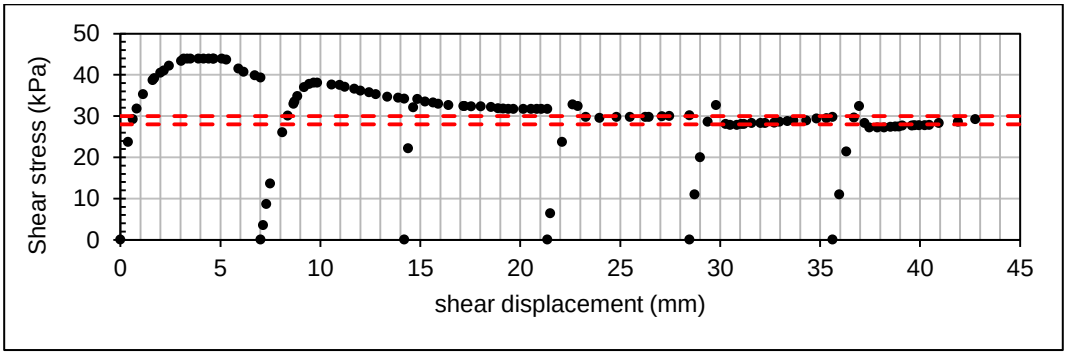

Figure 4.38 Shear Stress – Cumulative Shear Displacement, Kaolinite (100 kPa)

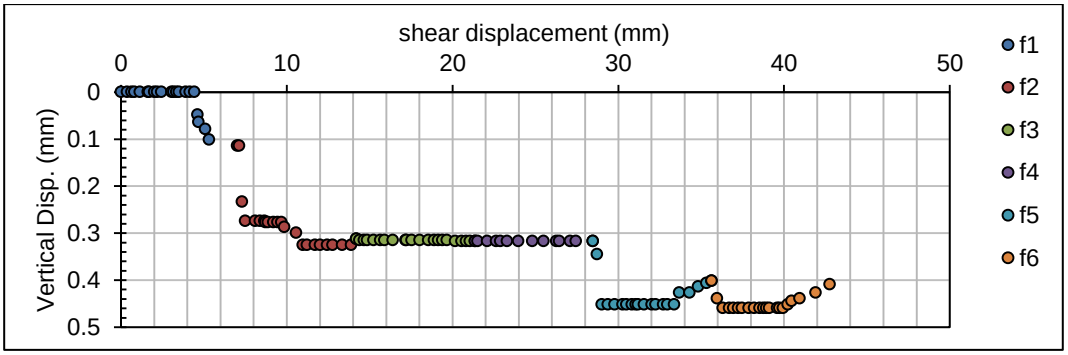

Figure 4.39 Vertical Displacement – Cumulative Shear Displacement, Kaolinite (100 kPa)

Strength test of kaolinite under 100 kPa has a set of fluctuations in large displacements that included two portion of linearized shear strength so, residual parameters are selected for a range between 28 and 30 kPa of shear strength as shown in the Figures 4.37 and 4.38. The friction angle is in the range of 15.6-16.7 degrees.

4.4.3.4 Kaolinite (200 kPa)

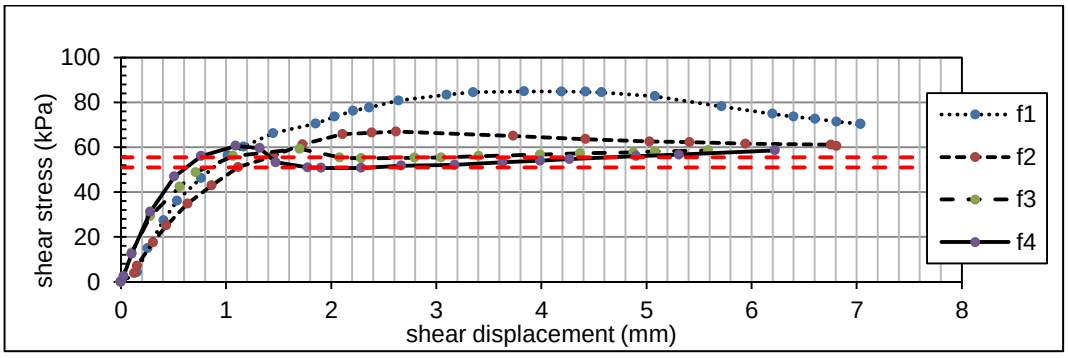

Figure 4.40 Shear Stress – Shear Displacement, Kaolinite (200 kPa)

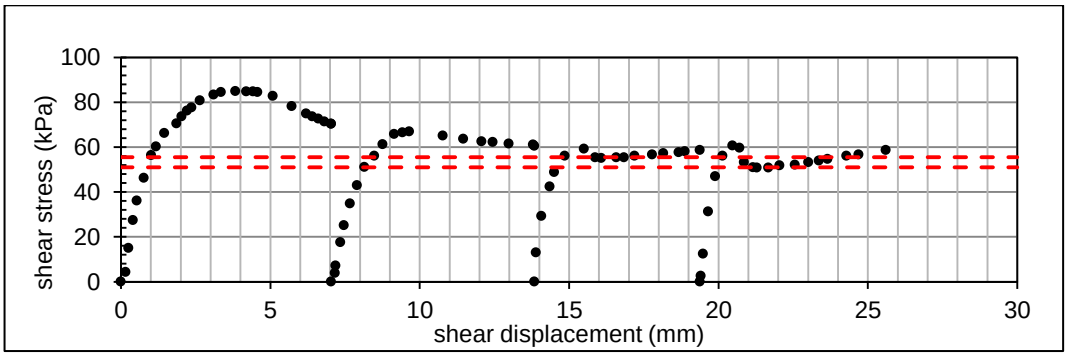

Figure 4.41 Shear Stress – Cumulative Shear Displacement, Kaolinite (200 kPa)

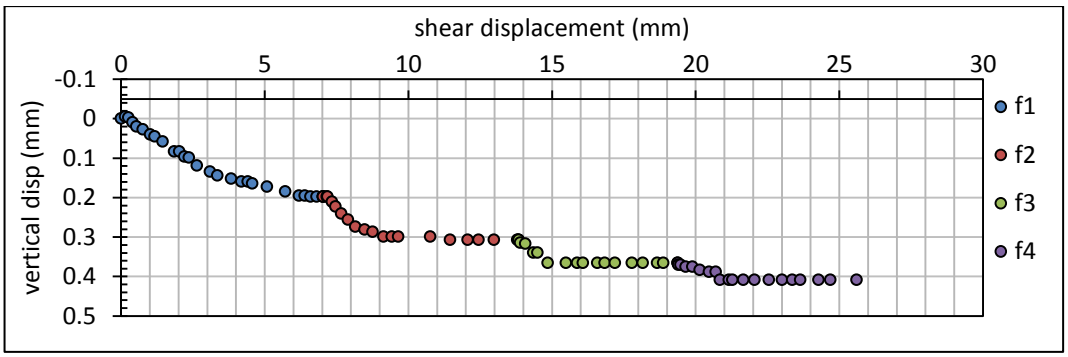

Figure 4.42 Vertical Displacement – Cumulative Shear Displacement, Kaolinite (200 kPa)

Similar to the previous test two different linear ranges are observed in the shear strength of kaolinite under normal effective stress of 200 kPa. Consequently as shown by red dashed lines two shear strength are selected as the residual shear strength in the tests which are 51 and 55.5 kPa that results in the friction angles of 14.3 and 15.5 degrees respectively.

4.4.3.5 Kaolinite (400 kPa)

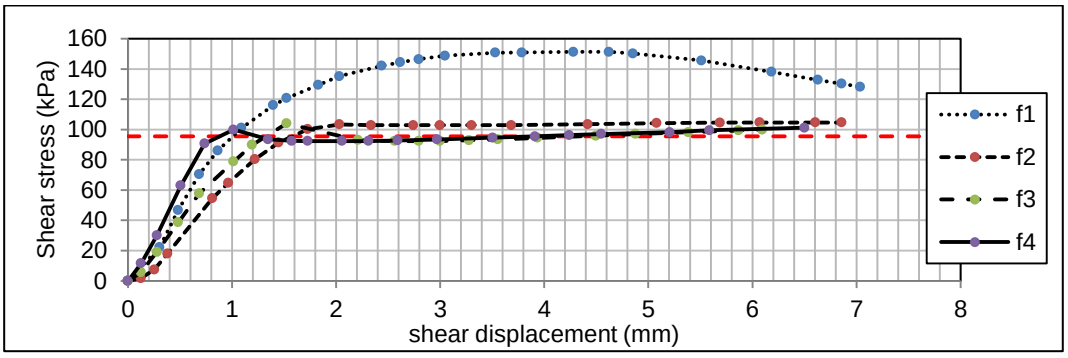

Figure 4.43 Shear Stress – Shear Displacement, Kaolinite (400 kPa)

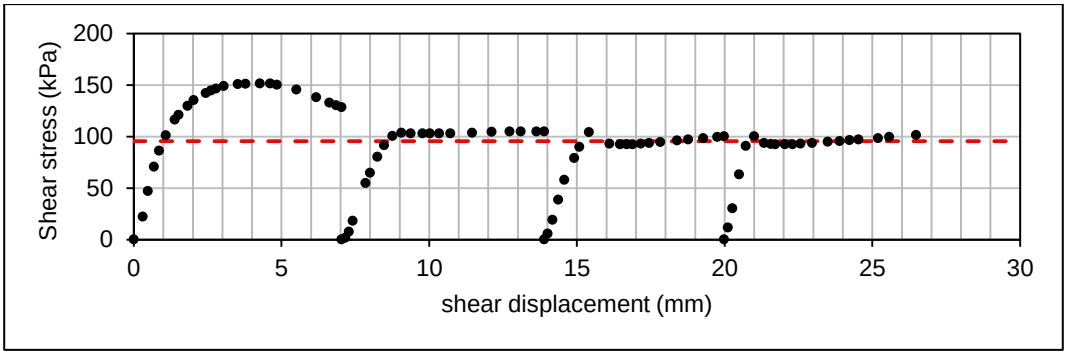

Figure 4.44 Shear Stress – Cumulative Shear Displacement, Kaolinite (400 kPa)

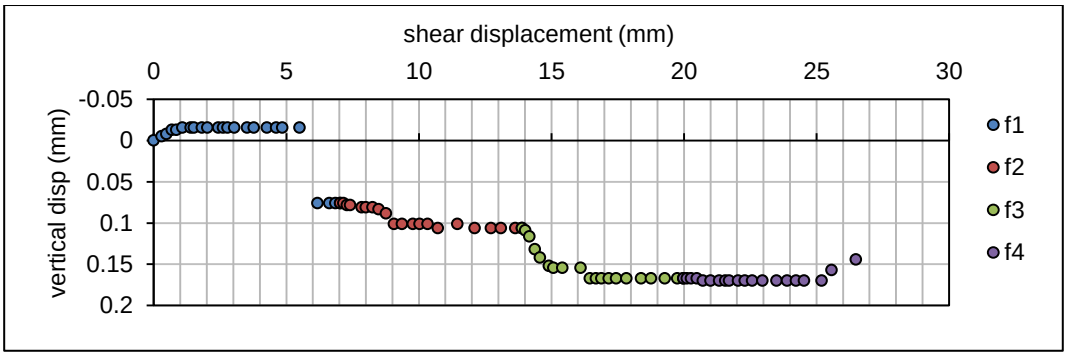

Figure 4.45 Vertical Displacement – Cumulative Shear Displacement, Kaolinite (400 kPa)

The measured residual friction angle of the kaolinite under 200 kPa effective normal stress is 13.4 degrees which is corresponding to 95.5 kPa shear strength.

4.4.3.6 Kaolinite (900 kPa)

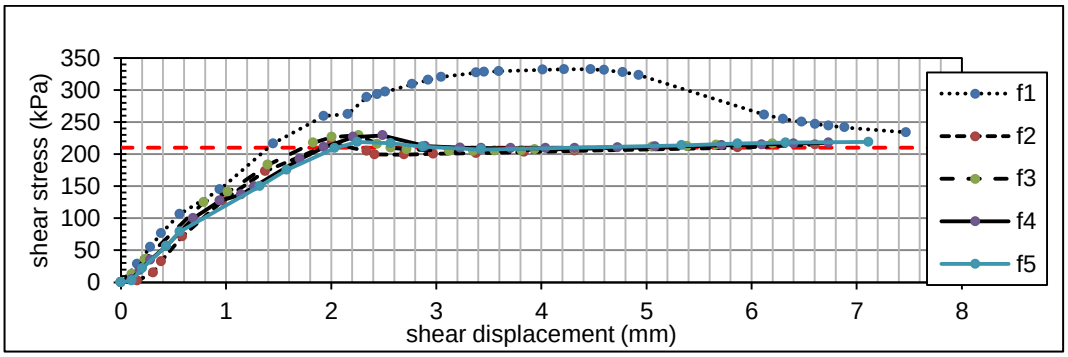

Figure 4.46 Shear Stress – Shear Displacement, Kaolinite (900 kPa)

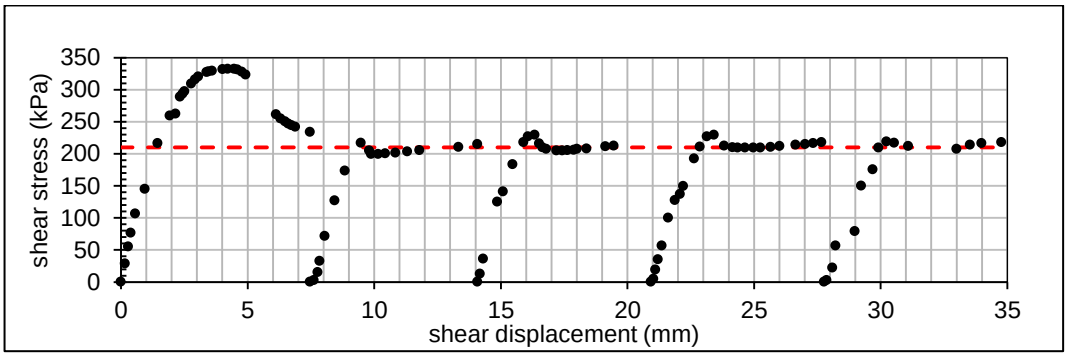

Figure 4.47 Shear Stress – Cumulative Shear Displacement, Kaolinite (900 kPa)

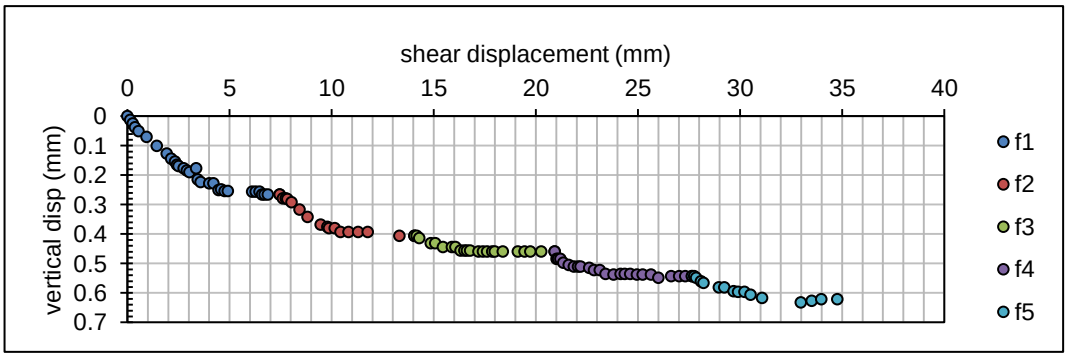

Figure 4.48 Vertical Displacement – Cumulative Shear Displacement, Kaolinite (900 kPa)

In the highest normal load of the test series, kaolinite reaches the residual state after 24 mm shear displacement. Resulted residual strength is 210 kPa and the residual friction angle is 13.1 degrees.

4.5 Residual Strength Failure Envelope

Since undisturbed samples were not available, remolded (intact and pre-cut) samples were prepared in the laboratory and consolidated to obtain an artificially produced stiff overconsolidated clay with OCR=4.0 for Ankara clay. Assuming a linear residual shear strength envelope, it is found that Ankara clay has 8.1 degrees residual friction angle for the effective normal stress range of 25 to 900 kPa (Figure 4.49).

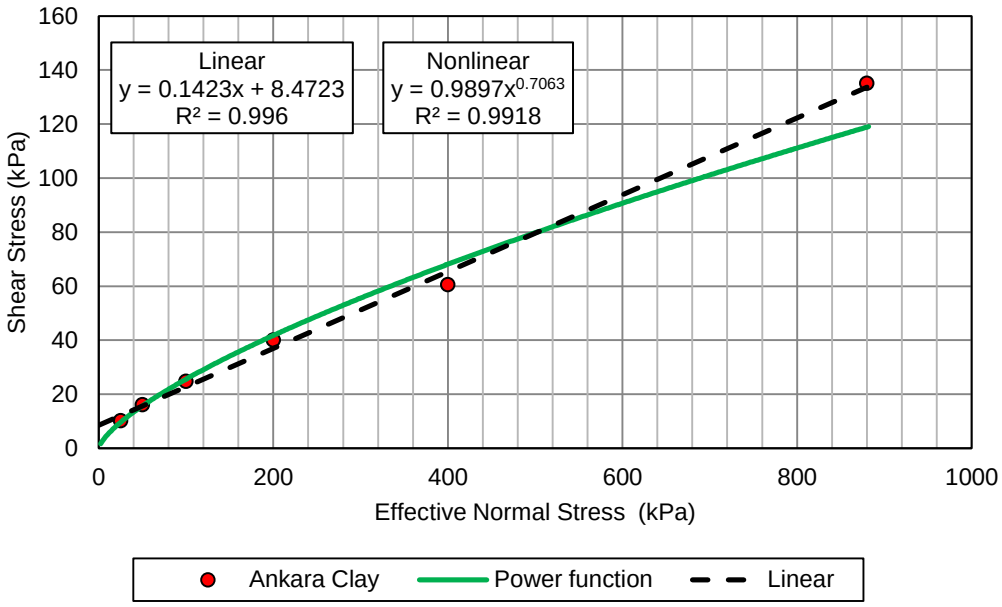

Figure 4.49 Residual shear strength envelope of Ankara Clay

Teoman et al. (2004) described three small landslides in Ankara clay and described the material as a clay and silt size material with locally sandy and gravely zones. Fines content was reported as 60-82%. The liquid limit of the material was LL=47-59%, and Ip=29-39%. Consolidated drained direct shear tests indicated a residual shear strength of on undisturbed samples gave residual parameters as c'=3-5 kPa and ϕ'_r =19-26 degrees. Back analyses results indicated c'=2-5 kPa and ϕ'_r =19-26 degrees. As reported by Teoman et al. (2004), Sonmez (2001) noted c'=15 kPa and ϕ'_r =15 degrees for the residual parameters of another sample of Ankara clay from another location. Mesri and Shahien (2003) gives for the Ip = 35% residual friction angle of 17 degrees (range 14-23 degrees) for the effective normal stress of 50 kPa.

It should be noted that Ankara clay has some variability in its properties such as the amount of clay-size particles, gravel content, % smectite in the clay-size fraction, plasticity index etc. from one location to another. Therefore it is possible that this material reported by Teoman et al. (2004) is quite different than the material in the current study. It should also be noted that the in order to define the residual condition, in direct shear test, several reversals (i.e. at least about 20 mm of cumulative forward displacement) could be necessary to be able to define the residual condition clearly. This is especially important for the undisturbed samples taken from the field that do not contain a shear plane in the field.

Ergun (1993) investigated a landslide in Erdemkent in Ankara-Cayyolu in Ankara clay material. The slope height was about 20 m and the landslide was about 150 m long. Direct shear tests were conducted on undisturbed samples to determine the residual shear strength parameters. Based on the laboratory tests c'=0-10 kPa and ϕ'_r =10-29 degrees were reported. Back-analysis carried out by Ergun (1993) found out that the shear strength parameters at the time of failure were c'=0 kPa and ϕ'_r =8-8.6 degrees. Ergun (1993) concluded in their report that the residual shear strength of the material was c'=0 kPa and ϕ'_r =8-10 degrees. This conclusion is in agreement with the current study.

Remolded (intact and pre-cut) samples were prepared in the laboratory and consolidated to obtain an artificially produced stiff overconsolidated clay with OCR=2.0 for Kaolinite clay. Assuming a linear residual shear strength envelope, it is found that Kaolinite clay has 13.4 degrees residual friction angle for the effective normal stress range of 25 to 900 kPa (Figure 4.50).

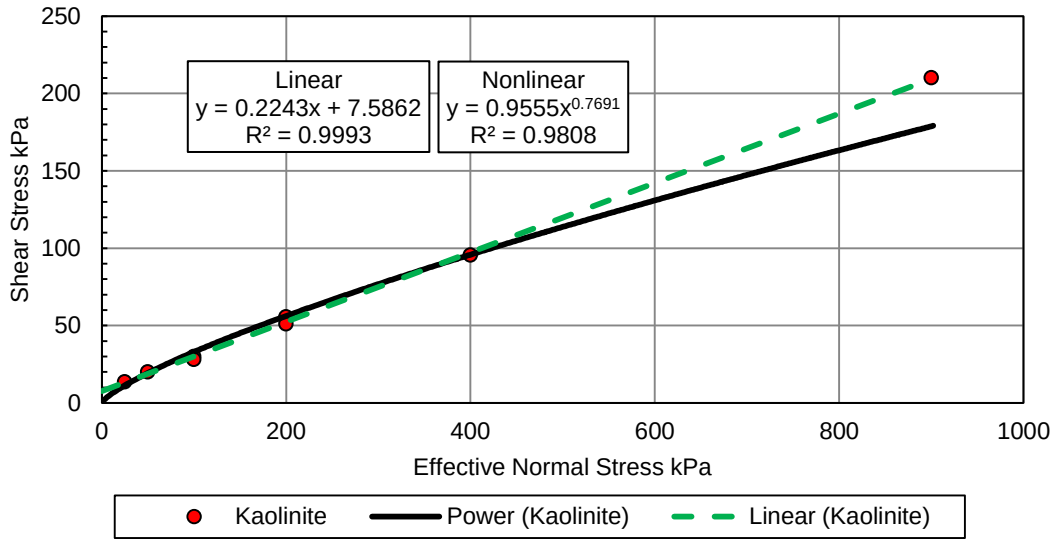

Figure 4.50 Residual shear strength envelope of Kaolinite

4.6 Shear Surface Investigation

After each test, the shear surfaces are investigated for a better interpretation of the shear strength trends during the shearing stages. Figure 4.51 illustrates some samples of the shear surface at the end of the residual test in which slickensided shiny surface is observed as in the real case slip surfaces . The point that must be taken into account is the nonuniform/irregular (undulating) shape of the shear surface which might be the result of load change due to change in the effective shearing area or the interaction between the soil particles and small generated local failures during the progressive failure.

(a)

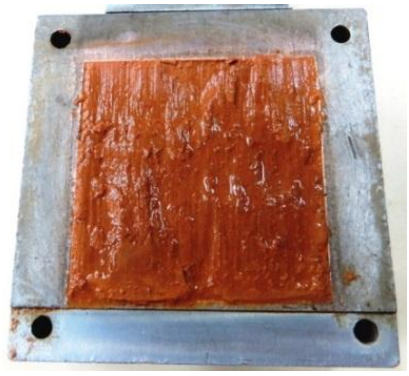

(b)

(c)

(d)

Figure 4.51 shear surface views from (a and b) Ankara Clay (c and d) Kaolinite

On the other hand, observed shear surface in the other method of sample preparation was much more uniform/planar and slickensided. In this approach the shear strength trend during the test also did not encounter any unusual alterations. A view of the precut shear surface after the test is presented in Figure 4.52.

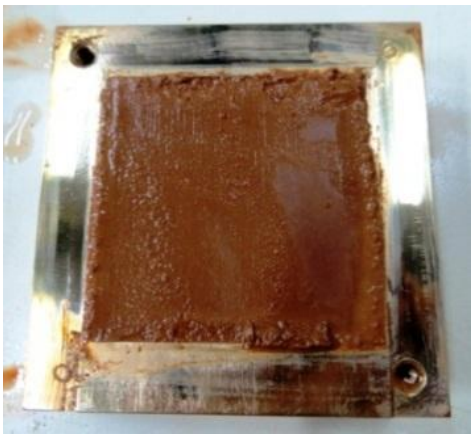

Figure 4.52 Shear surface of precut sample after the test

4.7 Interpretation of Test Results

4.7.1 Secant Internal Friction Angle at Different Normal Stresses

Figure 4.53 shows the trend of the decrease in secant residual friction angle with increasing normal stress for both Ankara clay and kaolinite. For Ankara clay the secant residual friction angle values start from 22 degrees at 25 kPa normal stress and decrease to 8.6 degrees at 900 kPa. For kaolinite secant residual friction angle of 28.6 degrees at 25 kPa normal stress decrease to 13.1 degrees at 900 kPa. This figure is also an indication of the nonlinearity of the residual shear strength envelope. The decrease in the secant residual friction angle seems to be the most significant at low normal stresses 50-100 kPa which may be relevant for shallow landslides.

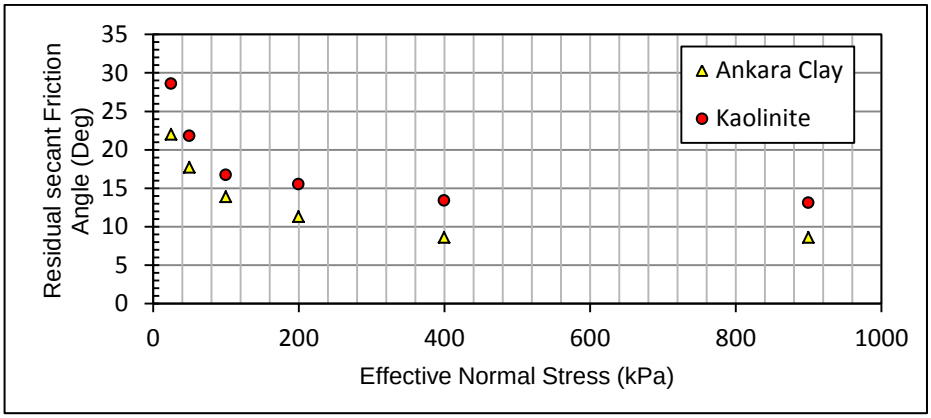

Figure 4.53 The correlation between secant residual friction angle and normal stress for the two soils tested in this study.

4.7.2 Residual shear strength and plasticity index correlations

Many researchers have investigated the empirical correlations between soil index properties and residual shear strength parameters. Figure 4.54 presents the test data on Ankara Clay and Kaolinite on the empirical trend provided by Mesri and Shahien (2003) for three different effective normal stresses.

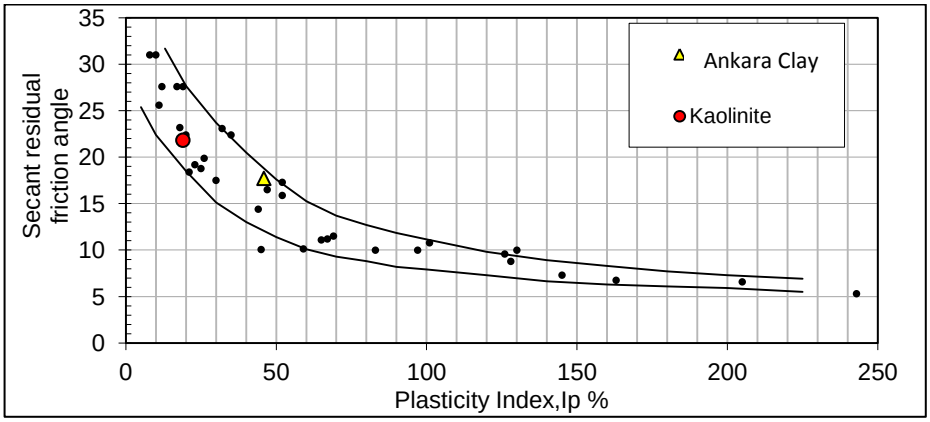

Figure 4.54 Residual Friction angle and Ip, for 50 kPa normal stress (Mesri and Shahien 2003)

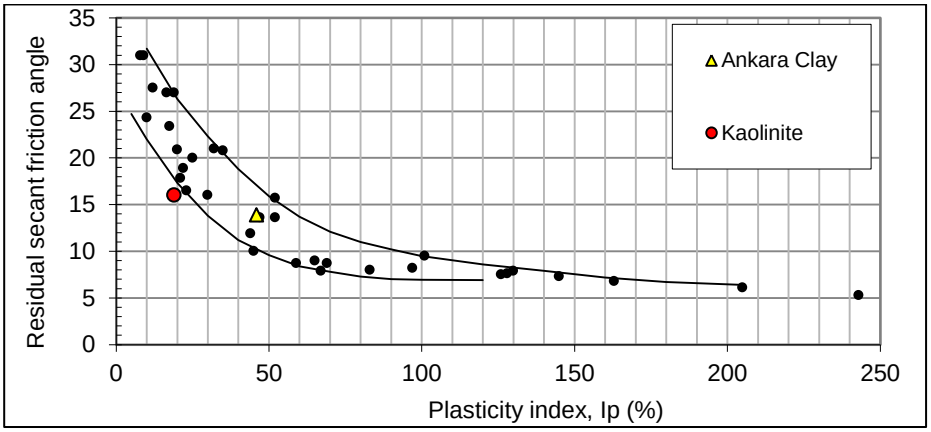

Figure 4.55 Residual Friction angle and Ip, for 100 kPa normal stress (Mesri and Shahien 2003)

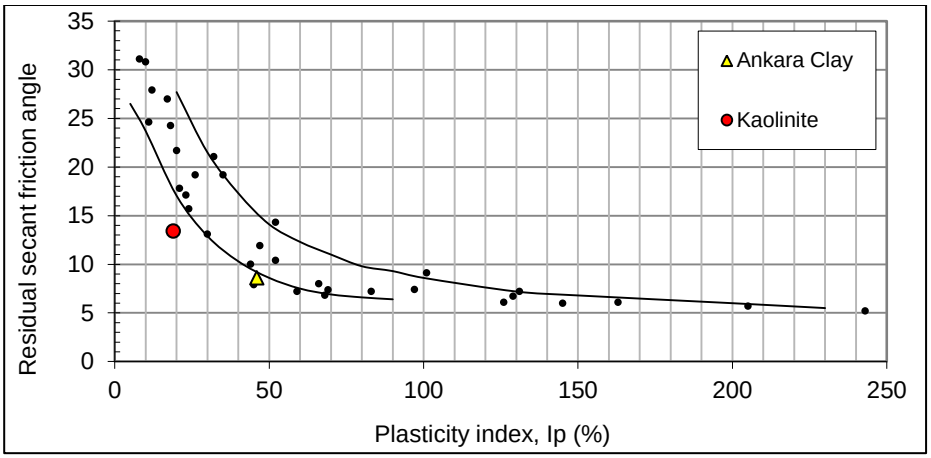

Figure 4.56 Residual Friction angle and Ip, for 400 kPa normal stress (Mesri and Shahien 2003)

4.7.3 Residual Shear Strength Failure Envelope in Comparison to Empirical Correlations

Mesri and Shahien (2003) empirical correlation is used to obtain the nonlinear residual shear strength envelope of Ankara clay. It must be emphasized that the data in Mesri and Shahien (2003) includes normal stress range of 50 to 400 kPa. In order to draw the shear strength envelope for this study up to 900 kPa normal stress, the equation is extrapolated. This extrapolation assumption may or may not be realistic. Figures 4.57and 4.58 also present a comparison of the generated failure envelops from the test results and the failure envelopes developed from empirical correlation of Mesri and Shahien (2003).

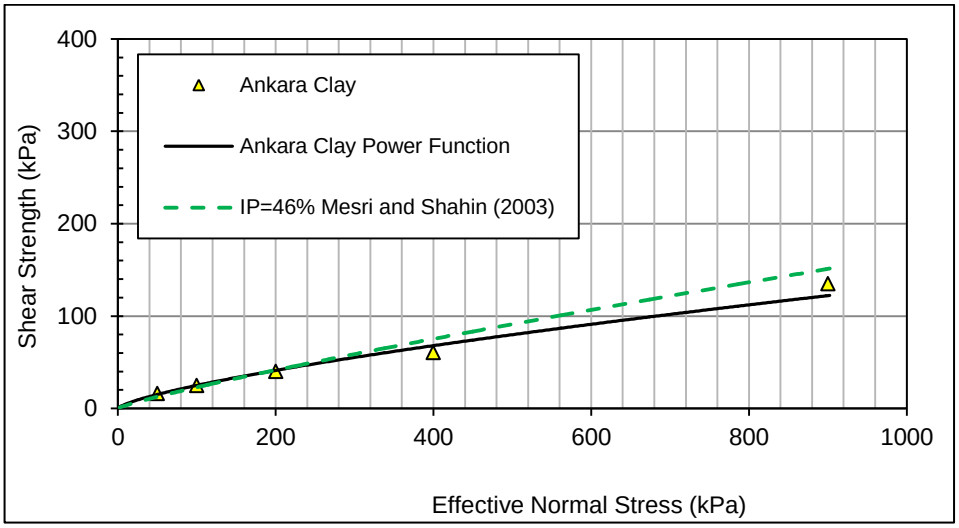

Figure 4.57 Ankara Clay's residual shear strength failure envelope compared with empirical envelopes from Mesri and Shahien (2003)

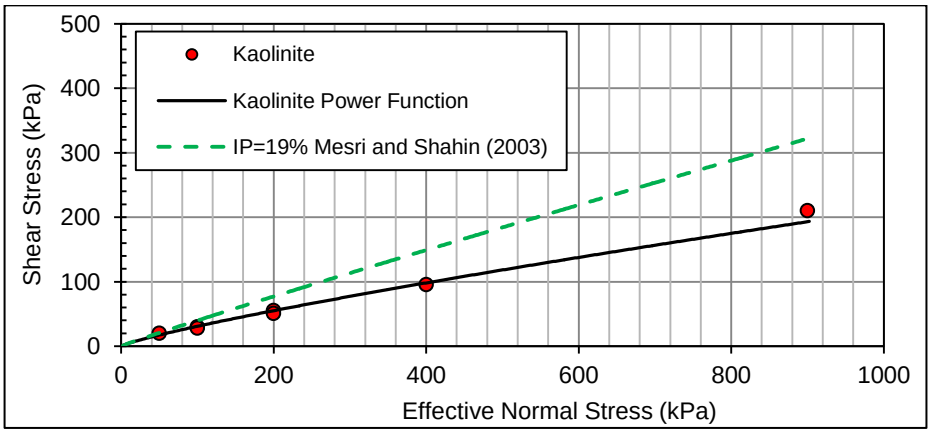

Figure 4.58 Kaolinite's failure envelope compared with empirical envelopes from Mesri and Shahien (2003)

4.7.4 Quantification of the amount of nonlinearity

Empirical correlations provided by researchers such as Mesri and Abdel-Ghaffar (1993) and Mesri and Shahien (2003) are in the form of a power function in which the amount of curvature is presented by the power of the variable in the functions. The function presented by Mesri and Abdel-Ghaffar (1993) for intact shear strength and the correlation that is proposed by and Mesri and Shahien (2003) for fully softened and residual shear strength are shown in equations 4.1 , 4.2 and 4.3 respectively.

$$s(r) = \sigma'_n \tan[\emptyset'_r]_s^{100} \left[\frac{100}{\sigma'_n}\right]^{1-m_r} \quad (4.1)$$

Where $\tan[\emptyset'_{fs}]_s^{100}$ is fully softened residual friction angle and $\tan[\acute{\emptyset}_r]_s^{100}$ is secant residual friction angle at $\sigma'_n = 100$ kPa.

Our proposed function is a power function in the form of $Y = AX^b$ ($\tau = A\sigma'^b$) . In order to compare the parameter that defines the curvature of the failure envelopes such as "m" in the correlations proposed by Mesri and Abdel-Ghaffar (1993) and Mesri and Shahien (2003) and "b" in our proposed functions, two correlations are uniformed as shown in the following procedure.

$$\begin{cases} \tau = A\sigma^b \\ s(r) = \sigma'_n \tan[\emptyset'_r]_s^{100} \left[\frac{100}{\sigma'_n}\right]^{1-m_r} \end{cases} \quad (4.2)$$

Then

$$A\sigma^b \cong \sigma'_n \tan[\emptyset'_r]_s^{100} \left[\frac{100}{\sigma'_n}\right]^{1-m_r} = \sigma_n' \times \tan[\emptyset'_r]_s^{100} \times 100^{1-m_r} \times {\sigma'_n}^{m_r-1} \quad (4.3)$$

$$A\sigma^b \cong \tan[\emptyset'_r]_s^{100} \times 100^{1-m_r} \times {\sigma'_n}^{m_r} \quad (4.4)$$

From equation 4.6 we can conclude that in both types of relationships m_r and b shows the curvature of the failure envelope and will show similar trends by changing related variables in different soil types.

To compare the change of b value and m_r value with the change of Plasticity Index values of some different soils Figure 4.59 is provided based on the available data from Mesri and Shahien (2003). The related data from Mesri and Shahien (2003) is also summarized in the Table 4.7. "b" values are obtained from the laboratory test data of Ankara Clay and Kaolinite and are presented in Table 4.6.

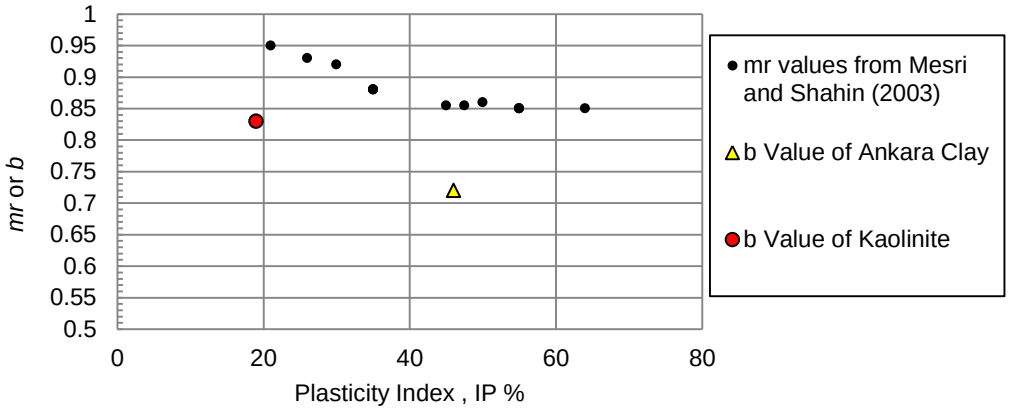

Figure 4.59 plasticity index and power correlations

Table 4.6 "*b*" values from experiments in this study

soil type	Ip (%)	"b" power
Kaolinite	19	0.83
Ankara Clay	46	0.72

Table 4.7 "m_r" values from Mesri and Shahien (2003)

soil type	Ip (%)	"mr"
London clay	50-60	0.85
Bearpaw shale	64	0.85
Santa barbara clay	35	0.88
Gault Clay	40-60	0.86
Lias clay	50-60	0.85
Lawton clay	15-40	0.98-0.86
Tertiary mudstone	30-40	0.9-0.86
Atherfield clay	21	0.95
Lugagnano clay	26	0.93
Oxford clay	45-50	0.86-0.85
Tertiary mudstone	30-40	0.9-0.86
Tault clay	40-50	0.86-0.85
London clay	50-60	0.86-0.84

4.8 The effect of area correction on residual strength parameters

In the direct shear testing, progressive shear displacement would result in a change in contact area of two shear box halves (Figure 4.60). Consequently, effective normal stress and shear stress must be calculated according to the corrected area. Terzaghi et al. (1996) states that this can be avoided if the data are interpreted based on the ratio of the shear stress and normal stress.

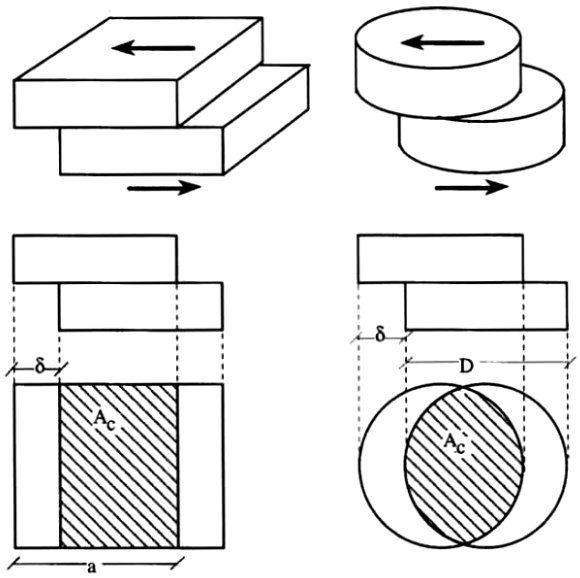

Figure 4.60 Change in the contact area in direct shear test (Bardet, 1977)

Since direct shear tests on the selected soils are conducted in square and cylindrical direct shear boxes, area correction method for both of the box types are explained (Bardet, 1977).

As shown in the Figure 4.60, in the square shaped direct shear box, A_c is the corrected area that is changing by the relative shear displacement of δ.

$$A_c = a(a - \delta) \tag{4.5}$$

Where *a*, is the length of the square box and δ is the relative shear displacement.

In addition, in the cylindrical box the corrected area is calculated as follows;

$$A_c = \frac{D^2}{2}(\theta - \frac{\delta}{D}\sin\theta) \tag{4.6}$$

Where $\theta = \cos^{-1}(\frac{\delta}{D})$ and θ is in radians.

Figure 4.61 and 4.62 present a comparison of the recorded direct shear test data with and without area corrections for two sample tests. It is also worthy of note that the effective normal stress for the recorded data is constant (e.g. 200 kPa in the Figure 4.61) but for the corrected data each data point has different effective normal stress which must be taken into account in interpretation of the data.

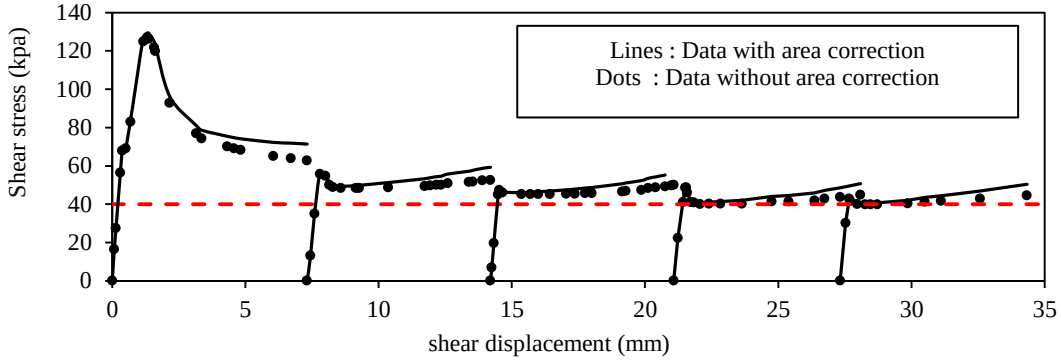

Figure 4.61 area correction in recorded data of Ankara Clay under 200 kPa effective normal stress in square box

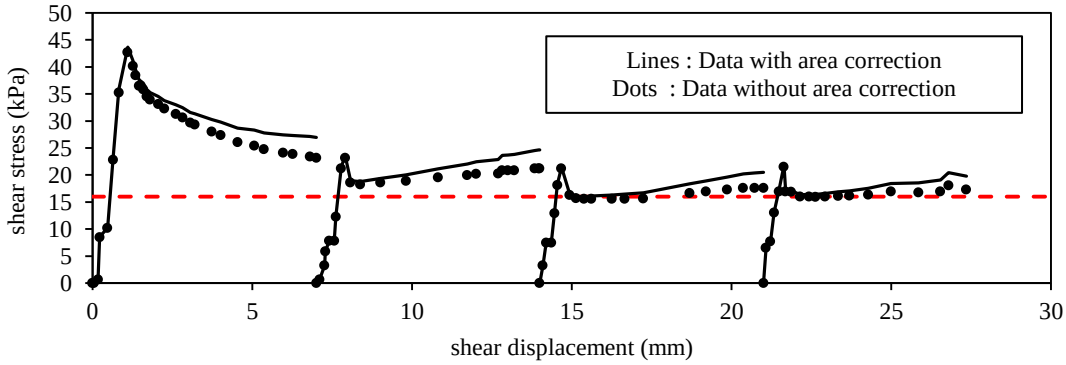

Figure 4.62 Area corrections in recorded data of Ankara Clay under 50 kPa effective normal stress in Cylindrical box

In order to investigate the effect of area corrections in the calculated residual shear strength parameters as well the amount of nonlinearity , for the corrected data point new failure envelopes are generated . Since the corrected data point are moved a little to the upper right side relative to previous point without area correction the observed change in the calculated parameters and the nonlinearity were negligible.

Tables 4.8 and 4.9 present the generated linear and nonlinear failure envelopes for Ankara clay and kaolinite, respectively. In addition in Figure 4.63 the residual shear strength failure envelope data points for Ankara clay and kaolinite with and without area corrections are illustrated.

Table 4.8 Effect of the area corrections in the shear strength failure envelope of the Ankara clay

Ankara Clay	without area correction	Residual Strength parameters (raw data)	with area correction	Residual Strength parameters (corrected data)
linear	y = 0.1377x + 9.7967	c= 9.8 kPa , ϕ=7.84 Deg.	y = 0.1375x + 9.9119	c= 9.9 kPa , ϕ=7.83 Deg.
linear zero inter cept	y = 0.1535x	ϕ = 8.7 Deg.	y = 0.1529x	ϕ = 8.7 Deg.
power function	$y = 0.9555x^{0.7691}$	-	$y = 0.9212x^{0.7183}$	-

Table 4.9 Effect of the area corrections in the shear strength failure envelope of the kaolinite clay

Kaolinite	without area correction	Residual Strength parameters (raw data)	with area correction	Residual Strength parameters (corrected data)
linear	y = 0.2245x + 7.4737	c= 7.5 kPa , ϕ=12.6 Deg.	y = 0.2255x + 7.6451	c= 7.6 kPa , ϕ=12.7 Deg.
linear zero intercept	y = 0.238x	ϕ = 13.4 Deg.	y = 0.2374x	ϕ = 13.3 Deg.
power function	$y = 0.6654x^{0.8335}$	-	$y = 0.6489x^{0.8402}$	-

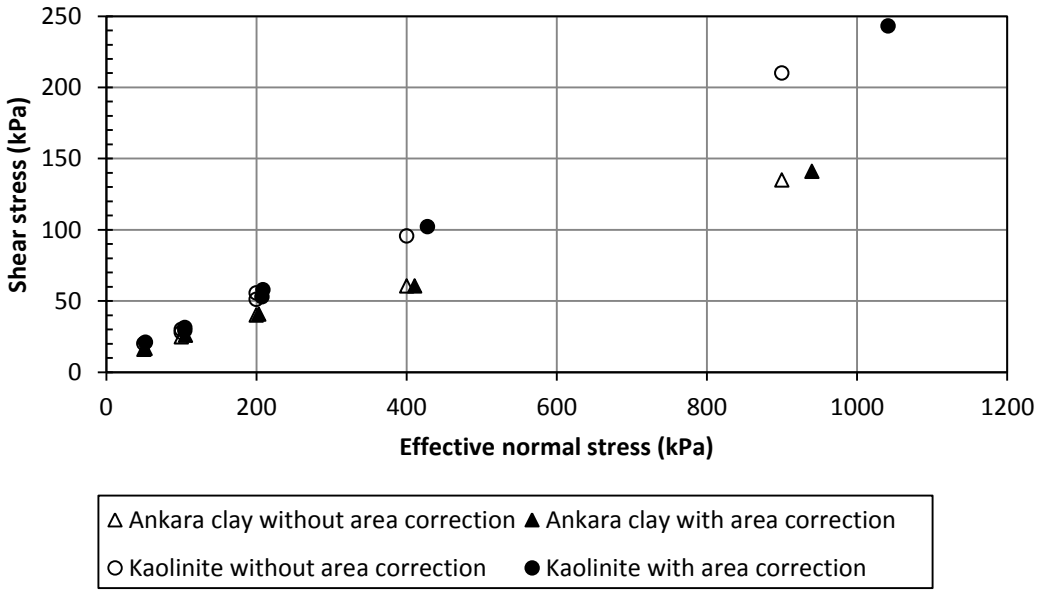

Figure 4.63 Ankara clay and kaolinite residual shear strength failure envelope data points.

CHAPTER 5

CASE HISTORIES AND PARAMETRIC STUDY

In this chapter, a number of reactivated landslide case histories are analyzed together with a parametric slope stability study in order to observe and demonstrate the practical significance (or lack thereof) of the nonlinearity of the residual shear strength envelope. In the following sections, firstly, a number of real life cases are evaluated and a parametric study is presented.

5.1 Balikesir Open pit mine

The investigated case is Balikesir open pit mine located in western central part of Turkey as shown in Figure 5.1 (a) and (b). This is one of the main borate mines in Turkey that has created immense economic benefits in more than one decade of production, and still has noticeable potential economic income.

(a) (b)

Figure 5.1 Location of the Balikesir open pit mine

In most of the engineering projects that there are excavations during construction, the soil or rock is locked in stresses. Releasing the existing stress would make the earth prone to failure during excavation. In addition, ground water level or even free water on the surface due to precipitations may significantly affect the excavation behavior from stability point of view. Figures 5.2 (a), (b) and (c) reveal the tension cracks detected on February 2011 near the peak of the hill. The cracks were reported to have about 700 meters length, about one meter width and a significantly deep depth. Observed tension cracks were the first clues of detecting the location of failure surface in the deep sliding mass. The cracks are considered as the scarp of landslide.

(a) (b) (c)

Figure 5.2 Observed tension cracks at the top of the hill near the open pit mine

Further investigations were performed towards the center of the open pit mine with the purpose of detecting actual failure surface. Different locations on the benches have been selected to drill two boreholes. As shown in the Figure 5.3, SK1 and SK2 boreholes were drilled at elevations of 93.1 m and 76.8 m respectively. Standard Penetration Test is conducted, soil samples are collected and inclinometers are installed in these boreholes. The lateral displacement of the sliding mass have been monitored in two boreholes by inclinometers. Scrutinizing the inclinometers' recorded data and the extracted soil profile from the boreholes, exact location of the failure surface has been detected on the toe of the sliding mass. Observed failure surface is extrapolated for the unknown portion, so that it passes from the existing tension cracks above the hill. Electrical resistivity tests are also used. Details of this study is presented in a consulting report by Duzgun et al. (2012).

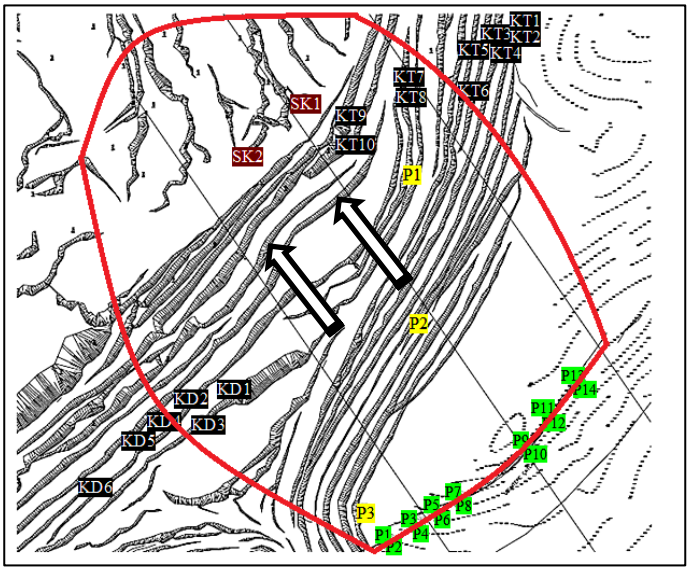

Figure 5.3 Location of boreholes and surface movement monitoring points (side boundaries, red lines, of the landslide are uncertain)

As the mine production phase proceeds, due to change in ground water level, seasonal precipitations or excavating the toe of slopes which keeps the slopes stable, local failures start throughout the trenches or in a large scale in a portion of the circular shape of the mine. Local failures demolished the

confining stresses. Consequently, driving forces will overtake the resisting shear strength of the earth material resulting in a factor of safety lower than one.

Soil profile estimated from site investigations shows a weak clayey layer adjacent to failure surface. Material properties for upper parts of the slope are estimated from previous investigation reports performed before the start of construction.

5.1.1 Laboratory and field tests and results

In-situ tests such as SPT test and electrical resistivity tests are utilized in addition to laboratory tests to determine soil types, properties, and location of the failure surface in the field. Electrical resistivity test results are presented in Figure 5.4 for four different profiles parallel to each other along the width of the sliding mass. Each of these profiles shows the electrical resistivity of earth materials beneath the installed wire line in different elevations parallel to contour lines.

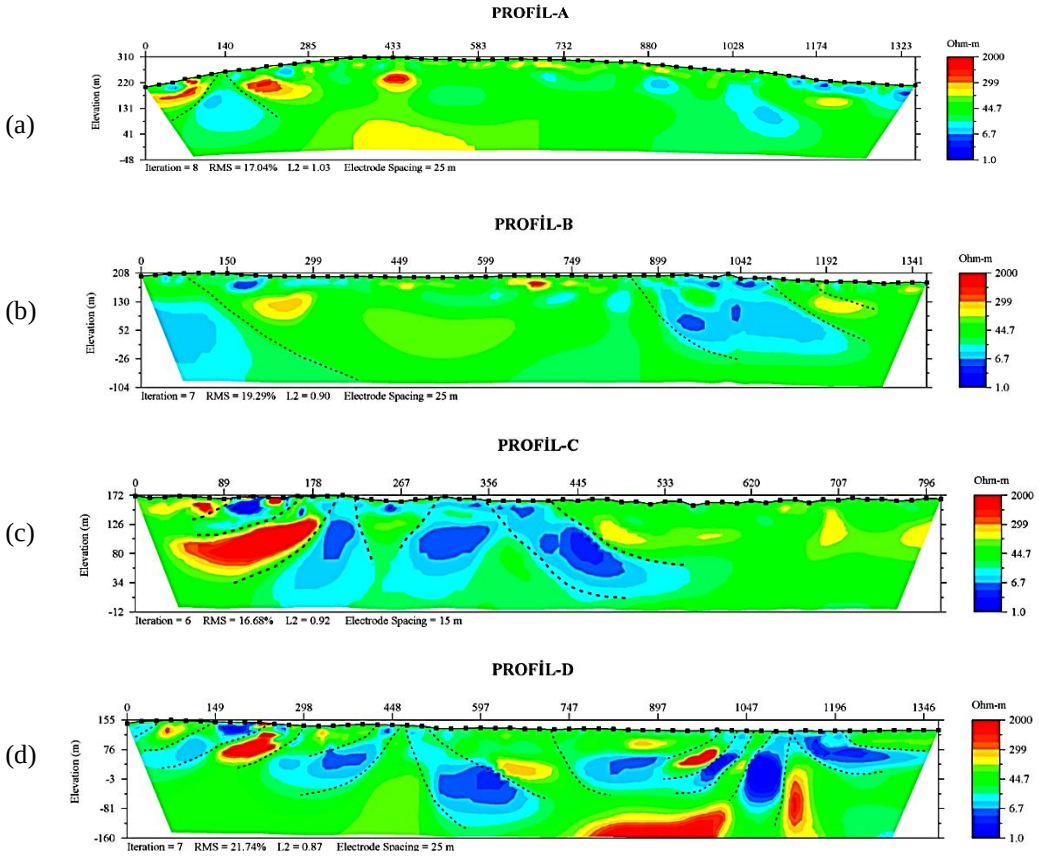

Figure 5.4 Electrical resistivity test results

In addition, samples taken to the laboratory are used to categorize and measure the strength parameters of the soils to be used in stability analyses. Index properties of available samples are determined by standard tests based on ASTM standards. Table 5.1 summarizes index properties of the samples.

Table 5.1 Index properties

borehole	SK1	SK1	SK1	SK1	SK2
Depth (m)	24.5-25	22.3-22.5	19.2-20	13.8-14	31.6-32
Specific Gravity	2.79	2.82	2.79	2.80	2.72
LL (%)	33	33	46	-	59
PI (%)	8	7	18	-	37

Failure surface was observed in clayey layer in two inclinometers installed in two boreholes. Consequently, consolidated drained direct shear tests according to ASTM D3080 standard are conducted on the clayey sample. Considering the slickenside surface observed in the borehole samples and the movements already observed in this site the shear strength that must be considered for stability analysis would be the residual shear strength. Therefore, reversal residual direct shear tests are performed to obtain the residual internal friction angle. Remolded samples are prepared from pulverized and air dried clayey soil. In sample preparation, the water content is set near the liquid limit of the clay, and then the pasty material is placed in the direct shear box as homogenous as possible to a specific height in layers of small thicknesses. The sample is consolidated under incremental loads with load increment ratio of one. Tests are performed at 100, 200, 400 and 900 kPa of effective normal stress after consolidation stage. Very low shearing rates, in the range of 0.024 millimeters per minute, are selected to prevent generation of the excess pore water pressure and allow the drainage during shearing.

5.1.2 Cross section of the landslide

Stability analysis is performed for two different cross sections of the sliding mass. One of the cross sections presented in the Figure 5.5 is the original profile of the mine slope and Figure 5.6. reveals the slope profile after excavating from the upper portion of the slope which is proposed for the failure mitigation in the mines construction plans. As shown in Figure 5.5, ground water level is considered in the toe of the slope because there were a drainage system which conveys the water level to a constructed canal near the mine which kept the water level in lower elevations.

5.1.3 Nonlinear function of the failure envelope (residual strength)

The data obtained from consolidated drained reversal direct shear test are utilized for constructing the residual shear strength failure envelope of the soil. Both linear and nonlinear failure envelopes and the related functions are illustrated in the Figure 5.7.

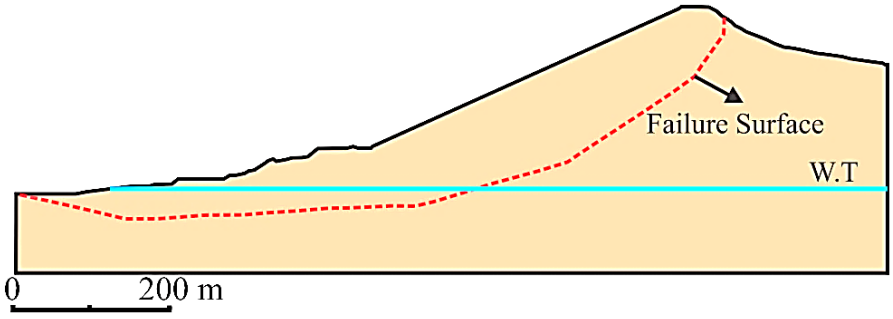

Figure 5.5 Balikesir Landslide cross sections original profile

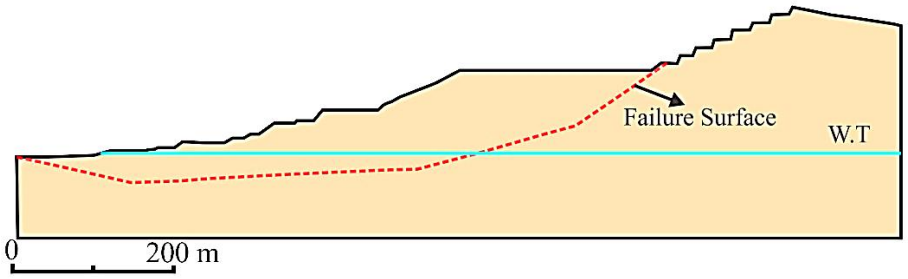

Figure 5.6 Balikesir Landslide cross sections, excavated upper part

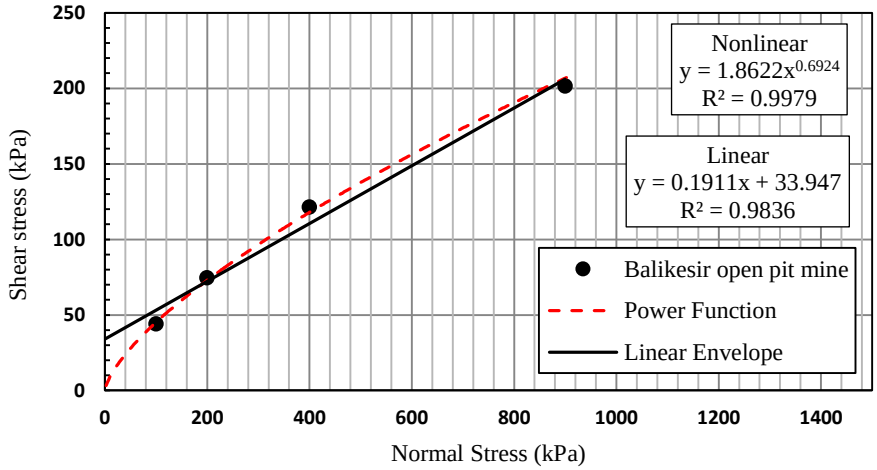

Figure 5.7 Linear and nonlinear residual shear strength failure envelope of Balikesir mine

5.1.4 Stability Analyses

A set of limit equilibrium stability analysis are performed for the available shear surface in both cross sections. In the analysis, non-linearity of the failure envelope is also taken into account and the linear and nonlinear factor of safeties are compared. For the analysis the limit equilibrium method (SLIDE v.6.0 software is utilized. In the linear failure envelope analysis material properties is selected from Mohr-Coulomb criterion from the investigation report which proposed a cohesion of 1 kPa and Internal friction angle of 19 degrees for the clay material. For the nonlinear failure envelope a user-defined function is given in the strength definition tab and normal and shear strength from the nonlinear power function is defined for the clay material as shown in Figure 5.8. The screen shot images of the slope stability analyses can be seen in figure 5.9.

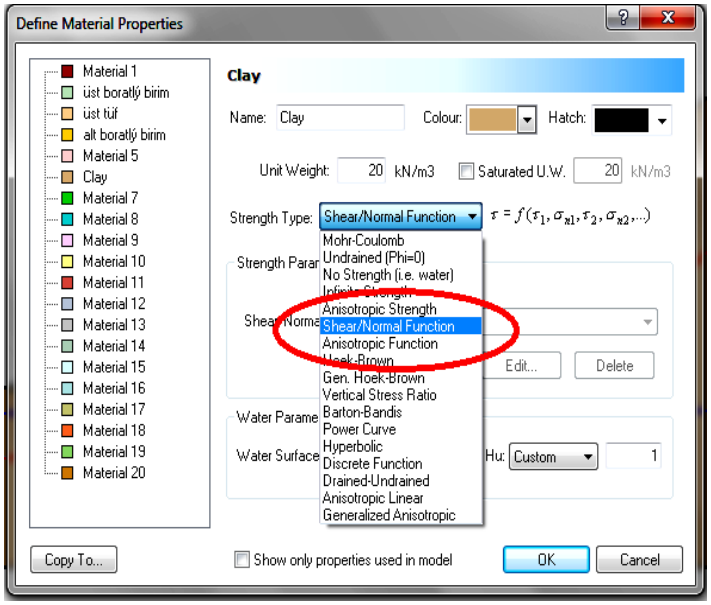

Figure 5.8 Defining nonlinear envelope for clayey material in SLIDE v.6.0 Program

Table 5.2 Linear and Non-linear material properties

Material	**Unit Weight kN/m^3**	**Linear Envelope**		**Nonlinear Function**
		C' (kPa)	Φ' (deg)	
Balikesir Clay	20	1	19	$\tau = 1.8622\sigma^{0.6924}$

Table 5.3 Stability analyses results

Cross Section	F.S. using linear shear strength envelope	F.S. using nonlinear shear strength envelope
Original Profile's F.S	1.1	0.7
Excavated Profile's F.S	1.9	1.2

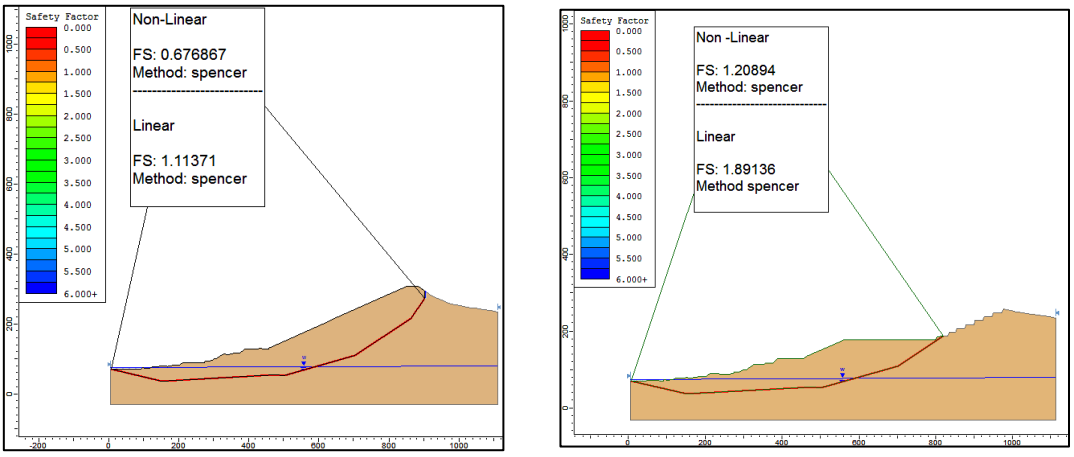

(a) (b)

Figure 5.9 Slope stability analyses results using linear and nonlinear shear strength envelopes (a) Original profile (b) Excavated profile

5.2 Jackfield Landslide

5.2.1 Site definition

This landslide occurred at the village of Jackfield, Shropshire, on the River Severn 1.25 miles downstream of Iron Bridge in 1952. The mass movement led to intensive damages to several houses and existing railway and road. Skempton (1964) mentions coverage of continuous erosions in the area, which results in a number of landslides.

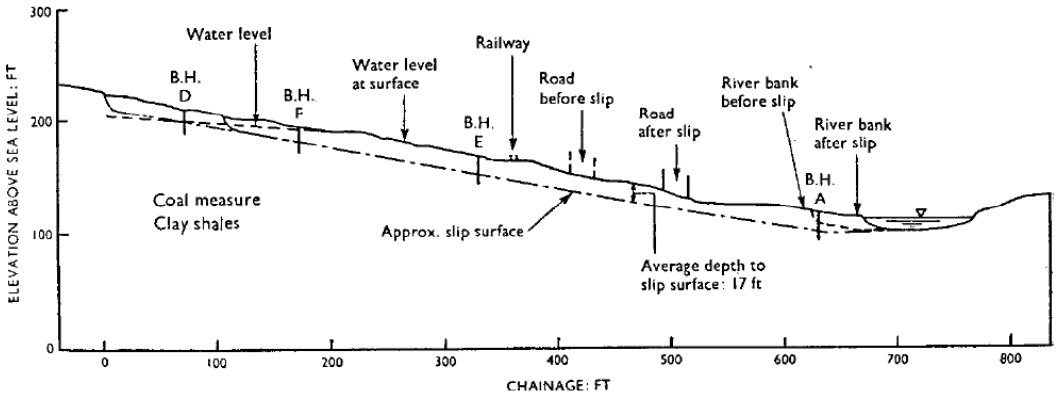

Figure 5.10 Cross section of the landslide (Henkel and Skempton 1954)

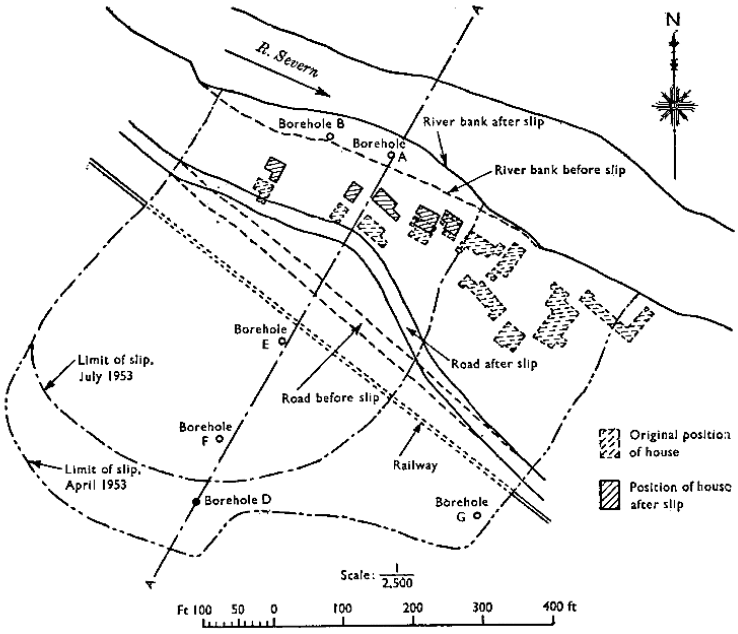

Figure 5.11 Plan view of the sliding limits and movement of the local houses (Henkel and Skempton 1954)

Initiation of the rapid ground movement was the result of continuous heavy rains during the winter in 1952. In July 1952, a maximum horizontal movement in the center of the slide and at the foot of the slide on the riverbank was reported as 60 ft (18 m) and 30 ft (9 m) respectively. The relative difference in the mass movement severely damaged the local brick houses as shown in Figure 5.12 (a) and (b).

(a) (b)

Figure 5.12 Damaged brick houses in Jackfield landslide (British Geological Survey)

To measure the ground water level and location of failure surface, a number of boreholes were drilled in various points as shown in Figure 5.10. Short-lengths of open jointed clay pipes were utilized as a liner of the boreholes to locate the depth of the sliding mass. Based on the site investigations it was concluded that this landslide is a "shallow rotational slide" (Henkel and Skempton 1954) although it looks like from the cross section given above that it is an "infinite-slope" type, translational slide.

5.2.2 Material properties

The extension of sliding area continued by April 1953, as shown on the plan view in Figure 5.10. Failure surface is observed in the zone of weathered, fissured clay extending to a depth of 20 ft. to 25 ft. below the surface. Consequently, Henkel and Skempton (1954) and Skempton (1964) performed a set of experiments on the clay layer. The index properties and drained residual shear strength test with direct shear box results of the clay samples are presented in table 5.4 and Figure 5.13 respectively. The initial tests performed by Henkel and Skempton (1954) are repeated and modified by Skempton (1964) and the results are utilized in stability analyses.

Table 5.4 Index properties of the clay sample

Liquid Limit (%)	45
Plasticity Index (%)	25
Density (lb/cu.ft)	130
PI/Clay-size Fraction	0.6

5.2.3 Nonlinear function of the failure envelope

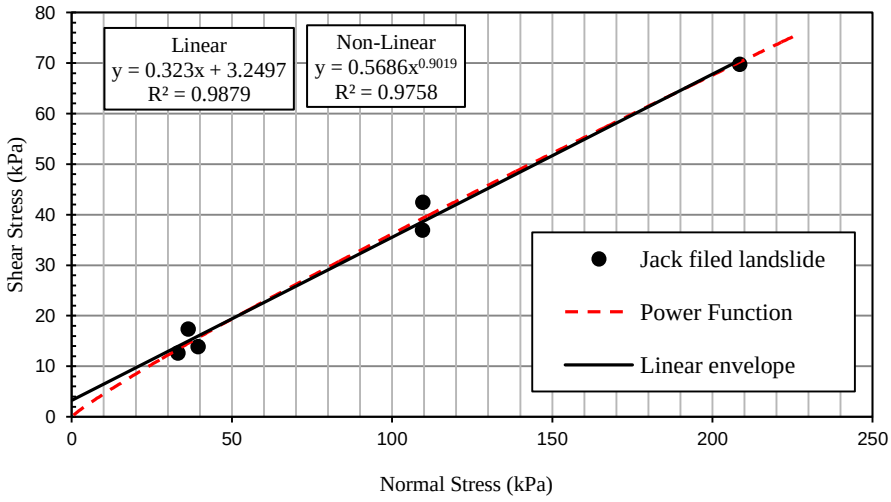

Figure 5.13 Linear and nonlinear failure envelopes

5.2.4 Stability Analyses

Stability analyses have been conducted on the Jackfield landslide as described in 5.1.4 and the linear and nonlinear residual shear strength envelopes are defined from the test data. Material properties and factor of safeties for the linear and nonlinear analyses are summarized in table 5.5 an 5.6 and Figure 5.14.

Table 5.5 Linear and nonlinear shear strength envelope of the material in Jackfield landslide

Material	Unit Weight	Linear Envelope		Nonlinear Function
Jackfield Clay	20 kN/m3	C' (kPa)	Φ' (deg)	$\tau = 0.568\sigma^{0.9019}$
		0	17	

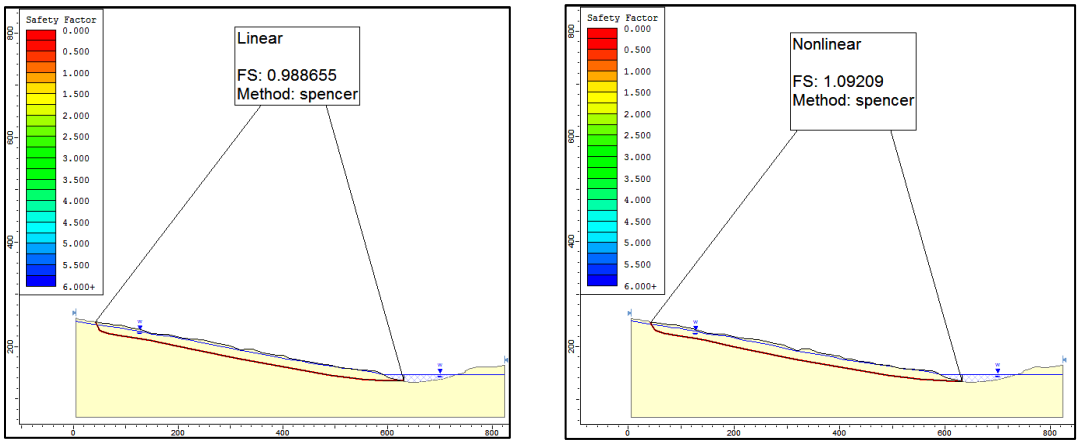

(a) (b)

Figure 5.14 The slope stability analyses results of using (a) Linear shear strength envelope (b) nonlinear shear strength envelope

Table 5.6 Stability analyses results

Cross Section	F.S. using linear shear strength envelope	F.S. using nonlinear shear strength envelope
Factor of Safety	1.0	1.1

5.3 Cortes de Pallas Landslide

5.3.1 Site introduction

Alonso et al. (1993) performed and study on Cortes de Pallas Landslide located in the province of Valencia, eastern Spain. Figure 5.15 shows the location of the landslide near the left bank of the Jucar River. Initiation of the landslide was due to quarry excavations. These excavations lead to reactivation of a preexisting landslide.

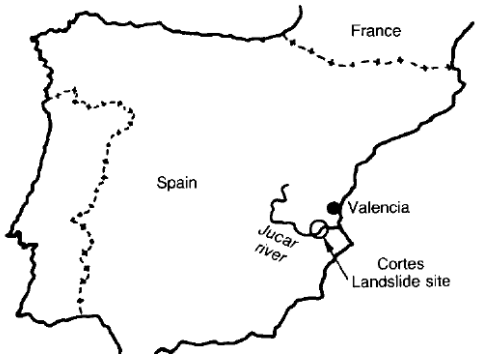

Figure 5.15 Location of the landslide, Alonso et al. (1993)

Alonso et al. (1993) have back analyzed the slope based on the monitored displacement and a set of strength and index properties test data performed in their laboratory and suggested an additional fill and excavation for destabilizing the reactivated landslide. Besides the lithological profile that has been obtained from boreholes in the landslide area, the inclinometer data which is presented in the Figure 5.16 shows that the failure surface is located in a 2 m depth in marl layer.

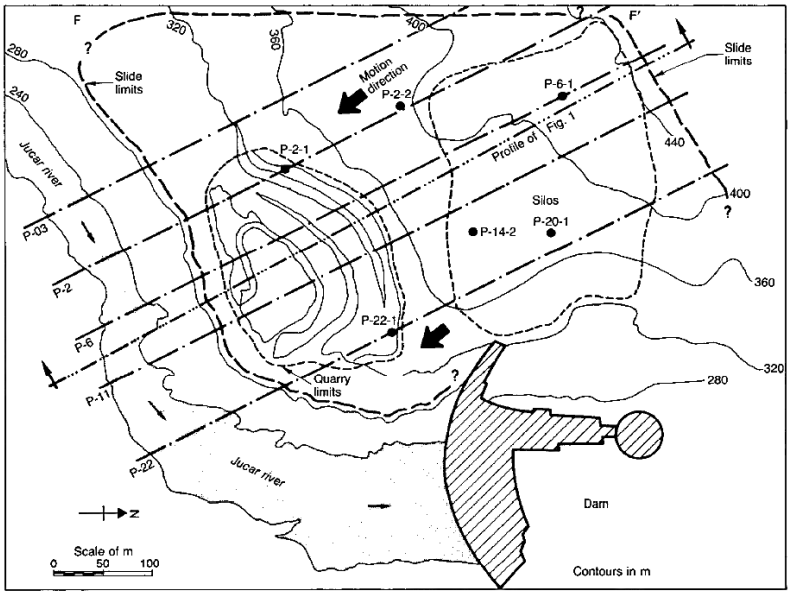

Figure 5.16 Direction of the landslide, boreholes, and cross section locations, Alonso et al. (1993)

5.3.2 Material properties and laboratory tests

Conducted laboratory tests on marl layer identified the layer as a low-plasticity clay with LL of 20%-28% and PL of 13%-14%. Drained direct shear test results conducted on marl samples are presented

in Figure 5.17. In these test series, the residual strength parameters are obtained after 4 cm of horizontal displacement.

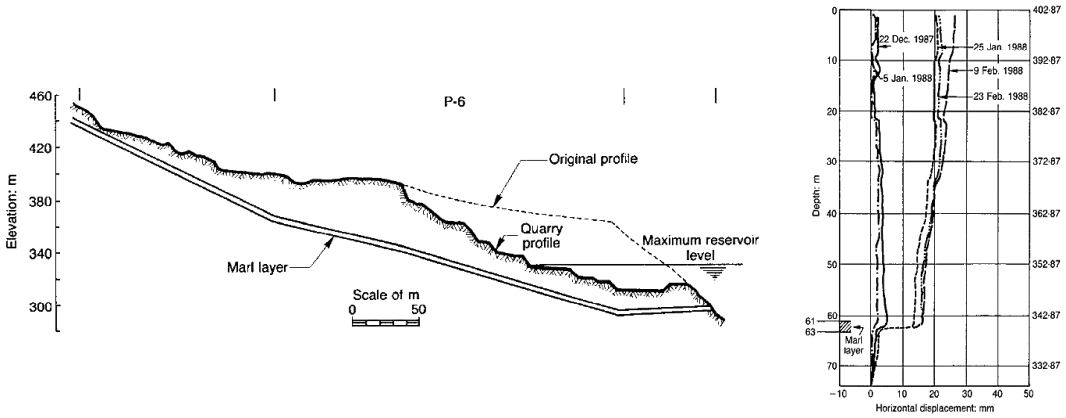

(a) (b)

Figure 5.17 (a) Cross section of the landslide from P-6 (b) Inclinometer data from borehole P-2-2 , Alonso et al (1993)

5.3.3 Nonlinear function of the failure envelope

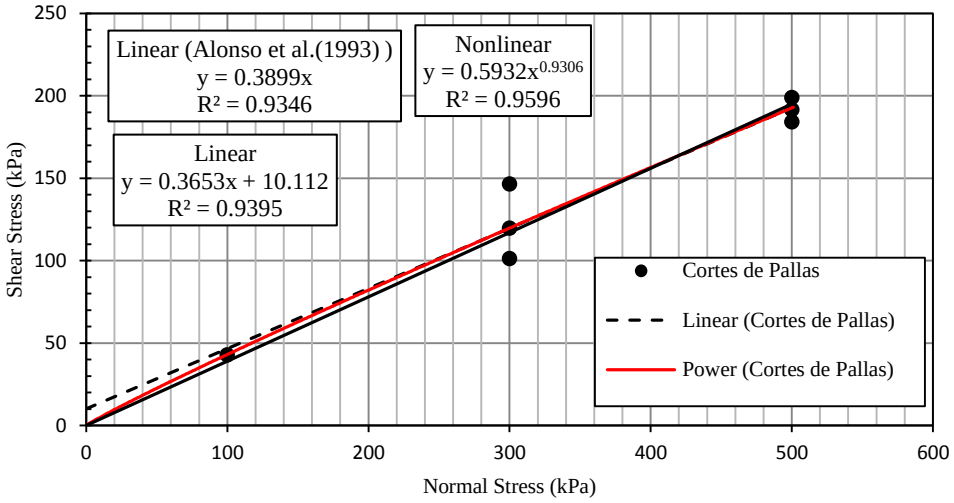

Figure 5.18 Failure envelopes from drained shear tests

5.3.4 Stability Analyses

Stability analysis of the Cortes De Palls landslide is performed as described in 5.1.4. In addition for the linear Mohr-Coulomb Strength criterion two envelopes are taken into account. One is the linear regression of the test data which has a non-zero intercept with the y axis and the other one that is proposed by Alonso et al (1993) is a linear envelope with zero intercept and the internal friction angle of 22 degrees.

Table 5.7 Linear and Non-linear shear strength envelopes

Material	Unit Weight	Linear Envelope		Linear Envelope (Alonso et al)		Nonlinear Function
		C' (kPa)	Φ' (deg)	C' (kPa)	Φ' (deg)	
Marl	20 kN/m^3	10	20	0	22	$\tau = 0.5932\sigma^{0.9306}$

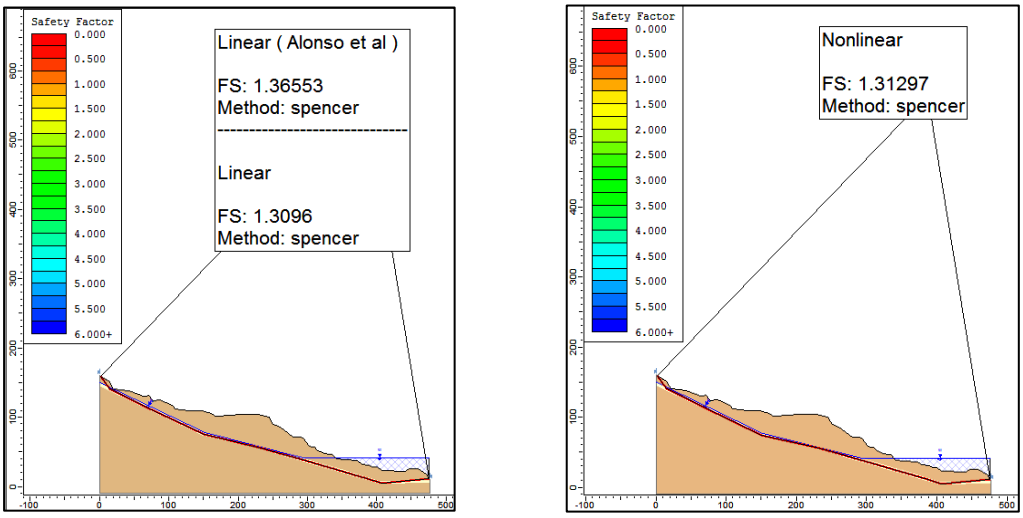

(a) (b)

Figure 5.19 The results of slope stability analyses using (a) Linear shear strength envelope (b) Nonlinear shear strength envelope

Table 5.8 Stability analyses results

	Using linear shear strength envelope	Using linear shear strength envelope of Alonso et al. (1993)	Using nonlinear shear strength envelope
Factor of Safety	1.3	1.4	1.3

5.4 Kutchi Otani landslide

5.4.1 Site introduction

As shown in Figure 5.20 the landslide located in southwestern part of Japan is reactivated in 2003. According to Gratchev et al. (2005) the mass movement with the rate of 1 mm per month caused a noticeable economic loss for the farmland located on this landslide. Monitoring the sliding area Gratchev et al. (2005) investigated the displacement behavior of the sliding mass in addition to the location of the shear surface and lithological composition of the area.

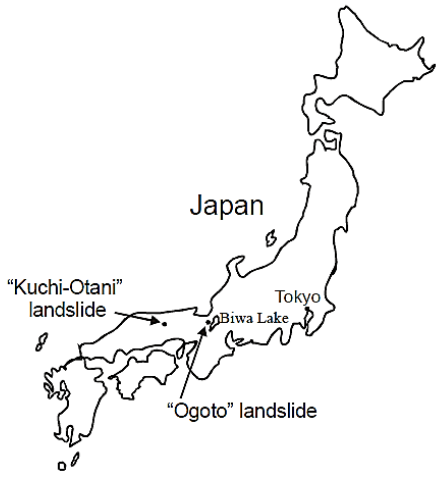

Figure 5.20 Location of the landslide

5.4.2 Site investigation and test results

Figure 5.22 illustrated the location of the drilled boreholes and installed inclinometers with which the geology and displacement behavior of the landslide is investigated. Materials obtained from the boreholes also shows three different layers of brownish clayey sand, amber silty clay and black clayey sand laid on black stiff mudstone.

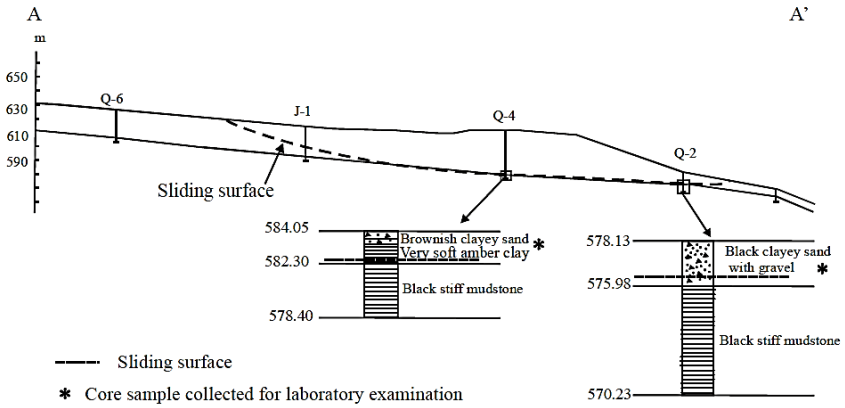

Figure 5.21 Cross-section of the landslide (Gratchev et al., 2005)

Based on the obtained data, Gratchev et al. (2005) provides a cross section of the Kuchi-Otani landslide in which the location of the failure surface as shown in the Figure 5.21.

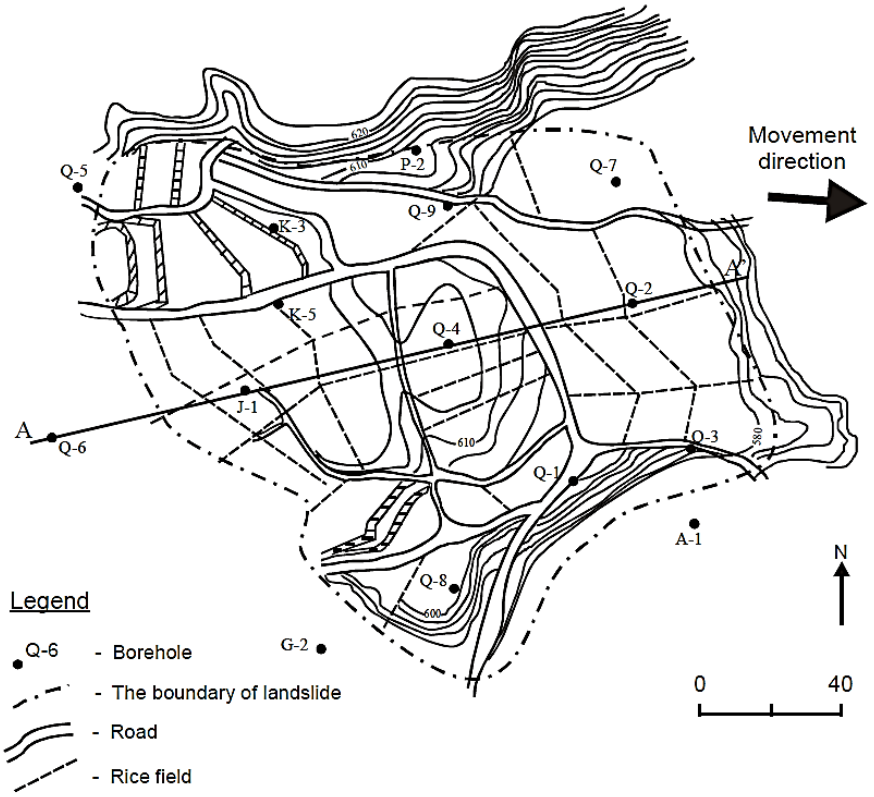

Figure 5.22 Location of the boreholes and direction of the landslide (Gratchev et al., 2005)

Soil samples taken from boreholes taken to the laboratory underwent initial index properties tests and X-ray diffraction test, test results are summarized in the table 5.3. Drained shear strength of the soil samples are also tested in a ring shear test setup.

Table 5.9 Material properties of the Kuchi-Otani landslide (Gratchev et al., 2005)

	Brownish Clayey sand	Amber silty sand	Black clayey sand
Liquid Limit (%)	88	96	39
Plasticity Index (%)	55	63	19
Clay-size Fraction (%)	11	66	8
Minerals	Quartz, Halloysite, Mica, Montmorillonite	Quartz, Halloysite, Mica	

5.4.3 Nonlinear function of the failure envelope

According to the ring shear test results published by Gratchev et al. (2005) linear and nonlinear failure envelope of the residual shear strength for three investigated soils are delineated in Figures 5.23, 5.24 and 5.25.

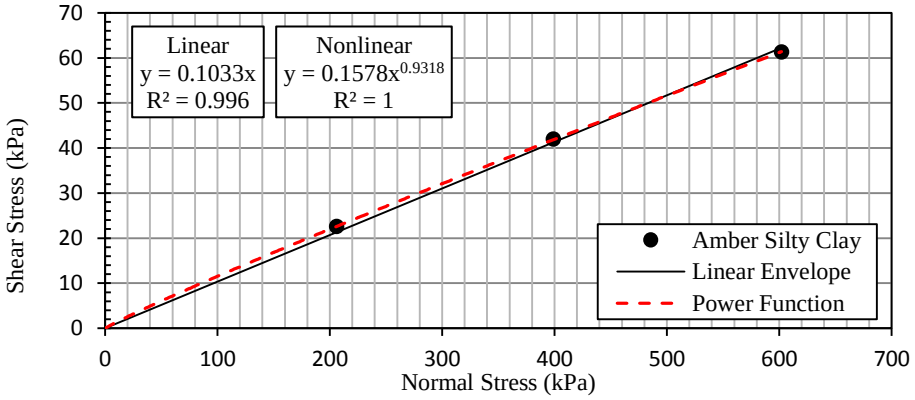

Figure 5.23 Residual shear strength failure envelope of Amber Silty Clay (After Gratchev et al., 2005)

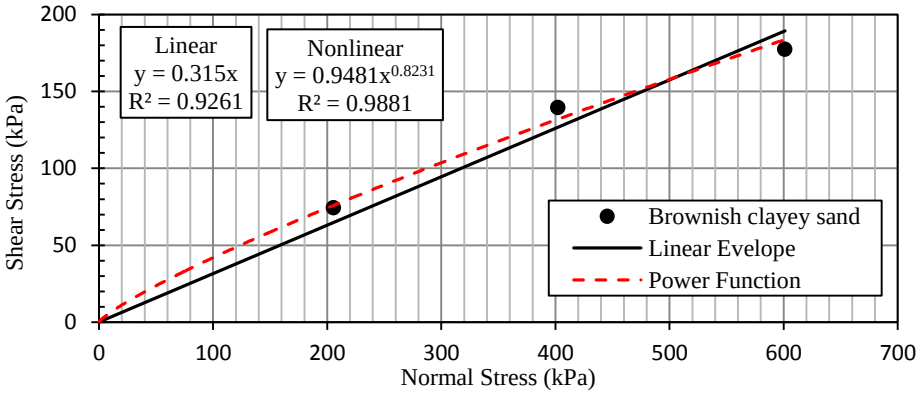

Figure 5.24 Residual shear strength failure envelope of Brownish Clayey Sand (After Gratchev et al., 2005)

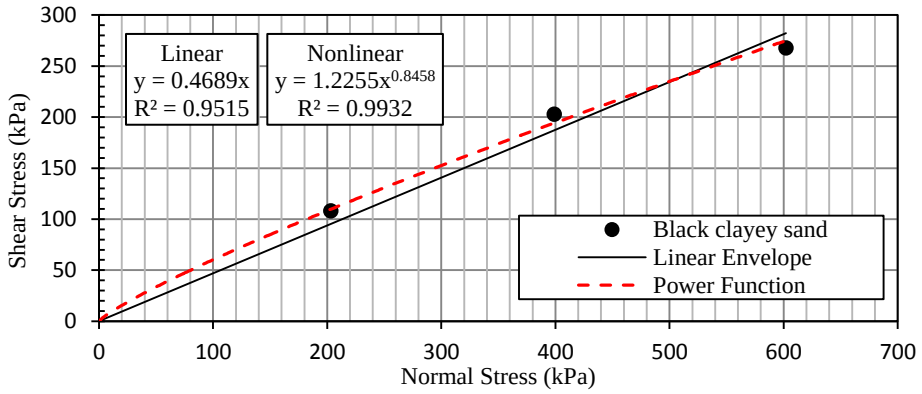

Figure 5.25 Residual shear strength failure envelope of Black Clayey Sand (After Gratchev et al., 2005)

5.4.4 Stability analyses

Stability analysis of the Kuchi-Otani landslide is performed following the procedure described in 5.1.4. Material properties adjacent to shear surface is defined based on extrapolation of the observed material layers shown in Figure 5.22. Gratchev et al. (2005) did not mention the ground water level condition. Consequently in the stability analyses the case is analyzed in half saturated condition with *Ru=0.25*.

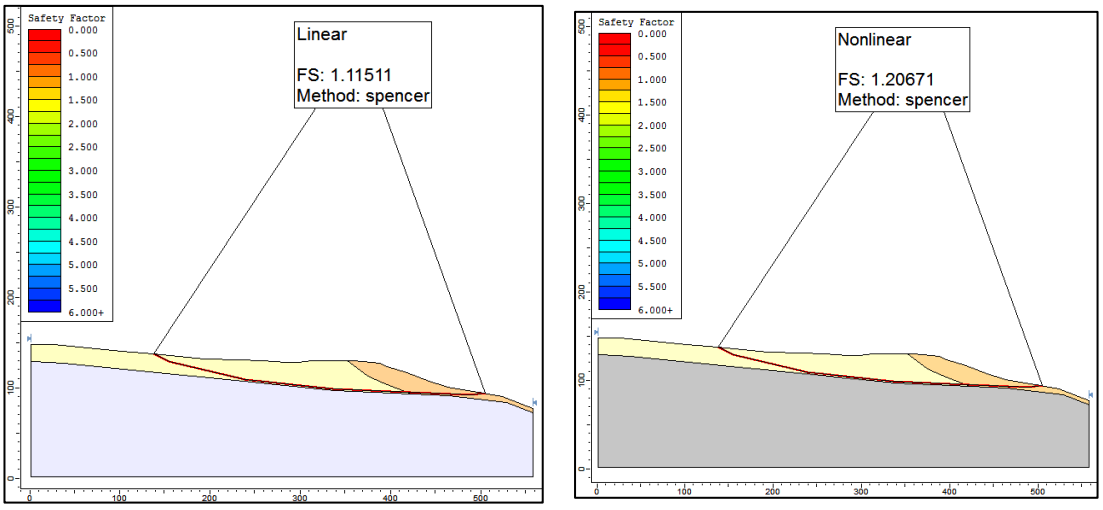

(a) (b)

Figure 5.26 The results of slope stability analyses using (a) Linear shear strength envelope (b) Nonlinear shear strength envelope

Table 5.10 Linear and Non-linear shear strength envelopes

Material	**Unit Weight kN/m^3**	**Linear shear strength envelope**		**Nonlinear shear strength envelope**
		C' (kPa)	Φ' (deg)	
Amber Silty Clay	20	0	5.8	$\tau = 0.1578\sigma^{0.9318}$
Brownish Clayey Sand	20	0	17.5	$\tau = 0.9481\sigma^{0.8231}$
Black Clayey Sand	20	0	25.8	$\tau = 1.2255\sigma^{0.8458}$

Table 5.11 Stability analyses results

	Using linear shear strength envelope	Using nonlinear shear strength envelope
Factor of Safety	1.1	1.2

5.5 Ogoto landslide

As shown in Figure 5.20, Ogoto landslide is located near Biwa lake in Japan near a residential area. After reactivation of the landslide in 2004, a series of investigations have been performed to prevent life and property loss due to possible failures. (Gratchev et al., 2005)

5.5.1 Site investigation and test results

Base on the obtained data from available boreholes two failure surfaces are detected in the sliding mass. The plan view of the sliding area and a cross section of the landslide is published by Gratchev et al. (2005) is presented in Figures 5.27 and 5.28. The boundaries of the soil 1 and soil 2 are not given in the Gratchev et al. (2005), therefore an interpretation has been made so that the smaller failure surface takes place in soil 1 and the bigger one in soil 2.

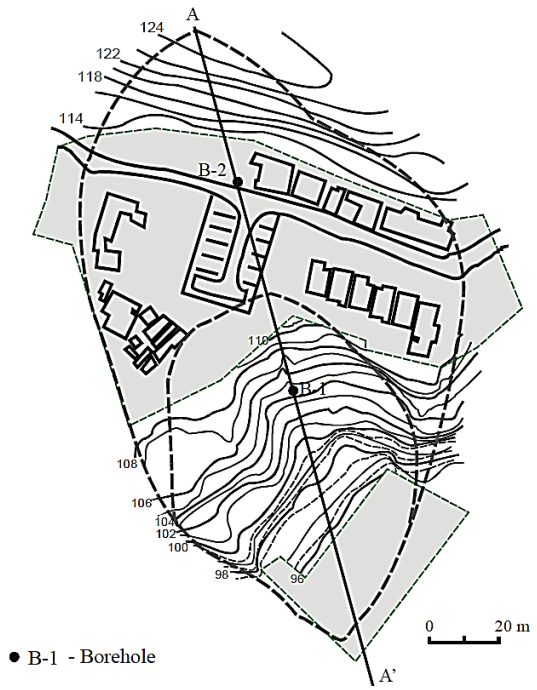

Figure 5.27 Plan view of the sliding mass, Ogoto landslide, Japan (Gratchev et al. (2005))

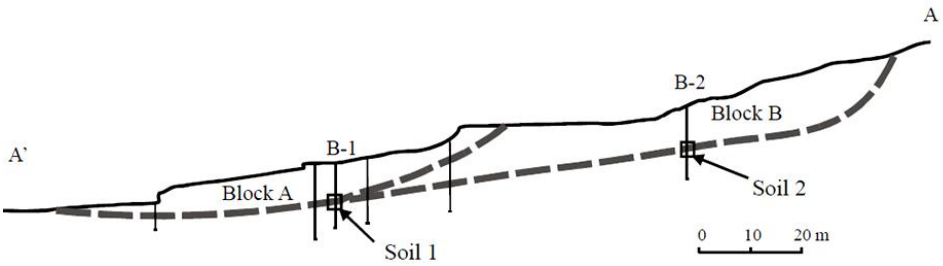

Figure 5.28 Plan view of the sliding mass, Ogoto landslide, Japan (Gratchev et al., 2005)

The failed mass contains two main blocks with different displacement rates. Block A moves with the rate of 0.05 mm/month which is 12 times faster than block B. From each block soil samples are taken to be tested in the laboratory. Soil 1 and Soil 2 are the soil samples taken from Blocks A and B respectively. Residual ring shear test results are provided in Figure 5.29.

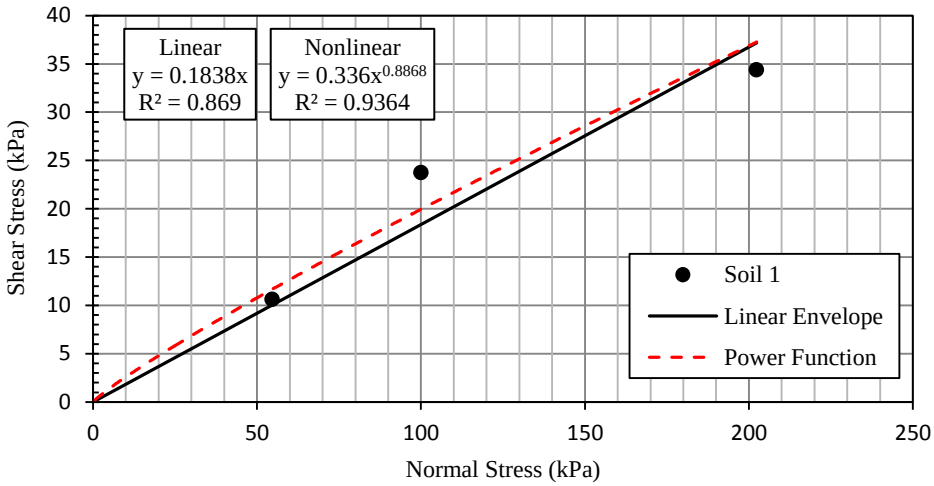

Figure 5.29 Residual shear strength failure envelope of Soil 1

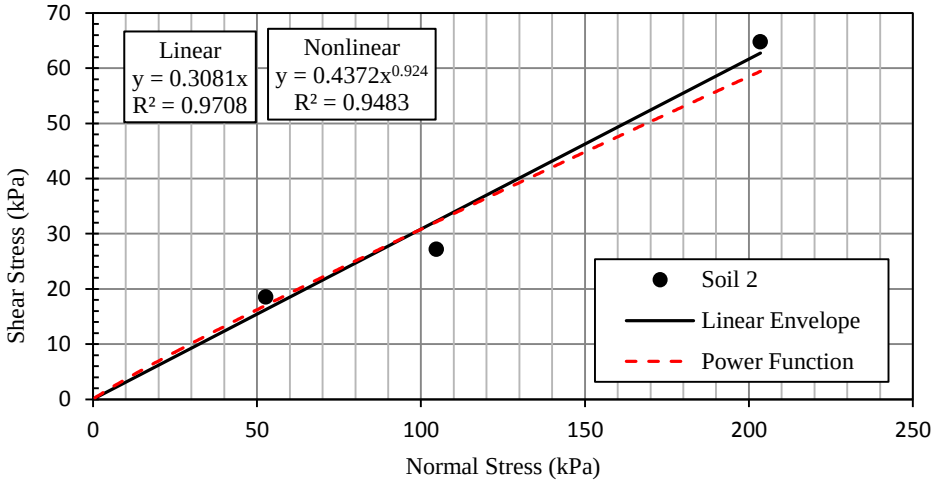

Figure 5.30 Residual shear strength failure envelope of Soil 2

Table 5.12 Material properties of the Ogoto landslide (Gratchev et al., 2005)

	Soil 1	Soil 2
Liquid Limit (%)	96	76
Plasticity Index (%)	57	50
Clay-size Fraction (%)	≈67	≈59
Minerals	Quartz, Halloysite, Mica	

5.5.2 Stability analyses

Stability analysis of the Ogoto landslide is also analyzed both for linear and nonlinear residual strength envelope of the materials based on the data published by Gratchev et al. (2005). In this landslide two different slip surfaces are detected and stability analysis is conducted for both of them.

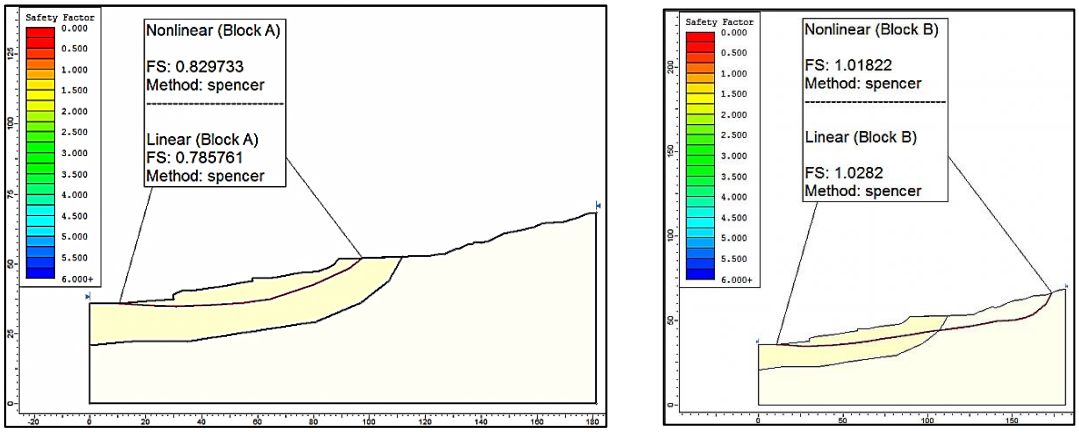

(a) (b)

Figure 5.31 The results of stability analysis of (a) Block A (b) Block B

Table 5.13 Linear and Non-linear shear strength envelope

Material	**Unit Weight kN/m^3**	**Linear shear strength envelope**		**Nonlinear shear strength envelope**
		C' (kPa)	Φ' (deg)	
Soil 1	20	0	5.8	$\tau = 0.1578\sigma^{0.9318}$
Soil 2	20	0	25.8	$\tau = 1.2255\sigma^{0.8458}$

Table 5.14 Stability analysis results

Factor of Safety	Using linear shear strength envelope	Using nonlinear shear strength envelope
Block A	0.8	0.8
Block B	1	1

5.6 Parametric Study

In order to evaluate the effect of some parameters, on the importance of nonlinearity of the shear strength envelope in F.S., such as slope height, normal stress range, ground water level a parametric study is conducted on two different types of slope: (1) a finite slope and (2) an infinite slope.

5.6.1 Finite Slope

In the initial step of the study, four different soils with different plasticity index ranges are selected and the initial slope geometry of the slopes in the most critical state with a factor of safety near to one when water level is at the ground surface was analyzed. In finite slopes, for simplicity, by using the "circular search" option in the SLIDE V.6.0 program, the most probable failure surface is predicted and selected as the starting point of the analyses. It should be noted that, the "circular failure surface search" option may not be fully accurate. In reactivated landslides, where residual shear strength is mobilized in the field, typically the shape of the most critical failure surface is noncircular, following some horizontal/subhorizontal, planar layer boundaries/discontinuities. Circular failure surface search, however, is a simple assumption that is used in this study. In the next step, the effect of change in pore water pressure distribution is investigated by changing the R_u (R_u is defined as the ratio of pore pressure to normal stress) values and monitoring the factor of safety both using linear and nonlinear shear strength envelopes. Utilized soil parameters and nonlinear functions of the shear strength envelope for all soil types are presented in table 5.15.

Table 5.15 Summary of the material properties

Material	Plasticity Index (%)	Unit weight kN/m3	Linear Envelope Parameters		Nonlinear Function
			c'	φ'	
Kaolinite	19	20	7.6	12.6	$y = 0.9555x^{0.7691}$
Santabarbara Clay	35	20	14	9.1	$\tau = 0.9988\sigma^{0.731}$
Ankara Clay	46	20	8.5	8.1	$\tau = 0.9897\sigma^{0.7063}$
USA mine Clay	75	20	15	6.6	$\tau = 0.7628\sigma^{0.7474}$

5.6.1.1 Ankara Clay

Searching for the initial geometry for the parametric study by utilizing Ankara clay as the soil body material is conducted for two different slope heights of 5 m and 20 m as shown in the Figure 5.32. In the 5 m and 20 m height slopes the final slope inclination is 20 degrees and 5 degrees respectively. Then by using the Mohr-Coulomb linear failure envelope, the slope angle for a critical condition is found. And for the selected geometry and a defined failure surface the effect of change in the water level location (represented by a change in R_u value) is summarized in the table 5.16 and Figure 5.33.

Table 5.16 Summary of the parametric study on Ankara clay

	Slope height = 5 m		**Slope height= 20 m**	
	Linear envelope	Nonlinear envelope	Linear envelope	Nonlinear envelope
Ru	FS		FS	
0	1.348	1.312	2.096	2.064
0.25	1.165	1.08	1.639	1.679
0.5	0.983	0.821	1.177	1.249

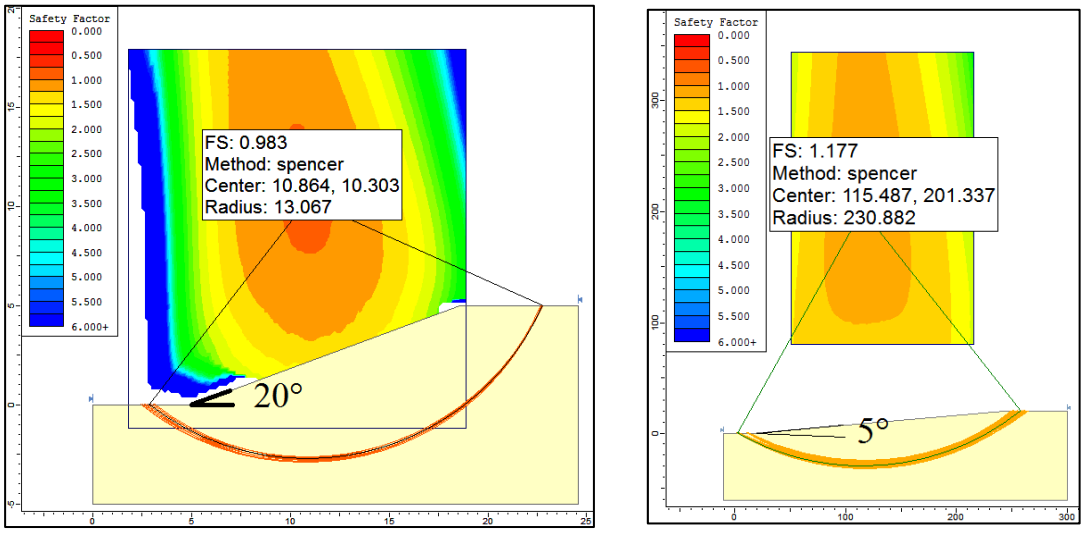

(a) (b)

Figure 5.32 The most probable failure surface in Ankara clay finite slope with the height of (a) 5 m (b) 20 m

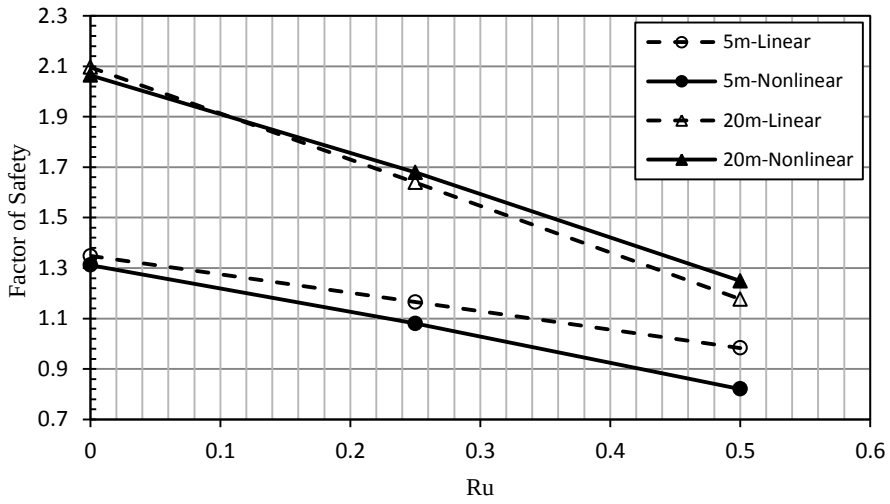

Figure 5.33 Results of parametric study in Ankara Clay

5.6.1.2 Kaolinite

The procedure of analyzing a finite slope in Kaolinite clay is the same as Ankara clay as described in 5.7.1.1. Figure 5.34 reveals the initial geometry of 5 m and 20 m slope. Table 5.17 and Figure 5.35 present the parametric study on Kaolinite clay.

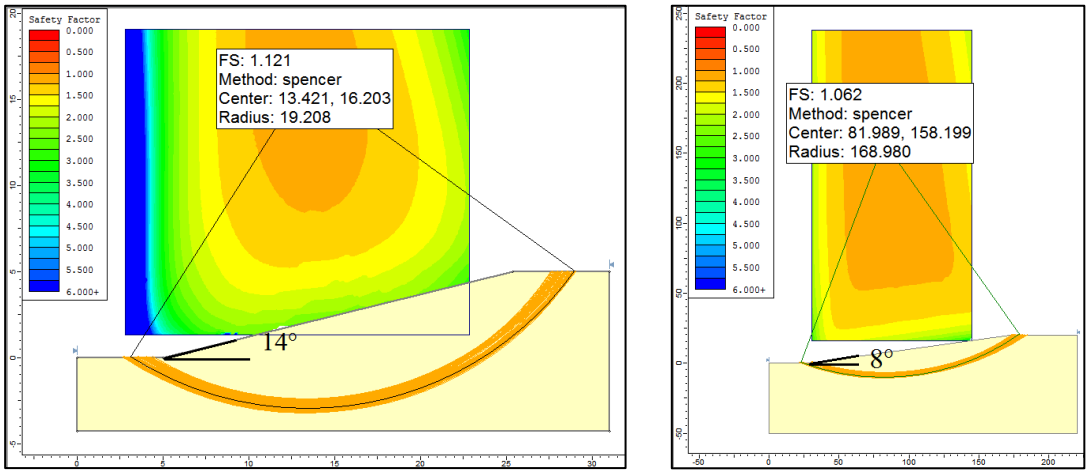

(a) (b)

Figure 5.34 The most probable failure surface in kaolinite finite slope with the height of (a) 5 m (b) 20m

Table 5.17 Summary of the parametric study on Kaolinite clay

	slope height = 5 m		**slope height =20 m**	
	Linear envelope	Nonlinear envelope	Linear envelope	Nonlinear envelope
Ru	FS		FS	
0	1.743	1.764	1.946	2.017
0.25	1.432	1.379	1.503	1.584
0.5	1.123	0.974	1.062	1.124

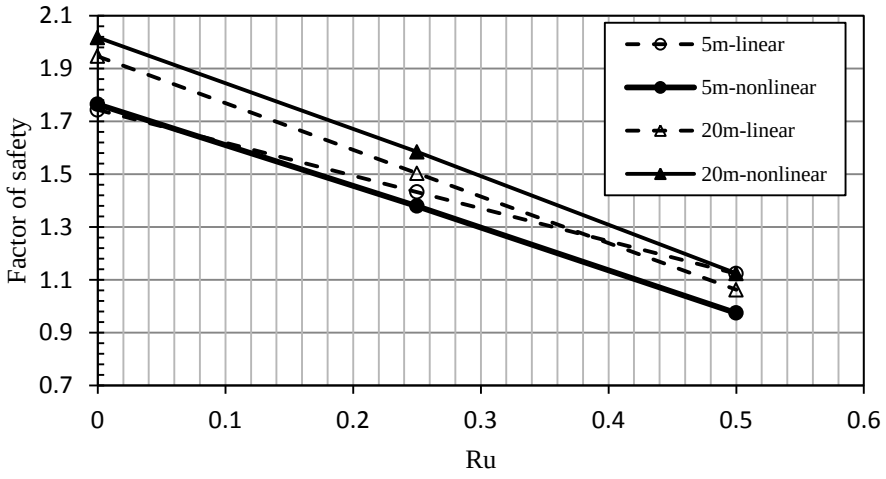

Figure 5.35 Results of parametric study in Kaolinite

5.6.1.3 Santa Barbara Clay

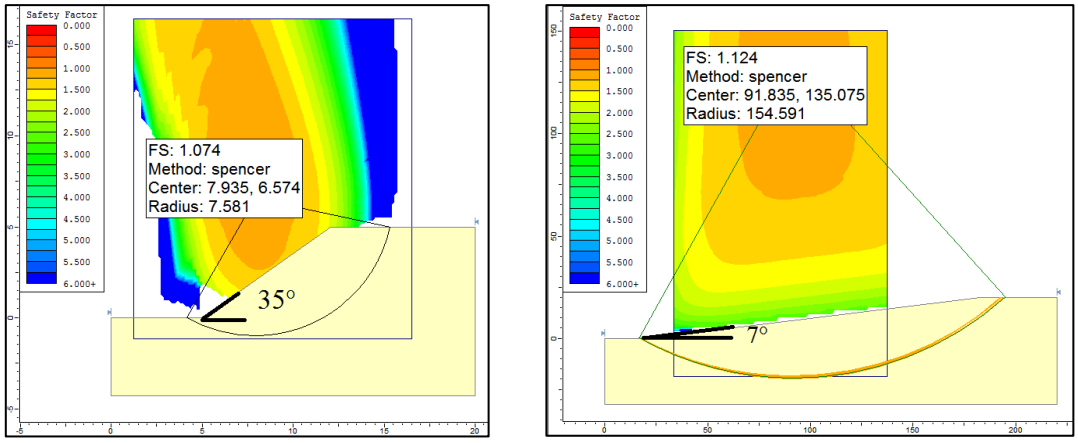

(a) (b)

Figure 5.36 The most probable failure surface in Santa Barbara clay finite slope with the height of (a) 5 m (b) 20 m

Table 5.18 Summary of the parametric study on Santa Barbara clay

	slope height = 5 m		**slope height =20 m**	
	Linear envelope	Nonlinear envelope	Linear envelope	Nonlinear envelope
Ru	FS		FS	
0	1.355	1.011	1.905	1.899
0.25	1.212	0.797	1.514	1.534
0.5	1.074	0.577	1.124	1.135

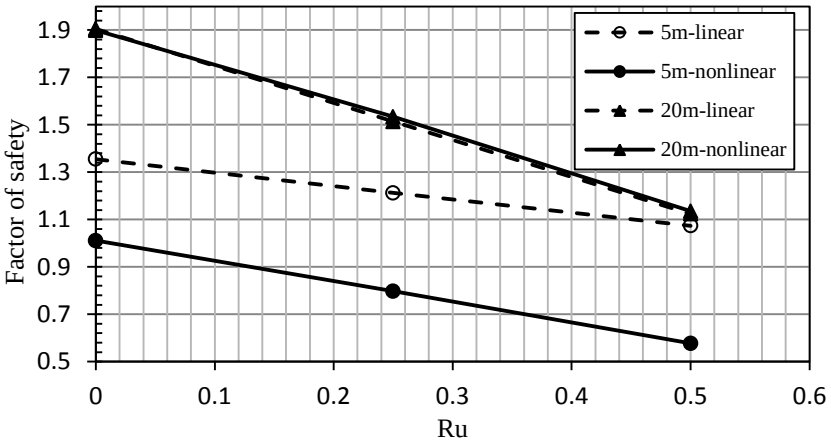

Figure 5.37 Results of parametric study in Santa Barbara Clay

5.6.1.4 Clay from a mine in USA

In order to have a wider range of plasticity in the studied materials a clayey soil from an unpublished data from a mine analysis in the United States is selected .The results are presented in the following tables and figures.

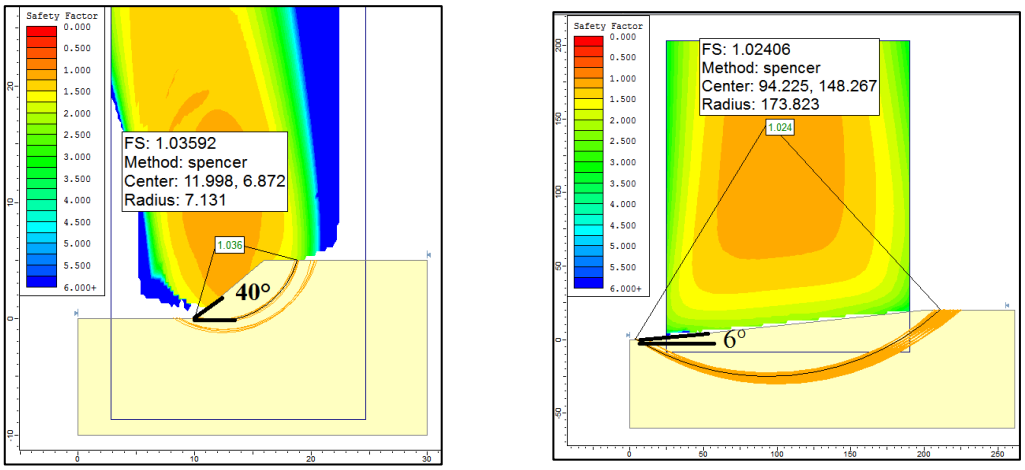

(a) (b)

Figure 5.37 The most probable F.S in USA mine clay finite slope with the height of (a) 5 m (b) 20 m

Table 5.19 Summary of the parametric study on Santa Barbara clay

	slope height = 5 m		**slope height =20 m**	
	Linear envelope	Nonlinear envelope	Linear envelope	Nonlinear envelope
Ru	FS		FS	
0	1.208	0.7	1.695	1.798
0.25	1.12	0.54	1.362	1.451
0.5	1.036	0.375	1.028	1.067

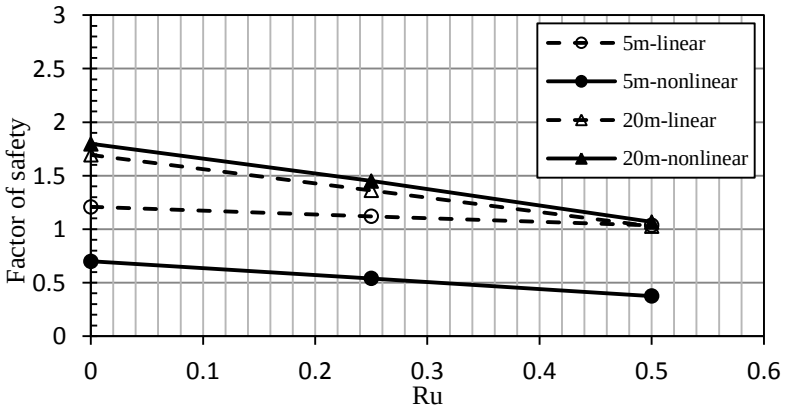

Figure 5.38 Results of parametric study in the Clay from the mine in USA

5.6.2 Infinite Slope

Another step of the parametric study is the same as the previous step but for an infinite slope. The change in the factor of safety for an initially defined geometry by the change in soil water level is investigated. In order to find the geometry a factor of safety of 1.1 is selected for the fully saturated soil and the slope angle is calculated.

Figure 39 reveals a schematic view of an infinite slope. The calculations for finding the initial slope geometry both for 5 m and 20 m failure surface thickness is shown for one soil and the other analysis results are presented in the following table.

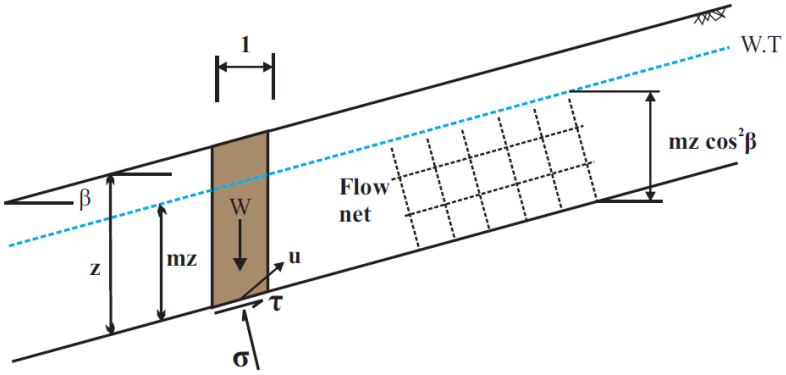

Figure 5.39 Infinite slope stability analyses (after Craig, 2004)

5.6.3 Ankara Clay

The following calculations present the stresses and factor of safety of an infinite slope in which σ is the total normal stress, σ' is the effective normal stress, τ is the shear stress, u is the pore pressure and β is the slope angle as shown in the Figure 5.39.

$$\sigma = \frac{F}{A} = \frac{w\cos\beta}{\frac{1}{\cos\beta}\times 1} = w\cos^2\beta \tag{5.1}$$

$$w = 1\times(z-mz)\gamma + mz\times\gamma_{sat} \tag{5.2}$$

$$\sigma = (1\times(z-mz)\gamma + mz\times\gamma_{sat})\cos^2\beta \tag{5.3}$$

$$\xrightarrow{\gamma_{sat}=\gamma} \sigma = \gamma z\cos^2\beta \tag{5.4}$$

$$u = mz\cos^2\beta\gamma_w \tag{5.5}$$

$$\sigma' = \sigma - u = (1\times(z-mz)\gamma + mz\times\gamma_{sat})\cos^2\beta - mz\cos^2\beta\gamma_w \tag{5.6}$$

$$\sigma' = \sigma - u = (1-r_u)\sigma \tag{5.7}$$

$$\sigma' = (1 - r_u)\,\gamma z cos^2\beta \tag{5.8}$$

$$\tau = \frac{F}{A} = \frac{w\ sin\beta}{\frac{1}{cos\,\beta} \times 1} = w\ sin\beta\ cos\beta \tag{5.9}$$

$$\tau = (1 \times (z - mz)\gamma + mz \times \gamma_{sat})\, sin\beta\, cos\beta \tag{5.10}$$

$$\xrightarrow{\gamma_{sat}=\gamma} \tau = \gamma z\, sin\beta\, cos\beta \tag{5.11}$$

$$F.S = \frac{Soil\ Shear\ Strength}{Disturbing\ Shear\ Stress} = \frac{\tau_{shear\ strength\ envelope}}{\tau_{slope}} \tag{5.12}$$

Linear failure envelope equation of Ankara Clay

$$\tau = 0.1377\ \sigma' + 9.7967 \tag{5.13}$$

$$\tau = 0.1377\ (1 - r_u)\,\gamma z cos^2\beta + 9.7967 \tag{5.14}$$

$$F.S_{linear} = \frac{0.1377\ (1 - r_u)\,\gamma z cos^2\beta + 9.7967}{\gamma z\, sin\beta\, cos\beta} \tag{5.15}$$

$$F.S_{nonlinear} = \frac{0.8959\ ((1 - r_u)\,\gamma z cos^2\beta)^{0.7225}}{\gamma z\, sin\beta\, cos\beta} \tag{5.16}$$

5.6.3.1 Infinite slope in Ankara Clay with water level at the ground surface

For γ=20 kN/m^3 and Z= 5 m

$r_u = 0.5$ and $\beta = 8.5$

$$F.S_{linear} = \frac{0.1377 \times (1 - 0.5) \times 20 \times 5 \times cos^2 8.5 + 9.7967}{20 \times 5 \times sin\,8.5\, cos\,8.5} = 1.13 \tag{5.17}$$

$$F.S_{nonlinear} = \frac{0.8959\ ((1 - 0.5) \times 20 \times 5 \times cos^2 8.5)^{0.7225}}{20 \times 5 \times sin\,8.5\, cos\,8.5} = 1.02 \tag{5.18}$$

5.6.3.2 Infinite slope in Ankara Clay with water level at mid-slope height

$r_u = 0.25$

$$F.S_{linear} = \frac{0.1377 \times (1 - 0.25) \times 20 \times 5 \times cos^2 11 + 9.7967}{20 \times 5 \times sin\,11\, cos\,11} = 1.36 \tag{5.19}$$

$$F.S_{nonlinear} = \frac{0.8959\,((1-0.25)\times 20\times 5\times cos^2 8.5)^{0.7225}}{20\times 5\times sin\,8.5\,cos\,8.5} = 1.36 \quad (5.20)$$

5.6.3.3 Infinite slope in Ankara Clay in dry condition

$r_u = 0.0$

$$F.S_{linear} = \frac{0.1377\times(1-0)\times 20\times 5\times cos^2 11 + 9.7967}{20\times 5\times sin\,11\,cos\,11} = 1.59 \quad (5.21)$$

$$F.S_{nonlinear} = \frac{0.8959\,((1-0.25)\times 20\times 5\times cos^2 8.5)^{0.7225}}{20\times 5\times sin\,8.5\,cos\,8.5} = 1.68 \quad (5.22)$$

5.6.3.4 Ankara Clay parametric study result summary

Table 5.19 Summary of the infinite slope parametric study on Ankara clay

	Failure Thickness = 5 m		**Failure Thickness = 20 m**	
	β = 8.5°		β =5°	
	Linear envelope	Nonlinear envelope	Linear envelope	Nonlinear envelope
Ru	FS		FS	
0	1.59	1.68	1.85	1.95
0.25	1.36	1.36	1.46	1.58
0.5	1.13	1.08	1.07	1.18

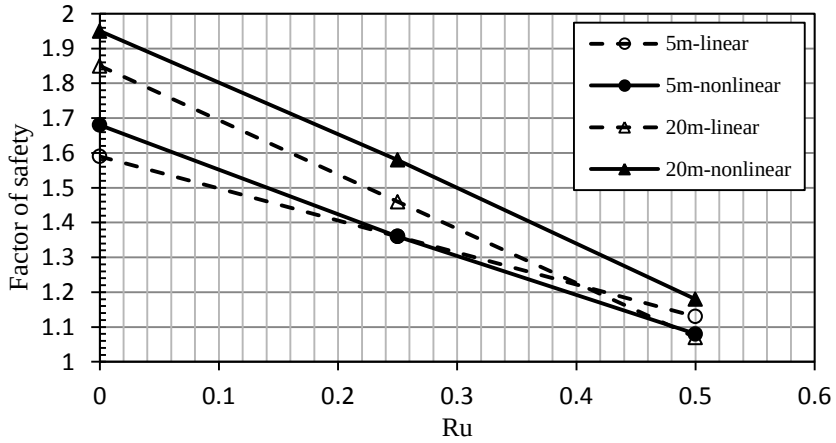

Figure 5.40 Results of infinite slope parametric study in the Ankara Clay

5.6.4 Kaolinite's parametric study results

Table 5.19 Summary of the infinite slope parametric study on Kaolinite

	Failure Thickness = 5 m		**Failure Thickness = 20 m**	
	β = 9°		β =6.5°	
	Linear envelope	Nonlinear envelope	Linear envelope	Nonlinear envelope
R_u	FS		FS	
0	1.59	1.68	2.07	2.11
0.25	1.36	1.36	1.59	1.67
0.5	1.00	1.98	1.11	1.19

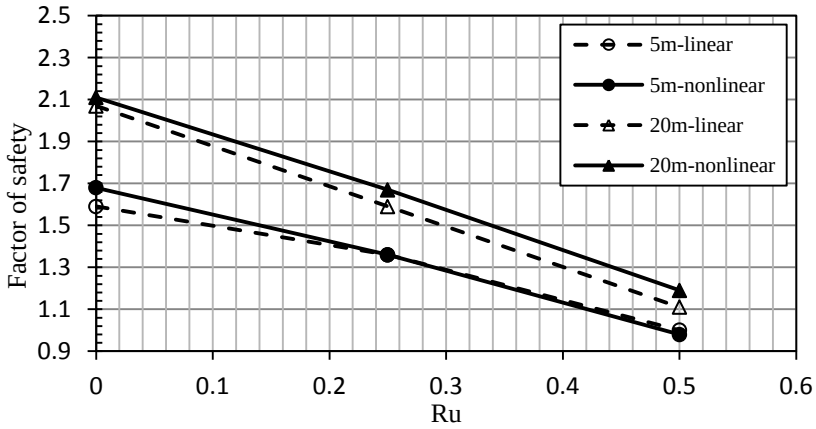

Figure 5.41 Results of infinite slope parametric study in the Kaolinite

5.6.5 Santa Barbara Clay's parametric study results

Table 5.20 Summary of the infinite slope parametric study on Santa Barbara Clay

	Failure Thickness = 5 m		**Failure Thickness = 20 m**	
	β = 11.5°		β =6°	
	Linear envelope	Nonlinear envelope	Linear envelope	Nonlinear envelope
R_u	FS		FS	
0	1.50	1.44	1.87	1.90
0.25	1.31	1.16	1.48	1.54
0.5	1.11	0.86	1.10	1.14

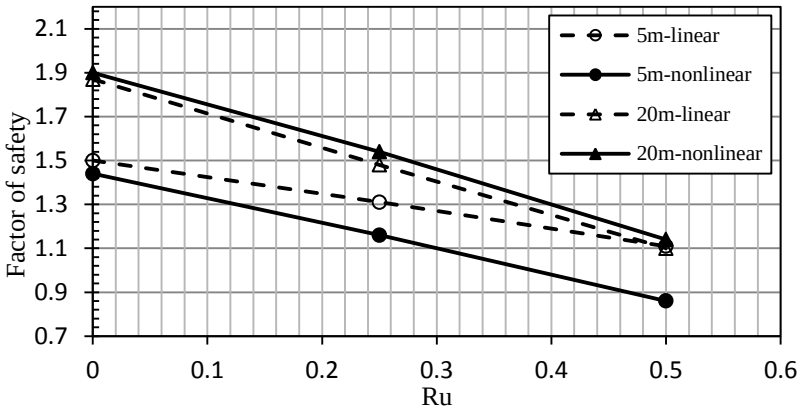

Figure 5.42 Results of infinite slope parametric study in the Santa Barbara Clay

5.6.6 USA mine Clay's parametric study results

Table 5.20 Summary of the infinite slope parametric study on USA mine Clay

	Failure Thickness = 5 m		**Failure Thickness = 20 m**	
	β = 11°		β =5°	
	Linear envelope	Nonlinear envelope	Linear envelope	Nonlinear envelope
Ru	FS		FS	
0	1.42	1.24	1.77	1.92
0.25	1.27	1.00	1.44	1.55
0.5	1.12	0.73	1.11	1.15

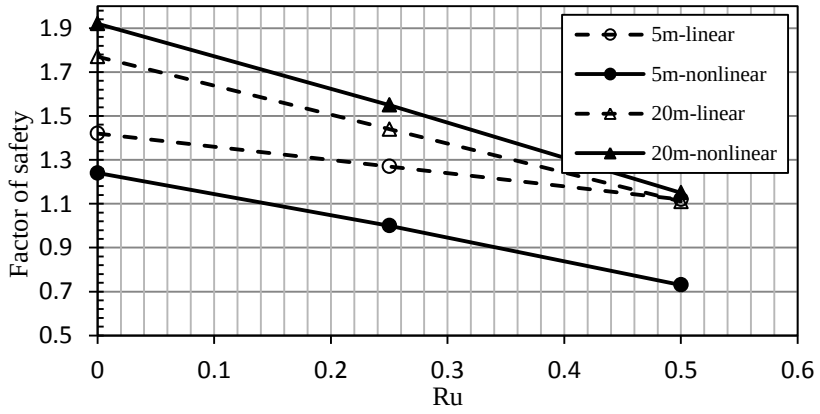

Figure 5.42 Results of infinite slope parametric study in the USA mine Clay

CHAPTER 6

SUMMARY AND CONCLUSIONS

6.1 Summarized points and conclusions

Some of the important results and conclusions of this study are given below:

1) The methodology:

In order to evaluate the validity and importance (or lack thereof) of nonlinearity of the shear strength envelope, laboratory reversal direct shear tests are carried out on two different artificially prepared overconsolidated clay materials with different plasticity values. The samples are sheared at effective normal stress values ranging from 25 to 900 kPa and the samples were initially overconsolidated with OCR 4.0 and 2.0 for Ankara clay and for kaolinite, respectively. Laboratory residual friction angle measurements from the literature were also collected to demonstrate the nonlinearity and to see the effect of plasticity index (Ip%) on the nonlinearity. Analyses of a number of selected reactivated landslide case histories are carried out. The practical significance of nonlinearity of residual shear strength envelope was also demonstrated by applying linear and nonlinear shear strength equations in a parametric slope stability study.

2) Residual shear strength of stiff Ankara clay:

Since undisturbed samples were not available, remolded (intact and pre-cut) samples were prepared in the laboratory and consolidated to obtain an artificially produced stiff overconsolidated clay with OCR=4.0. Assuming a linear residual shear strength envelope, it is found that Ankara clay has 8.1 degrees residual friction angle for the effective normal stress range of 25 to 900 kPa.

Ergun (1993) investigated a landslide in Erdemkent in Ankara-Cayyolu in Ankara clay material. The slope height was about 20 m and the landslide was about 150 m long. Direct shear tests were conducted on undisturbed samples to determine the residual shear strength parameters. c'=0-10 kPa and $\varphi'r$ =10-29 degrees were reported. Back-analysis carried out by Ergun (1993) found out that the shear strength parameters at the time of failure were c'=0 kPa and $\varphi'r$ =8-8.6 degrees. Ergun (1993) concluded in their report that the residual shear strength of the material was c'=0 kPa and φ'_r =8-10 degrees. This conclusion is in agreement with the current study.

3) Effect of specimen preparation on residual friction angle:

Two different specimen preparation methods from remolded specimens prepared in laboratory (pre-cut and intact, with and without a shear plane, respectively) gave similar residual secant friction angles for Ankara clay at 400 kPa shearing effective normal stress. The fact that these two methods gives similar results has been reported in the literature (Mesri and Gibala 1972, Tiwari and Marui 2004). In one of the methods, a remolded sample was overconsolidated in the direct shear box (initially there was no shear plane) then sheared. This sample gave 8.6 degree secant residual friction angle at 400 kPa effective normal stress. In the second method, same material was remolded into the

upper and lower halves of the shear box separately, overconsolidated separately, then assembled together, (i.e. there was a distinct plane between the two halves of the shear box). This sample gave 7.6 degrees secant residual friction angle at 400 kPa effective normal stress. These results are in agreement and accuracy of ±1 degree is also reported as reasonable in the literature (Skempton 1985, Bromhead and Dixon 1986, Tiwari and Marui 2004, Meehan 2006, Eshraghian 2007).

4) Residual shear strength under large normal stresses :

In the literature there is very limited data on shear strength tests at large normal stresses. The residual shear strength envelopes of both Ankara clay and kaolinite are nonlinear, and can be represented by a power function (the cohesion is zero). The secant residual friction angle of kaolinite was 28.6 degrees at 25 kPa normal stress and it decreased to 13.1 degrees at 900 kPa. If the residual shear strength is tried to be represented by a linear envelope, we would find residual friction angle of 13.4 degrees. This is quite different from the range of friction angles 13.1-21.8 in the nonlinear envelope. For Ankara clay these friction angles were 22 and 8.6 degrees, for 25 and 900 kPa effective normal stresses, respectively. A linear envelope would give residual friction angle of 8.1 degrees. Therefore, there is significant nonlinearity. The power "b" is similar to Mesri and Shahien (2003's) m_r parameter indicating the quantity of nonlinearity. The power coefficient (the degree of nonlinearity) changes with plasticity index.

5) No vertical movement of shear plane:

In the reversal direct shear tests very small amount of vertical displacement is observed during shearing (0.03 to 0.20 mm for Ankara clay and 0.17-0.62 mm for kaolinite), as it is the typically expected case for overconsolidated clays. The material in the shear plane is in the "recompression" part of the void ratio versus log effective stress plot. This proves that the shear plane did not move into the shear box during shearing and simulates field preexisting shear planes correctly.

6) Displacement required to reach residual:

As has been pointed out by Morgenstern (1977) and Mesri and Shahien (2003) large deformations may not be necessary in bedded deposits where shearing is restricted to laminations/discontinuities or interfaces. For the Selborne cut-slope experiment in Gault clay, after the slope was cut, horizontal movements near the toe were observed, by an amount 10 to 20 mm (Cooper et al. 1998). It was found out that the planar basal part of the surface parallel to the bedding formed as a single, highly polished and striated slickenside just above the slope toe. Similar conclusions can be drawn based on our laboratory test results (on remolded specimens without a pre-cut shear surface) that 17-37 mm cumulative shear displacements were required to reach residual condition.

7) Empirical relations to estimate residual friction angle:

It is observed that the empirical relations based on liquid limit, plasticity index of the material (such as Mesri and Shahien 2003, Stark et al. 2005) can predict the residual friction angle accurately.

8) For which conditions nonlinearity of shear strength envelope is important:

Based on laboratory reversal direct shear experiments, residual shear strength lab test results collected from literature, back-analysis of reactivated landslides and a parametric study, the nonlinearity of the residual shear strength envelope is evaluated. Nonlinearity is especially important to consider for the landslide cases where the average effective normal stress on the shear plane is small (i.e. ≤ about 50 kPa), both for translational and rotational slope failures. For slopes with such small effective normal stresses, using a linear shear strength envelope overestimates the F.S. (more significantly for the case of high pore pressures in the slope). Low effective normal stresses can be observed when depth of shear plane is shallow, (or in other words the slope height is small). It can also happen if the groundwater table is closer to ground surface, (i.e. high water pressures, high ru values and smaller effective stress values on the shear plane). Factor of safety of the slope would be overestimated if a linear shear strength envelope is used for these landslides, which is unconservative (unsafe) and may lead to dangerous consequences. For the materials with high plasticity, the nonlinearity of the shear strength envelope is significant and should be taken into account. By plotting the plasticity index versus the power "b" of the nonlinear shear strength envelope, the effect of plasticity can be observed. Although there is significant scatter, a general conclusion can be drawn such that as the plasticity index of the material is increasing, the power "b" of the nonlinear shear strength envelope is decreasing, which means a more significant nonlinearity. For less plastic materials, using linear and nonlinear shear strength envelopes does not affect the F.S. much.

9) Reversal direct shear tests can be used to determine residual friction angle:

Reversal direct shear tests can give reliable results as long as they are conducted properly on overconsolidated clay samples and sheared until defining residual shear strength condition very clearly (i.e. at least three forward shearing or minimum cumulative shear displacement of 20 mm).

6.2 Future work recommendations

1) For the future studies the soils utilized in the experimental and analytical sections of this study can be investigated for their exact mineralogy to check the available correlations between the amount of a specific clay mineral on the residual shear strength parameters.

2) In order to investigate the particle alignment in the shear surface at the residual state, samples from the shear surface could be taken to be investigated by Scanning Electron Microscope.

3) Based on the conclusions it can be concluded that there is a significant nonlinearity in lower effective normal stresses, so a set of additional reversal direct shear tests could be performed to estimate the amount of nonlinearity in the low effective normal stress ranges more precisely.

4) While it is recognized that preforming the shear surface in the direct shear test samples gives the same results in comparison to the intact sample tests without a shear surface, a complete set of precutted sample tests can be performed to see its effect on the nonlinearity of the entire shear strength envelope.

5) Reanalyzing more landslide case histories would clarify the effect of the parameters such as failure mechanism, soil properties and ground water level condition on the calculated factor of safety in the stability analysis.

6) Adding more test data from the literature is recommended to clarify the existing correlations between soil properties and amount of nonlinearity in the residual shear strength failure envelope.

REFERENCES

Agrawal, K. B. (1967). "The influence of size and orientation of sample on the undrained strength of London Clay." Ph.D. thesis, University of London.

Alonso, E. E. Gens, A. Lloret, A. (1993) "The landslide of Cortes de Pallas, Spain", Géotechnique, Volume 43, Issue 4, 01 December 1993 , pages 507 –521.

Anayi, J. T., Boyce, J. R., and Rogers, C. D. (1988) Comparison of alternative methods of measuring the residual strength of a clay, Transportation Research Record, 1192, 16-26.

Baker, R. (2004). "Nonlinear Mohr Envelopes Based on Triaxial Data." Journal of Geotechnical and Geoenvironmental Engineering, 130(5), May, pp. 498-506.

Bardet, J.P. (1997) "Experimental Soil Mechanics", Prentice-Hall, Inc., Upper Saddle River, New Jersey.

Biscaye, P.E. (1965) "Mineralogy and sedimentation of recent deepsea clay in the Atlantic Ocean and adjacent seas and oceans", Geol Soc Am Bull 76:803–832.

Bishop A.W., Henkel D.J. (1962) "The measurement of soil properties." Edward Arnold Publishers Ltd, London.

Bishop, A.W. (1971). "The influence of progressive failure on the choice of the method of stability analysis.", Géotechnique, 2, 168-172.

British Geological Survey's website , (2012), http://www.bgs.ac.uk/landslides/IronbridgeGorge.html.

Bromhead, E.N. (1979) "A simple ring shear apparatus, Ground Engineering.", v.12(5), p.40-44.

Bromhead, E.N. and Dixon, N. (1986) The field residual strength of London clay and its correlation with laboratory measurements, especially ring shear tests, Technical Note, Geotechnique, p.449-452.

Chandler, R.J. (1966). "The measurement of residual strength in triaxial compression." Geotechnique Volume 16, Issue 3, pages181–186.

Chandler, R.J. (1984a) "Recent European Experience of landslides in overconsolidated clays and soft rocks," Proc. 4th Int. Symposium on Landslides, Toronto, v.1, p.61-81.

Colotta, T., Cantoni, R., Pavesi, U., Robert, E., and Moretti, P. C. (1989). "A correlation between residual friction angle, gradation and index properties of cohesive soil." Geotechnique, 39 No 2, 343-346.

Cooper, M.R., Bromhead, E.N., Petley, D.J., and Grant, D.I. (1998). "The Selborne cutting stability experiment," Géotechnique, 48(1), 83-101.

Craig, R. F. (2004). Craig's Soil Mechanics. London: Spon Press.

Culmann, C. A.(1866). "Die Graphische Statik.", Meyer und Zeller, Zurich.

Dewoolkar, M. M., and Huzjak, R. J. (2005) ."Drained residual shear strength of some claystones from Front Range Colorado.", Journal of Geotechnical and Geoenvironmental Engineering, 131(12), 1543-1551

De Mello, V.B.F. (1977). “Reflections on design decisions of practical significance to embankment dams.” 17th Rankine lecture.“ Geotechnique, 27(3), 281-354.

Duzgun, H.S., Akkar, S., Huvaj, N., Akgun, A. and Aras, C. (2012) Bigadiç Bor İşletme Müdürlüğü Simav Açık Ocağı-Uzuntepe’de Görülen Çatlakların İncelenmesi Projesi, METU Revolving Fund Consulting Project, unpublished report (in Turkish).

Eid, H.T. (1996) “Drained shear strength of stiff clays for slope stability analyses”, PhD thesis, Univ. of Illinois at Urbana-Champaign, Ill.

Erol, O. (1973). Geomorphological outlines of the Ankara area (Summary). Map 1:100.000. Ankara University, D.T.C.F. Publication, No:16, Geomorphology Maps, Ankara, No.1, 29 p.

Ergüler, Z.A., Ulusay, R (2003), “Engineering characteristics and environmental impacts of the expansive Ankara Clay, and swelling maps for SW and central parts of the Ankara (Turkey) metropolitan area” . Environmental Geology. 44: 979-992.

Ergun, M.U. (1993) Ankara-Cayyolu S.S. Erdemkent Arsa ve Yapı Kooperatifi Heyelan Etüdü, Middle East Technical University, Revolving Fund Consulting Project, unpublished report (in Turkish).

Eshraghian, A. (2007) Hazard analysis of translational earth slides in the Thompson River Valley, Ashcroft, British Columbia, Ph.D. Thesis,. Dept. Civil and Env. Eng., University of Alberta, Edmonton, Alberta

Gratchev, I. Sassa, K. Fukuoka H.(2005) ” The shear strength of reactivate landslides” . Annuals od Disas. Prev. Res. Inst. Kyoto University . No 48. B .

Grelle,G.Guadagno,F.M. (2010) “Shearmechanismsandviscoplasticeffectsduring impulsive shearing”. Ge´otechnique 2010; Volume 60, Issue 2, p:91–103.

Haefeli, R. (1951).” Investigation and Measurements of the Shear Strengths of Saturated Cohesive Soils”. Géotechnique, Volume 2, Issue 3, 01 June 1951 , pages 186 –208.

Hatipoglu, M. (2011) Determination of Residual Shear Strength With Ring Shear Test and Affecting Factors, Istanbul Technical University, PhD Thesis.

Henkel, D.J., and Skempton, A.W., 1954, A landslide at Jackfield, Shropshire, in a heavily over-consolidated clay: Geotechnique, v. 5, (2), p. 131-137.

Huvaj-Sarihan, N. (2009) “Creep movements of reactivated landslides”, Proc. 4th Young Geotechnical Engineers Conference, 2-4 October 2009, Alexandria, Egypt.

Huvaj-Sarihan, N. (2009). “Movement of reactivated landslides.” Ph.D. thesis, Univ. of llinois at Urbana-Champaign, Urbana, IL.

Hvorslev, M.J. (1937). “Uber die Festigkeitseigenschaften gestoerter bindiger Boden.”, (On the physical properties of undisturbed cohesive soils). Ingeniorvidenskabelige Skrifter, A, No. 45, Copenhagen. English translation (1969), US Waterways Experiment Station.

Kenney, T.C. (1967) “The influence of mineral composition on the residual strength of natural soils.” Proc. Geotechnical Conference on Shear Strength Properties of Natural Soils and Rocks. 1967, Oslo, v.1, 123-129, NGI, Oslo, Norway.

Kenney, T.C. (1977). “Residual Strengths of Mineral Mixtures.” Ninth International Conference on Soil Mechanics and Foundation Engineering, Vol. 1, Japan, pp. 155–160.

La Gatta, D.P. (1970). “Residual Strength of Clays and Clay-Shales by Rotation Shear Tests.” Harvard Soil Mechanics Series No. 86. Harvard University, Cambridge.

Lemos, L. J. L., Skempton, A. W. & Vaughan, P. R. (1985). “Earthquake loading of shear surfaces in slopes.” Proc. 11th Int. Conf. Soil Mech. Found. Engng, San Francisco, CA 4, 1955–1958.

Lemos, L. J. L. (2003). “Shear behaviour of pre-existing shear zones under fast loading: insights on the landslide motion.” Proceedings of the international conference on fast slip movements prediction and prevention for risk mitigation, Sorrento.

Li, X.(2007), “Finite element analysis of slope stability using a nonlinear failure criterion”, Computers and Geotechnics, Vol. 34 ,127–136.

Maksimovic, M. (1979). "Limit equilibrium for nonlinear failure envelope and arbitrary slip surface." Third Int. Conf. on Numerical Methods in Geomechanics, Aachen, 769-777.

Maksimovic, M. (1988). "General slope stability software package for micro-computers." 6th Int. Conf. on Numerical Methods in Geomechanics, 3, Innsbruck, Austria, 2145-2150.

Maksimovic, M. (1989). “Nonlinear Failure Envelope for Soils.” Journal of Geotechnical Engineering, ASCE Vol. 115 (4), April. pp. 581-586.

Meehan , C. L. (2006) An Experimental Study of the Dynamic Behavior of Slickensided Slip Surfaces, PhD Thesis, Virginia Polytechnic Institute and State University.

Meehan C.L., Brandon T.L., Duncan J.M., Tiwari B (2010) “Direct shear testing of polished slickensided surfaces.” Landslides, Journal of the International Consortium on Landslides, Springer, 7(2), 157–167

Meehan, C. L., Tiwari, B., Brandon, T. L., and Duncan, J. M. (2011). " Triaxial Shear Testing of Polished Slickensided Surfaces." Landslides, 8, 449-458.

Mesri, G., and Abdel-Ghaffar, M.E.M. (1993). “Cohesion intercept in effective stress-stability analysis.”, J. Geotech. Engrg., ASCE, 119(8), 1229-1249.

Mesri, G., and Cepeda-Diaz, F., (1986). “Residual Shear Strength of clays and shales.”, Geotechnique, 36(2), p. 269-274.

Mesri G. and Gibala, R. (1972). “Engineering Properties of a Pennsylvanian Shale”. in Stability of Rock Slopes, Proc. 13th Symp. On Rock Mech., Urbana, IL, (ed. Cording E.), p.57-75.

Mesri, G. and Huvaj-Sarihan, N. (2012). ”Residual Shear Strength Measured by Laboratory Tests and Mobilized in Landslides.” J. Geotech. Geoenviron. Eng., 138(5), 585–593.

Mesri, G., and Shahien, M., (2003). “Residual shear strength mobilized in first-time slope failures, J. Geotech. Geoenviron.”. Eng., ASCE, v. 123, n. 4, p. 12-31.

Mohr, O. (1882). “Ueber die Darstellung des Spannungszustandes und des Deformationzustandes eines Korperelementes und uber die Anwendung derselben in der Festigkiteslehre.” Civilengenieur Vol.28, No.113-156. (also Technische Mechanik, 2nd ed. 1914).

Morgenstern, N.R. (1977). “Slopes and excavations”, State of the Art Report, Proc. 9th Int. Conf. Soil Mech. Found. Engrg., 2, 567-581.

Noor, M.J.Md. Derahman, A. (2011), “Curvi-linear shear strength envelope for granitic residual soil grade VI.”, Unsaturated Soils: Theory and Practice 2011, Kasetsart University, Thailand, ISBN 978-616-7522-77-7.

Nusier, O.K. Almohd (Ayasrah), I.M. Jaradat, R.A. (2008), “Nonlinearity of Shear Strength and Stress-Strength Behavior and Induced Stress Predictions.” International conference on construction and building technology. ICCBT. kuala lumpur, Malaysia, Malaysia.

Ordemir, İ., Soydemir, C. and Birand, A. (1977). “Swelling Problems of Ankara Clays.” In: 9th Intentional Conference of Soil Mechanics and Foundation Engineering, Tokyo, Vol.1, 243-247.

Perry, J. (1994), “A technique fr defining non-linear shear strength envelopes and their incorporation in a slope stability method of analysis.” Q. J. Eng. Geol., 27(3), 231-241.

Sezer, G. A.; Turkmenoglu, A. G., Gokturk, E. H., (2003),”Mineralogical and sorption characteristics of Ankara clay as a landfill liner”. Applied Geochemistry, Vol. 18, pp. 711–717.

Skempton, A.W. (1964). “Long-term stability of clay slopes.” Géotechnique, 14(2), 77–101.

Skempton, A. W. (1985). “Residual strength of clays in landslides, folded strata and the laboratory.” Géotechnique, 35(1), 3–18.

Skempton, A.W., and Petley, D.J. (1967). “The strength along structural discontinuities in stiff clays,” Proc. Geotech. Conf., Oslo, 2, 29-47.

Sonmez, H. (2001) “Investigation of the behaviour of fissured clays,” PhD Thesis, Hacettepe University, Ankara, Turkey.

Stark, T.D., Choi, H., and McCone, S. (2005) “Drained shear strength parameters for analysis of landslides.”, ASCE Journal of Geotechnical and Geoenvironmental Engineering, 131(5), p.575-588.

Stark T.D. and Eid, H.T. (1994). “Drained residual strength of cohesive soils.”, J. Geotechnical Eng., 120(5), 856-871.

Stark T.D. and Eid, H.T. (1997). “Slope stability analyses in stiff fissured clays.”, J. Geotech. Geoenviron. Eng. 123(4), 335-343.

Stark, T. and Hussain, M. (2010). ”Shear Strength in Preexisting Landslides.” J. Geotech. Geoenviron. Eng., 136(7), 957–962.

Stark, T.D., Vettel, J.J. (1992). “Bromhead Ring Shear Test Procedure.”. Geotechnical Testing Journal - GEOTECH TESTING J , vol. 15, no. 1, 1992.

Teoman, M.B., Topal, T., Isık N. S. (2004) Assessment of slope stability in Ankara clay: a case study along E90 highway, Environmental Geology, v. 45:963–977.

Terzaghi, K., Peck, R.B., and Mesri, G. (1996). “Soil Mechanics in Engineering Practice.”, 3rd Edition, John Wiley and Sons.

Tiedeman, (1937). “Ueber die Schubfestigkeit bindiger Boden.” (On the strength of cohesive soils). Die Bautechnik, Vol.15, pp. 400-403, 433-35.

Tika, T.E. and Hutchinson, J.N. (1999) “Ring shear test on soil from the Vaiont landslide slip surface.” Géotechnique 49 (1), 59-74

Tika, T. E., Vaughan, P. R. & Lemos, L. J. L. (1996). “Fast shearing of pre-existing shear zones in soil.” Ge´otechnique 46, No. 2, 197–233.

Tiwari, B. (2007). “Residual shear strength of tertiary mudstone and influencing factors.”, Progress in Landslide Science, Springer Special publication, 135-145.

Tiwari, B. Ajmera, B. (2011). A new correlation relating the shear strength of reconstituted soil to the proportions of clay minerals and plasticity characteristics, Applied Clay Science, 53, 48-57.

Tiwari, B. Marui, H. (2005). “A new method for the correlation of residual shear strength of the soil with mineralogical composition.” J. Geotech. Geoenviron. Engng ASCE 131, No. 9, 1139–1150.

Townsend, F.C., Gilbert, P.A., (1976). “Effects of specimen type on the residual strength of clays and clay shales.” Soil specimen preparation for laboratory testing. ASTM STP 599, American Society for Testing and Material, pp. 43–65.

University of Idaho college of Agricultural and Life science‘s website (2012). http://www.cals.uidaho.edu/soilorders/vertisols_07.htm

Vithana, S.B., Gibo, S., Nakamura, S., Kimura, S. (2009). “Influence of overconsolidation ratio on residual strength of Kamenose & Miaowan landslide soils under laboratory conditions.” The International Society of Offshore and Polar Engineers. Proceedings of 19th Offshore (Ocean) and Polar Engineering Conference, Osaka Japan, 21–26 June, 2, pp. 246–249.

Vithana, S.B. Nakamura, S. ,Sho Kimura, Gibo, S. (2012). “Effects of overconsolidation ratios on the shear strength of remoulded slip surface soils in ring shear”. Engineering Geology 131–132, p: 29–36.

Voight, B. (1973). “Correlation between Atterberg plasticity limits and residual shear strength of natural soils.” Geotechnique, 23,2 pages :265–267.

Wright, S. G. (2005). “Evaluation of Soil Shear Strengths for Slope and Retaining Wall Stability Analyses with Emphasis on High Plasticity Clays.” Project No. 5-1874-01, Center for Transportation Research, The University of Texas at Austin, (August 2005): 90 pgs.

Yang, X.L. Yin, J.H. (2004), “Slope stability analysis with nonlinear failure Criterion”. J Eng Mech ASCE; Vol. 130(3):267–73.